Roles of Cell Junctions and the Cytoskeleton in Substrate-free Cell Sheet Engineering

Qi Wei

Submitted in partial fulfillment of the

requirements for the degree of

Doctor of Philosophy

in the Graduate School of Arts and Sciences

COLUMBIA UNIVERSITY

2014

ABSTRACT

Roles of Cell Junctions and the Cytoskeleton in Substrate-free Cell Sheet Engineering

Qi Wei

In multicellular organisms, one-cell-thick monolayer sheets are the simplest tissues, yet they play crucial roles in physiology and tissue engineering. Cells within these sheets are tightly connected to each other through specialized cell-adhesion molecules that typically cluster into in discrete patches called cell-cell junctions. Working together, these junctional organelles glue cells to their neighbors and integrate the cytoskeletons into a mechanical syncytium. Human bodies offer many vivid illustration of how a cell sheet physiology changes considerably during development and diseases, as shown in epidermal blistering and certain cardiomyopathy, which requires it to be mechanically durable and capable of transducing a variety of mechanical signals. Despite the extensive molecular and clinical work on cell junctions, relevant *in vitro* experimental data are often masked by cell-substrate interactions due to a lack of suitable experimental methods. It is therefore important to develop novel *in vitro* methods for characterizing how junctional proteins, as well as tightly associated cytoskeletal proteins, may modulate various cellular behaviors, such as viability and apoptosis, cell-cell adhesiveness and tissue integrity.

Control over cell viability is a fundamental property underlying numerous physiological processes. Cell-cell contact is likely to play a significant role in regulating cell vitality, but its

function is easily masked by cell-substrate interactions, thus remains incompletely characterized. In the first part of the thesis, we developed an enzyme-based whole cell sheet lifting method and generated substrate- and scaffold-free keratinocyte (N/TERT-1) cell sheets. Cells within the suspended cell sheets have persisting intercellular contacts and remain viable, in contrast to trypsinized cells suspended without either cell-cell or cell-substrate contact, which underwent apoptosis at high rates. Suppression of junctional protein plakoglobin weakened cell-cell adhesion in cell sheets and suppressed apoptosis in suspended, trypsinized cells. These results demonstrate that cell-cell contact may be a fundamental control mechanism governing cell viability and that the plakoglobin is a key regulator of this process. The study also lays groundwork for future characterization and manipulation of viable cell sheets for cell sheet engineering purpose.

Cell sheet engineering, characterized by non-invasive harvest of cultured cell monolayer as a scaffold-free sheet, was recently developed. Particularly, cell sheet engineering based cardiac tissue engineering has emerged as an alternative method for the repair of damaged heart tissue. Such an engineered cell sheet offers a new way to study cell junctions when substrate interactions are no longer dominant. While this method is promising, it is limited by the fragility and shrinkage of the sheets as well as the lack of information regarding the characteristics of such sheets. In this part of the thesis we pursued two related research projects by developing a novel partial-lift method to generate strong, unshrunk substrate-free and scaffold-free cell sheets, first using skin cells and then further refined and expanded it to cardiac cells primarily due to the ease with which they can be manipulated, their similarities in cell junctions and potential clinical applications. These partially-lifted cell sheets engage primarily in cell-cell interactions, yet are amenable to biological and chemical perturbations and, importantly, mechanical conditioning.

This simple yet powerful tool was then deployed to test the hypothesis that the lifted cells would exhibit substantial reinforcement of key cytoskeletal and junctional components at cell-cell contacts, and that such reinforcement would be enhanced by mechanical conditioning. Results further demonstrate that the mechanical strength and cohesion of the substrate-free cell sheets strongly depend on integrity of the actomyosin cytoskeleton and junctional protein plakoglobin. Moreover, our results showed dissociating cell-substrate interactions and implementing mechanical conditioning could enhance contraction, calcium signaling, alter viscoelastic property, and thus improve the functional cell-cell coupling in the cardiac sheets.

In sum, this thesis represents a first systematic examination of junctional regulating of cell viability and mechanical conditioning on cells with primarily cell-cell interactions. The information gained from this study will help advance our understanding of cell-cell interactions and improve cell sheets biomechanical properties. For tissue engineering purpose, our dispase-based partial-lift cell sheet harvesting method has the advantage of being biocompatible, easily applicable, rapidly collectable and stretchable, compared to currently available techniques. This simple yet powerful partial lift technique has enormous potential for fabricating clinically applicable skin and cardiac tissues.

Table of Contents

List of Figures

List of Tables

Acknowledgements

I would never have been able to finish my dissertation without the guidance of my committee members, help from colleagues and support from my family.

I would like to express my deepest gratitude to my advisor, Dr. Hayden Huang, for his guidance, caring, patience, support and providing me with an excellent atmosphere for doing research. His infectious enthusiasm and unlimited zeal for biology-medicine-engineering have been major driving forces through my graduate career at Columbia. I would like to thank my committee members Dr. Gordana Vunjak-Novakovic, Dr. Lance Kam, Dr. Angela Christiano and Dr. David Owens for their guidance over the years from Ph.D. qualifying exam to thesis proposal to final defense. They have been invaluable sources of inspiration and motivation on how to conduct rigorous and meaningful scientific studies.

I am indebted to many fellow Columbia Biomedical Engineering (BME) colleagues. My research would not have been possible without their helps. I would like to thank Biomechanics and Mechanotransduction lab members past and present, particularly Jarett Michaelson and Venk Hariharan, who always willing to help and give their best suggestions. I also extend my gratitude to many faculty members in Engineering School for instructing me how to become a top-notch engineer, and in Business School for providing me opportunities to think out of engineering box; BME staff that that keeps our department running, especially Keith Yeager, Jarmaine Lomax, Michelle Cintron, Paulette Louissaint, and Shila Maghji; BME classmates and visiting scholars for being friends and for their support they have lent to me during my enjoyable and memorable stay at Columbia and New York City, especially Bin Zhou, Xinzhi Zhang, Bin Lou, Emmanuel Dumont, Keenan Bashour, Edward Judokusumo, Ji Wang, Eric Yu, Siheng He and many more.

I would like to thank my former supervisor, Dr. Don McClure, for his guidance over the years I worked at Eli Lilly. Don watched me grow from a rookie to a bioprocess engineering expert, recommended me to chase my dream and constantly encouraged me to reach higher during my study at Columbia. I would also like to thank my Lilly colleagues for the support they have lent to me, for keeping me updated with Company and industry trend and for offering me job positions during my career at and beyond Indianapolis.

Finally, I would like to thank my parents for their unconditional love. They were always encouraging me with their best wishes and supporting me with their best efforts to ensure that I would have access to the best education and opportunities. And finally, my very special thanks to my beautiful wife, Zhiyan, and lovely son, Steven, for her consideration to accompanying me from Connecticut to New York to New Jersey, for their love and support that made these achievements possible.

Dedication

For wife Zhiyan Zeng and son Steven Chuqi Wei

Chapter 1 Introduction

1.1 The structure and composition of cell junctions

In multicellular organisms, both cell–cell and cell–matrix adhesion are vital for the formation, composition, architecture, and function of tissues. However, significant pathways involved in tissue integrity and function are determined to a large part by adhesion and communication between individual cells, which are in turn mediated by cell junctions [1-7]. Recent studies provided much insight into the molecular composition and structure of cell junctions, and investigators are starting to understand the underlying mechanisms of their diverse functions [8-17]. This introduction chapter briefly reviews the basic classification of cell-cell junctional structures and some of their representative proteins. Their roles in development, disease and signaling are briefly outlined, followed by a section on contemporary methods for probing cell-cell interactions and some recent developments. For more details, please refer to the IRCMB review article we recently published [13].

In vertebrates, cell-cell junctions can be classified into four functional classes: (1) adherens junctions and (2) desmosomes, which mechanically link cells by bridging the cytoskeleton of adjacent cells, (3) communicating junctions, or *gap junctions*, which chemically and electrically couple neighboring cells, and (4) occluding junctions, or *tight junctions*, which are essential for establishing barrier function across a cell layer [18-28]. Working together, these four cell junctional classes play vital roles in development, health and disease [8,29-32] (Figure 1.1).

Cell-cell interactions drive numerous physiological processes and help enable coordinated functioning in multicellular organisms [7,33]. Many cell-cell interactions have not

been well-characterized, partially because much work was devoted to examining cell-matrix interactions, and partially because studying cell-cell associations comes with a long list of challenges. First, cell-cell associations are generally more geometrically complex. Second, various extracellular matrices are readily isolated or purchased, while cell-cell junctions rely more on specific receptor-receptor interactions, which in turn rely on expensive antibodies or purified receptors. Finally, effects of cell-cell interactions are very difficult to isolate from cell-substrate interactions in adherent cells. The reverse is a bit simpler – some cell models can work with sparsely plated cells. But generating consistent cell culture conditions where cell-cell interactions dominate is not always a simple matter.

As a result of these and other challenges, insights into cell-cell interactions have been somewhat slow in coming. While we can now generate artificial scaffolds of various materials, geometries/patterns, adhesion molecules and mechanical properties (e.g., stiffness), there are few analogous tools for cell junctional studies [34-42]. However, with the recent development of more advanced methods, the critical role of cell-cell junctional proteins in regulating various cell processes is rapidly becoming more appreciated [37,43].

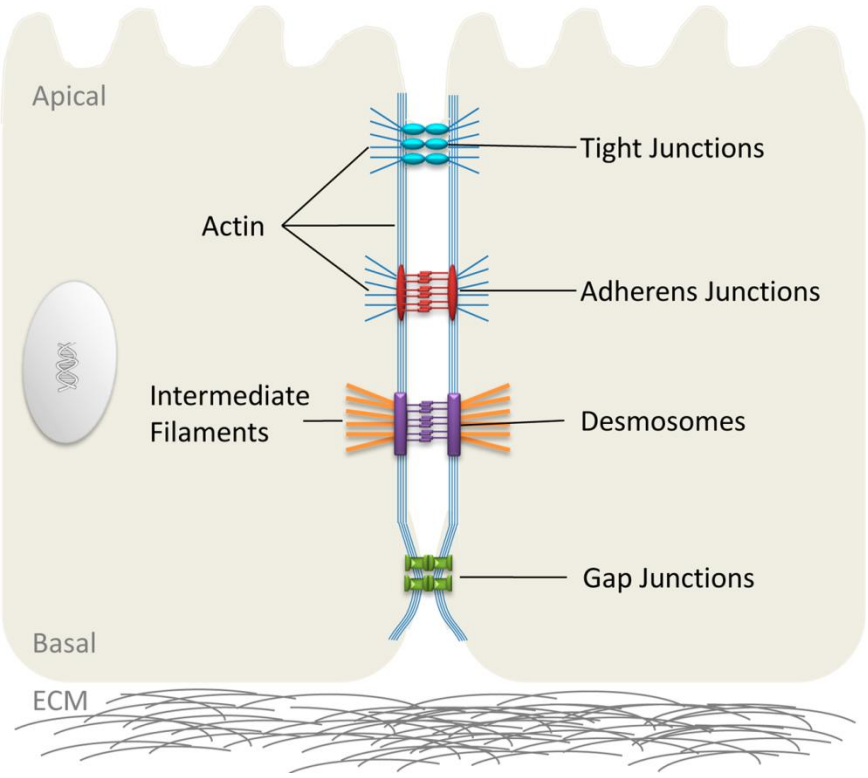

Figure 1. 1 The four main cell junctional classes.

From apex to base are the (1) adherens junctions, which serve as actin anchors, (2) desmosomes, which serve as intermediate filaments anchors, (3) tight junctions, which are selective permeability barriers, and (4) gap junctions, which function as electrical and chemical couplers for adjacent cells [13].

1.2 Cell junctions in development and diseases

Development of any multicellular organism is likely impossible without precisely regulated cell-cell adhesion. Many developmental processes, including embryonic compaction and cell fate determination, are guided by a dynamic balance dependent on intercellular junctions, mechanical stresses and the cytoskeleton [31,44]. Tissue morphogenesis and organogenesis post early

development require a constant and precisely executed remodeling of cell junctions. This process is accompanied by dramatic cytoskeletal remodeling that facilitates the changes in cell shape and motility [44]. To some extent, embryonic morphogenesis results largely from epithelial sheet stretching, contraction, migration and deformation [31]. The mechanical forces generated by dynamic rearrangements of cell junctions and the cytoskeleton thereby facilitate the morphological changes that transform flat cell sheets into three dimensional structures [44].

The coordinated control of cell junctions by various signaling pathways plays an essential role in human health and disease. Observations from a variety of studies, including naturally occurring and engineered mutations, through animal models and *in vitro* experiments, provide valuable information about the critical functions of cell junctions and associated diseases. In recent years, a large number of naturally occurring human mutations have been reported in genes that encode components of the four major cell junctional classes. Defects in those junctional proteins have been linked to various inherited disorders, including skin and hair disorders, cardiomyopathies, sensory defects, psychiatric disorders and cancers [45-49]. These genetic disorders also provide valuable insight for investigating the relative contributions of mechanical stress response and signaling pathways to the pathogenic process. A comprehensive, timely compendium of human genes and genetic disorders can be found at Online Mendelian Inheritance in Man (OMIM) [50,51].

Of the four major cell junctional classes, desmosomes are expressed in many cells, with considerable interest in their role in epidermal and cardiac disease [52]. Mutations were identified in many desmosomal components [53]. Collectively, these mutations demonstrate the important role of desmosomal proteins in skin, hair, and cardiac function. Many mutations in desmosomal components are associated with both dominant and recessive disorders [45].

Additionally, desmosomal cadherins are also the target of some auto-immune and infectious diseases, such as pemphigus vulgaris and pemphigus foliaceus [54-58].

Plakoglobin-deficient transgenic mice exhibit severe cardiac defects and skin fragility [59]. Mutations in the human plakoglobin gene have been found to be the cause of diseases such as Naxos disease, an autosomal-recessive disorder involving heart, skin, and hair abnormalities [60]. Further, mutations in plakoglobin, along with many other desmosomal genes, are implicated in arrhythmogenic right ventricular dysplasia/cardiomyopathy (ARVD/C) [61]. The characteristic pathological hallmark of ARVD/C is fibrofatty replacement of healthy cardiac tissue, with myocyte apoptosis and cardiac rhythm dysfunction [62]. Though the exact mechanism remains elusive, it has been hypothesized that the mutations could affect the structure and distribution of cell junctional proteins, and interferes with canonical Wnt/β-catenin signaling pathway (Figure 1.2). In support of this hypothesis, nuclear localization of plakoglobin was shown to inhibit Wnt/β-catenin signaling, ultimately leading to apoptosis [11,63]. Of considerable interest in researching this condition is the clarification of the mechanism underlying disease progression, including its apparently variable penetrance and the potential influence of mechanical stresses in modulating the condition.

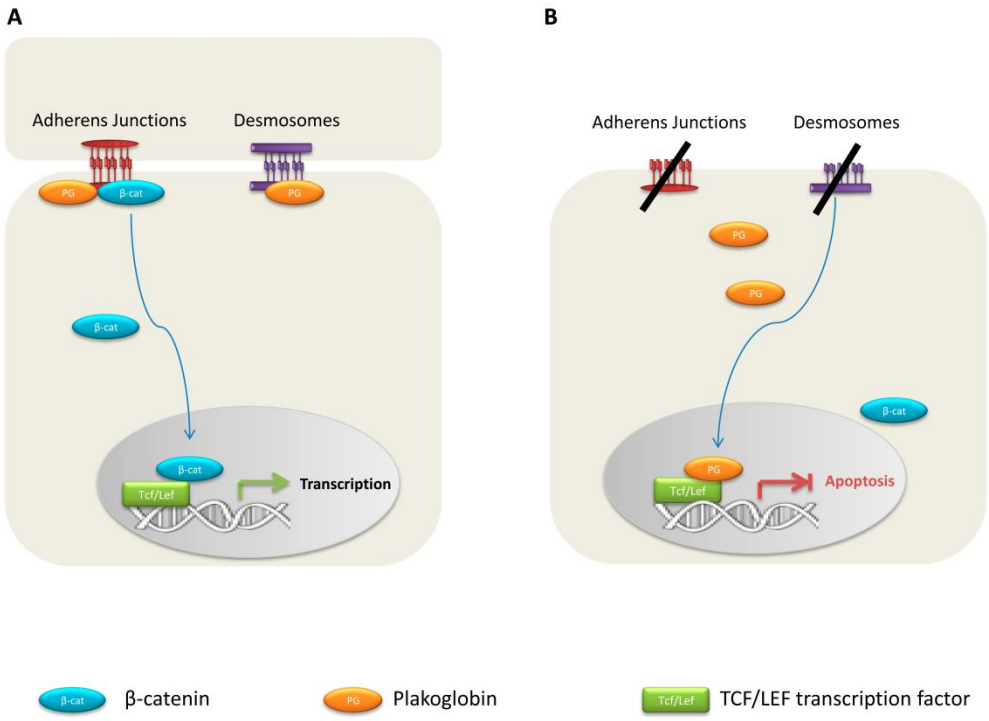

Figure 1. 2 Plakoglobin may participate in the Wnt/β-catenin signaling pathway to regulate signaling and apoptosis.

(A) A simplified model of the canonical Wnt/β-catenin pathway shows that normally, Wnt signaling leads to β-catenin translocation into the nucleus, where it acts in conjunction with TCF/LEF to activate specific target genes. In contrast, plakoglobin is normally confined to the desmosomes and adherens junctions. (B) When cell-cell junctional structures are disrupted, plakoglobin translocates into the nucleus, where it displaces β-catenin. The plakoglobin-TCF/LEF complex ultimately results in cell apoptosis through mechanisms that are yet to be elucidated [13].

1.3 Cell junctions and the cytoskeleton in signaling

In addition to their structural functions, it is becoming increasingly clear that components of the cell junctions also possess diverse signaling capabilities. Recent evident suggests that their dual function may facilitate changes in cellular morphology and gene expression [44]. Indeed, the adhesive properties themselves may facilitate intercellular signaling pathways by bridging the opposing membranes of neighboring cells. Furthermore, many junctional proteins, such as β-catenin, plakoglobin and plakophilin have been reported to localize in the nucleus of cells [64-68]. Although their nuclear functions remain incompletely resolved, the widespread nuclear expression of these proteins has led to the hypothesis that they may be involved in certain transcriptional and signaling machinery.

Connections between cell junctions and the cytoskeleton profoundly influence cell structure and function. Of the three major cytoskeletal components (actin, microtubules and intermediate filaments), actin plays what may be considered the most prominent role in the regulation of cell-cell contacts, by sustaining the cross-junctional force balance, which subsequently determines cell-cell contact patterns. Reciprocally, by providing a powerful mechanical coupling between the actin network of adjacent cells, the cadherin-catenin complex integrates intracellular and intercellular forces across developing tissues [32]. The desmosome-intermediate filament network helps distribute mechanical stresses throughout the embryonic tissues and contribute to the regulation of intercellular adhesion and tissue integrity [48]. Cell junctions also depend on the presence of the microtubules, which facilitates transportation of key

proteins (such as classic and desmosomal cadherins and associated armadillo proteins), to the plasma membrane [69,70].

Mechanotransduction refers to the process of converting mechanical forces into biochemical signaling responses, which requires the integrity of cell junction (and cell-extracellular matrix)- cytoskeletal associations [8,9,11,29,71]. Of particular interest here are the studies of a kinetic organ- the heart. The morphology of heart changes considerably during development and disease, via either adaptive or maladaptive remodeling that requires cardiomyocytes to be mechanically durable and biologically capable of transducing a variety of environmental signals [72]. During these remodeling processes, the cytoskeleton plays a pivotal role in both sensing mechanical signals and mediating structural remodeling and functional responses within the cardiomyocytes. Studies have demonstrated that junctional cadherins facilitate the bi-directional transmission of cytoskeletal tension between cells, function as mechanosensors by actively remodeling the cytoskeleton and reinforcing cell–cell junctions in response to tugging forces [73,74]. However, the mechanism of mechanosensing remains unknown. Moreover, besides neighboring cells, cytoskeletal architecture is sensitive to many factors in the extracellular microenvironment, such as cell shape, ECM component, stiffness and topology [72]. Notably all previous studies were performed in conventional adherent cell culture models which maintain cell-substrate interactions and as a result, may introduce noise into the readouts. From a cell junction perspective, it would be interested to see how the cytoskeleton senses mechanical signals and mediates structural remodeling without the interference from cell-substrate interactions.

1.4 Techniques for studying cell junctions

Many conventional molecular biology methods were deployed to examine junctional regulation of cell behavior. These include transfection, immunoblotting (western blotting), cell tracking for migration, wound healing, cell-substrate adhesion assays, and immunofluorescence staining. For studies focusing on junctions in particular, however, investigators have had to develop some new approaches to more precisely characterize cellular properties.

A measure of how junctional proteins may respond to external stimuli can be acquired by quantifying the fluorescence signal for an immunofluorescently stained sample. This measurement was used to demonstrate increases in gap junction and desmosomal proteins in various cell types in response to applied cyclic stretch [75,76]. Measurement of forces generated across cell junctions required an adaptation of classical traction-force microscopy by including a constraint regarding the total force in a region of cells. Using this constraint, Trepat et al demonstrated that cell-cell forces are not uniform in confluent patches of cells; rather there are focal locations of high cell-cell forces, apparently near the edges of cell "islands," with a mostly-low force interior [77]. Micropatterning, expanding from its ability to shape individual cells, is now being used to shape small groups of contacting cells, whether to precisely control the contacting geometry or to arrange the type of contacting cells, such as for heterotypic interactions [78]. Recently, the use of micropillars has given rise to precise studies of cell-cell forces in cell pairs [74] or in cells that are exposed to external mechanical stimuli [79].

One of the most vexing problems in examining cell-cell interactions is to precisely measure the adhesion force between contacting cells – that is, the amount of force necessary to separate adjacent cells – in the cells' natural environment. Three common techniques to

approximate this measurement are double micropipette aspiration [80], cell aggregate assays, and cell sheet assays. Double micropipette aspiration relies on partially aspirating a cell in each of two pipettes, allowing the cells to contact, and then aspirating one of the cells to separate them. Cell aggregate assays rely on use of a hanging drop culture to generate a small cluster of cells which do not adhere to a substrate, which are then collected and sheared, often by pipetting or vortexing, to measure aggregate cohesion strength [81,82]. Cell sheet assays use confluent monolayers of cells. In most cases, the monolayer is dissociated from the surface using enzymatic compounds like dispase and then sheared [11,82]. Alternative methods of dissociating the monolayer, such as thermo-responsive polymers or soluble matrix could also be used [83,84] (Figure 1.3). A deform-drag method may be used to assess the relative strength of cell-cell to cell-matrix adhesion, although it appears to be best applied to cell types having modest cell-matrix adhesion strength [76].

One main advantage of using cell sheet assays in contrast to cell aggregate assays is that in the case of the former, the cells are plated normally until immediately prior to the assay. While use of hanging drops or micropipette aspiration is not without advantages, the fact that the cells remain in suspension for extended times may lead to changes in baseline behavior, which may in turn affect adhesion readouts, for normally adherent cells. In the case of micropipette aspiration, a clear readout of the actual adhesion forces is not always easily obtainable, although there are mathematical models that can be used to help provide some estimates. Use of micropipettes that flex can lead to more direct extraction of forces using the beam equation, although plating cells on the tips can be challenging. Alternative methods are being developed. For example, “teethed” plates that can be separated after cells attach may eventually lead to force quantification [85].

Another challenge is to determine the role of junctional proteins when cell-cell contact is the dominant mechanism by which the cell receives information regarding the environment. There appears to be some evidence that cells need force generation to thrive; when the substrate is too soft, for example, cells will tend to cluster and form cellular networks that they otherwise wouldn't on stiffer substrates [86]. Thus it would appear that the machinery for cellular regulation by junctional proteins is extant but is usually attenuated by cell-substrate interactions. Indeed, the balance between cell-cell and cell-substrate forces can be considered to be regulated together, perhaps by one unifying mechanism [87]. Consider that the matrix within an organism is generally self-generated; thus there may be promise in engineering cells in the absence of external substrates [11], since cell-substrate contact is not necessary for cell survival.

Another approach to examine the properties of cell-cell interactions uses a substrate coated with a cell-cell adhesion molecule and either a cell or another object coated with a cell-cell adhesion molecule. Such studies have the advantage that a particular protein (usually a receptor) is targeted but the results are likewise limited to that single interaction. Such studies have been done using atomic force microscopy and micropillars [13,88,89].

1.5 Cell sheet based cardiac tissue engineering for heart repair

Heart disease, including myocardial infarction (MI) and congestive heart failure (CHF), is currently the leading cause of death in the USA and is rapidly becoming one of the leading causes of global mortality [90,91]. Both MI and CHF are characterized by cardiac muscle damage caused by massive cardiomyocyte death and reduced cardiac function. Though recent studies have demonstrated that there is a limited regeneration potential in the adult heart, the

turnover capability of the heart itself after MI cannot compensate for the loss of large-scale tissue and contractile function [92,93]. Many therapies, including various pharmaceuticals and surgical interventions, have been developed to slow down the progression to heart failure; however, these treatments do not restore contractile function to the affected heart tissue [94] and can only increase the patient's life expectancy of heart failure patients by a few years [95]. Ultimately, heart transplantation is the gold standard for treating CHF [96]. Unfortunately, the benefits of heart transplantation are limited by the growing donor scarcity and further complicated by the need for lifelong immunosuppressant therapy [97,98]. Consequently, there exists a need for alternative strategies.

Cellular therapy aiming to use cells to regenerate new cardiomyocytes and improve cardiac function has emerged as a promising alternative therapeutic option for heart diseases [99]. Two common strategies are currently being pursued, including *in situ* cellular cardiomyoplasty and cardiac tissue engineering. The *in situ* cellular cardiomyoplasty strategy directly delivers or injects cells directly into the post-myocardial infarction heart [100,101]. Though several clinical trials demonstrate statistically significant improvement in heart function, this improvement is often not clinically relevant and the functional benefit is mostly transient [102,103]. Many hurdles remain including cell retention, survival of the engrafted cells, cell differentiation, immune rejection and integration of transplanted cells with host tissue.

An alternate strategy is cardiac tissue engineering, which aims to create functional tissue constructs that can reestablish the structure and function of injured cardiomyocytes. Generally speaking, the technique uses a combination of cells and three-dimensional biomaterials/scaffolds in highly controllable environments, such as a bioreactor with proper biophysical stimulation, which can mediate cell differentiation and functional assembly (Figure 1.3) [84,99,104-107]. The

use of tissue engineering techniques results in improved cell retention over *in situ* cellular cardiomyoplasty and generates cardiac tissue through control of the *in vitro* culture conditions. Some common cardiac tissue engineering approaches currently being pursued include *in situ* delivering cells entrapped in injectable biomaterials into the infarcted heart, *in vitro* engineering of stem cell- seeded tissue constructs, *in vitro* engineering of cardiac tissue constructs followed by *in vivo* implantation, and cell sheet tissue engineering [108]. More recently, cardiac cell sheet tissue engineering has attracted considerable interest (Figure 1.4) [109,110]. This technique allows cultured cells to detach from temperature-responsive substrates without the disruption of intercellular junctions that are critical for myocardial function. Furthermore, cell sheet engineering permits the development of simple cardiac tissues without the use of biomaterial scaffolds. However, to date, cardiac sheets generated for tissue engineering purposes are fragile. It is not currently known whether the scaffold-free cardiac tissues could withstand the persistent mechanical stresses required to function as cardiac muscle. Mechanical stimulation has been demonstrated as an attractive strategy for the tissue engineering of functional cardiac tissues [111-115]. It would be interesting to see if subjecting the scaffold-free 2D cell sheets to mechanical stretch would also induce hypertrophic changes in overall gene expression and benefit the functional cell-cell coupling in cardiac sheets. Notably all previous studies were performed using conventional adherent cell models which maintain cell-substrate interactions and as a result, may introduce mixed responses into the readouts. A suitable experimental method for mechanical conditioning, characterizing and improving cardiac sheet biomechanical properties, in the absence of cell-substrate interactions, is still lacking.

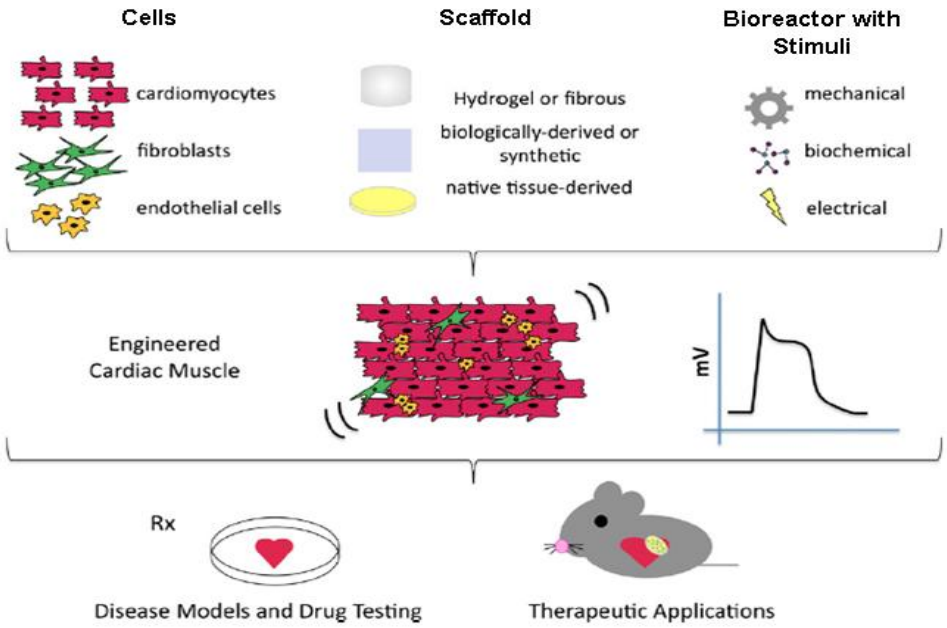

Figure 1. 3 Current cardiac tissue engineering approaches.

Several approaches have been used to generate 3D cardiac patches in vitro, including scaffold-free stackable 2D cell sheets and 3D constructs in or on scaffold biomaterials. The bioreactor provides environmental control and biophysical stimulation (such as electrical excitation, mechanical stretch, and electrical stimulation) to these 2D or 3D constructs. The resulting engineered cardiac tissue constructs can be used to reestablish the structure and function of injured myocardium (*in vivo*); moreover, they can also serve as high-fidelity models for studies of cardiac development, disease modeling and drug testing (*in vitro*). Adapted from [107].

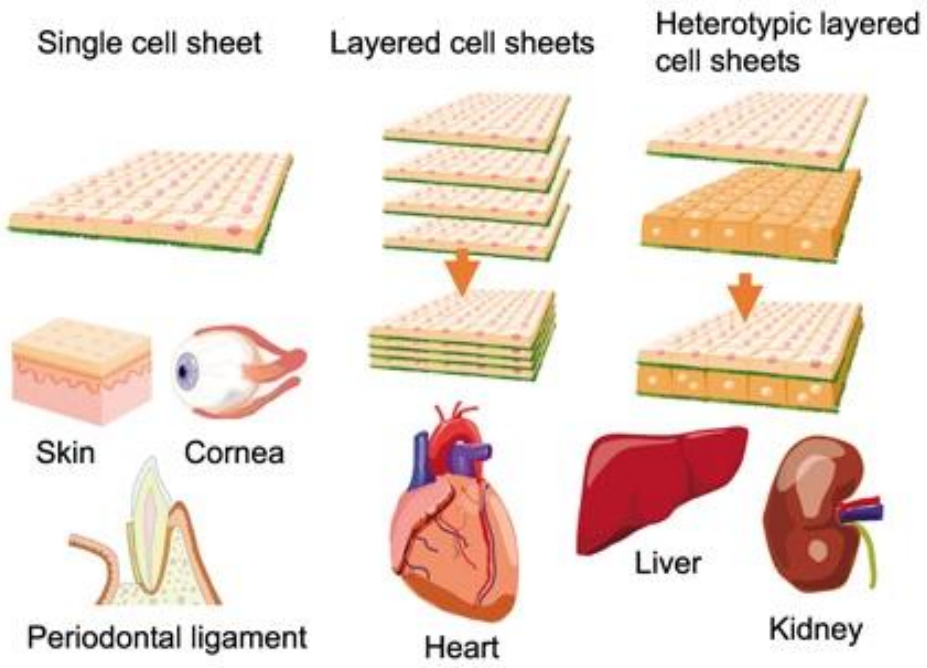

Figure 1. 4 Nanotechnology-based cell sheet engineering as a platform technology for regenerative medicine.

Researchers have developed "cell sheet engineering" by utilizing nanotechnology-based temperature-responsive culture dishes. Such cell sheets have been generated for a wide variety of laminar tissues, such as skin, heart, corneal and renal components. Adapted from [36].

1.6 Overview of the thesis

In multicellular organisms, one-cell-thick monolayer sheets are the simplest tissues, yet they play crucial roles in physiology and tissue engineering [116-119]. Cells within these sheets are tightly attached to each other through cell-cell junctions. Cell sheet engineering is a new area of research that focuses on characterizing how cells respond when substrate interactions are limited or eliminated [43]. Such an engineered cell sheet offers an unprecedented way to study cell

junctions when substrate interactions are no longer dominant. While this method is promising, it is limited by the fragility and shrinkage of the sheets as well as the lack of information regarding the characteristics of such sheets. It is therefore important to develop and apply novel *in vitro* methods for characterizing how junctional proteins may modulate cellular responses, such as apoptosis and viability, cell sheet biomechanics and tissue integrity [120-122].

The framework of this thesis consists of three major projects:

The study presented in Project 1 (Chapter 2) developed an enzyme-based cell sheet engineering technique and study of how cell junctional proteins regulate cell apoptosis and viability. Keratinocytes were used in this study primarily due to the ease with which they can be manipulated and their especially abundant cell junctions. This study also lays groundwork for future characterization of viable engineered cell sheets.

The study presented in Project 2 (Chapter 3) explores a novel strategy to generate partially-lifted cell sheets that are amenable to biological and chemical perturbations, and more importantly, mechanical conditioning and characterization. The partial-lift technique was first applied to keratinocyte. How cell junctional proteins regulate cell sheet biomechanics and tissue integrity were examined. This study also provide a solid foundation for extend partial-lifting technique to cardiac sheet engineering due to existing similar junctional structures between epidermal and cardiac tissues.

The study presented in Project 3 (Chapter 4) refined the partial-lift technique and adapted it for cardiac cells. Moreover, we characterized microrheology, contraction and calcium signaling of the cardiac cell sheets, which are critical for their potential clinical applications.

1.6.1 Project 1: United We Stand: cell-cell contact preserves cell viability

Control over cell viability is a fundamental property underlying numerous physiological processes. Cell spreading on a substrate was previously demonstrated to be a major factor in determining the viability of individual cells [6]. In multicellular organisms, cell-cell contact is likely to play a significant role in regulating cell vitality, but cell-cell signaling is easily masked by generally and difficult to isolate from cell-substrate interactions, thus remains incompletely characterized. Whether adhesion to other cells is important to cell viability is the central question of this study.

We show that suspended immortalized human keratinocytes cell sheets with persisting intercellular contacts exhibited significant contraction, junctional actin localization, and reinforcement of cell-cell adhesion strength. Further, cells within these sheets remain viable, in contrast to trypsinized cells suspended without either cell-cell or cell-substrate contact, which underwent apoptosis at high rates. Suppression of plakoglobin weakened cell-cell adhesion in cell sheets and suppressed apoptosis in suspended, trypsinized cells. These results demonstrate that cell-cell contact may be fundamental control mechanism governing cell viability and that the junctional protein plakoglobin is a key regulator of this process. Given the near-ubiquity of plakoglobin in multicellular organisms, these findings could have significant implications for understanding cell adhesion, modeling disease progression, developing therapeutics and improving the viability of tissue engineering protocols. These results provide a solid foundation for future characterization and manipulation of viable cell sheets for cell sheet engineering purpose.

1.6.2 Project 2: Characterization of partially-lifted keratinocyte cell sheets

In this part of the thesis we developed a novel method to generate partially lifted substrate-free and scaffold-free keratinocyte cell sheets.

There is a need to characterize biomechanical cell-cell interactions, but due to a lack of suitable experimental methods, relevant *in vitro* experimental data are often masked by cell-substrate interactions. This study describes a novel method to generate partially-lifted substrate-free cell sheets which engage primarily in cell-cell interactions, yet are amenable to biological and chemical perturbations and, importantly, mechanical conditioning and characterization. A PDMS mold is used to isolate a patch of cells, and the patch is then enzymatically lifted. The cells outside the gasket remain attached, creating a partially-lifted cell sheet. This simple yet powerful tool enables the simultaneous examination of lifted and adherent cells. This tool was then deployed to test the hypothesis that the lifted cells would exhibit substantial reinforcement of key cytoskeletal and junctional components at cell-cell junctions, and that such reinforcement would be enhanced by mechanical conditioning. Results demonstrate that the mechanical strength and cohesion of the substrate-free cell sheets strongly depend on integrity of the actomyosin cytoskeleton and the cell-cell junctional protein plakoglobin. Both actin and plakoglobin are significantly reinforced at junctions with mechanical conditioning. These results represent a first systematic examination of mechanical conditioning and the cytoskeleton on cells with primarily intercellular interactions.

1.6.3 Project 3: Characterization of partially-lifted cardiomyocyte cell sheets

Cardiac cell sheet tissue engineering has recently emerged as a promising alternative therapeutic option for heart diseases [109,110]. However, these scaffold-free cardiac sheets are fragile and it remains to be seen whether they could withstand mechanical forces required to function as cardiac muscle. Further, these cardiac sheets shrink significantly after detached from substrates and thus impairs their ability to provide sufficient coverage in the cardiac tissues being repaired. Mechanical stretch has been utilized to improve the functionality of engineered myocardial tissues *in vitro* [75,123,124]. Notably, however, all previous studies were performed using the conventional adherent cell models which maintain cell-substrate interactions and as a result, may introduce mixed responses into the readouts. A suitable experimental method for mechanical conditioning, characterizing and improving cardiac sheet biomechanical properties, in the absence of cell-substrate interactions, is still lacking.

In this part of thesis we further refined the partial-lift technique originally developed in skin cells and expanded it to cardiac cells primarily due to the ease with which they can be manipulated, their similarities in cell junctions and potential clinical applications. Results show that lifted cardiac cells exhibit changes to the distribution of cytoskeletal and junctional proteins, with reinforcement occurring at cell-cell junctions, and that such reinforcement is enhanced by mechanical conditioning. Further results demonstrate that the mechanical strength and cohesion of the substrate-free cell sheets strongly depend on integrity of the actin cytoskeleton and the cell junctional protein plakoglobin. Moreover, we characterized the properties of the cardiac cell sheet using microrheology, contraction and calcium signaling assays, to assess their potential for

clinical applications. Direct experimental investigations on cardiac cell sheets without interference of cell-substrate interactions will greatly enhance our understanding of cell-cell interactions and improve cardiac cell sheets mechanical properties. For tissue engineering purpose, our dispase-based partial-lift cell sheet harvesting method has the advantage of being biocompatible, easily applicable, rapidly collectable and stretchable, compared to currently available techniques. This simple yet powerful partial lift technique has enormous potential for fabricating clinically applicable cardiac tissues.

1.7 Related publications

Journal publications:

Wei Q, Hariharan V, Huang H (2011) Cell-cell contact preserves cell viability via plakoglobin. *PLoS ONE* 6(10): e27064

Wei Q, Reidler D, Shen MY, Huang H (2013) Keratinocyte cytoskeletal roles in cell sheet engineering. *BMC Biotechnology*. 13:17

Wei Q, Huang H (2013) Insights into the role of cell-cell junctions in physiology and disease. *Intl Rev Cell Mole Bio*. B978-0-12-407694-5

Wei Q, Huang H (2013) Characterization of partially-lifted cell sheets. *Tissue Engineering, Part A.* 10.1089/ten.TEA.2013.0274

Wei Q, Huang H (2014) Mechanical conditioning of cardiac myocyte sheets. *Biomechanics*. (Submitted)

Conference presentations:

Wei Q, Hayden Huang (2010) Plakoglobin controls cell viability through cell-cell contact. *American Society for Cell Biology Conference*

Wei Q, Reidler D, Huang H (2011) Cell junctions and cytoskeleton regulate cell-cell adhesion strength. *Biomedical Engineering Society Conference*

Wei Q, Huang H (2013) Intercellular adhesion, cytoskeletal organization and signaling in a substrate-free cell monolayer. *Biophysical Society Conference*

Wei Q, Huang H. (2014) Strengthening substrate-free and scaffold free cardiac cell sheets via mechanical conditioning. *Biophysical Society Conference*

Chapter 2 Cell-cell contact preserves cell viability via plakoglobin

2.1 Introduction

Cell-cell interactions, which occur via specialized adhesion structures in cell junctions, regulate a variety of functions in multicellular organisms, including differentiation, barrier formation, tissue function and signal transduction [8,9]. Despite these critical roles, cell-cell signaling is generally difficult to isolate from cell-substrate interactions, with the result that the latter has been studied more extensively. For example, many studies demonstrate that cell membrane receptors that mediate cell adhesion to the extracellular matrix (ECM) play a central role in sensing external mechanical stimuli, such as fluid shear stress, and transduce these signals into downstream intracellular changes [2-5,10]. One key finding is that cell viability is controlled via geometric factors, being dependent on cell spreading but not contact area per se [6]. Thus, cell-substrate adhesion is one critical regulator of cell life. Whether adhesion to other cells is important is the central question of this study.

Recent work has emphasized the multiple critical roles that cell-cell junctional proteins play in regulating the various facets of development, life and disease. For example, recent studies in arrhythmogenic right ventricular cardiomyopathy (ARVC) demonstrate that mutations in desmosomal proteins are thought to lead to alterations in cardiac and sometimes, dermal tissues. In particular, nuclear localization of the desmosomal protein plakoglobin is thought to lead to apoptosis [63], suggesting a role for junctional proteins in establishing or maintaining cell vitality.

The exact role of cell junctions and the relative impact of cell-substrate versus cell-cell interactions in preserving cell life remain unclear. In particular, it is clear that cells can, at least

transiently, remain viable when plated sparsely (maintaining cell-substrate contact with spreading but having minimal or no cell-cell contact). However, normal culture conditions typically rely on establishing cell-cell contact and in fact, some cells are not viable when lacking cell-cell contact, even when appropriate substrate is plentiful [125]. We hypothesize that cell-cell contact is a fundamental regulator of cell viability, and based on ARVC-related observations, we propose that plakoglobin is a key regulator of cell-cell based viability. That is, when cells are in contact with each other, plakoglobin normally resides at the junctions. When junctions are disrupted, plakoglobin is no longer junctional and cell apoptosis will increase. Determining this has been difficult because regulation of plakoglobin has, up to date, mostly been studied in adherent cells with protein mutation models, which maintains cell-substrate interactions and as a result, may introduce noise into the readouts.

To test our hypothesis, we strategically divided immortalized human keratinocytes into three treatment groups: (1) control, which were cells with both cell-cell and cell substrate contacts; (2) dispase-lifted, which were cells suspended as an intact cell sheet, so that cells maintained cell-cell contact but lost cell-substrate contact, and (3) trypsinized, which were cells that were trypsinized and maintained in suspension dishes as single cells so that the cells had neither cell-cell nor cell-substrate contact. We characterize dispase-lifted cells that maintain cell-cell, but not cell-substrate, contact and show that the cell sheets exhibit contraction, maintain junctional actin, reinforce cell-cell adhesion, and suppress apoptosis in a plakoglobin-dependent manner. Keratinocytes were chosen for this study in part due to existing interest in keratinocyte cell sheet cohesion for dermal tissue engineering and in part because they exhibit strong cell-cell interactions, including desmosomes. This study laid the groundwork for future characterization and manipulation of viable cell sheets for cell sheet engineering purpose. Such an engineered cell

sheet offers a novel way to study cell junctions when substrate interactions are no longer dominant, enable us to further develop and apply novel *in vitro* enzyme-based cell sheet lifting methods for manipulating and characterizing how junctional proteins may modulate cellular responses, such as cell sheet biomechanics and tissue integrity, which are critical for future clinical applications.

2.2 Methods

2.2.1 Cell culture

Immortalized human keratinocytes (N/TERT-1) were maintained as described elsewhere [126]. Briefly, cells were expanded and propagated in keratinocyte serum-free media (abbreviated ker-sfm, media, reagents and supplements from Invitrogen, Carlsbad, CA, unless otherwise stated), supplemented with rEGF (0.2 ng/mL) and BPE (25 μg/mL), $CaCl_2$ (Sigma, St. Louis, MO, 0.4mM), and penicillin/streptomycin. To grow cells to high confluence, cells were switched to a medium consisting of a 1:1 mixture of ker-sfm and a medium DF-K, the latter consisting of a 1:1 mixture of DMEM and Ham's F-12, supplemented with rEGF (0.2 ng/mL) and BPE (25 μg/mL), L-glutamine (1.5 mM) and penicillin/streptomycin.

2.2.2 Antibodies and reagents

The primary mouse monoclonal antibodies anti-plakoglobin (γ-Catenin) and anti-GAPDH (Novus Biologicals) were used for immunoblotting. Immunofluorescence staining was performed using the anti-plakoglobin antibody as the primary and Alexa Fluor 594 goat anti-mouse IgG as the secondary antibody (all at 1:1000 dilutions). Alexa Fluor 488 conjugated phalloidin at a concentration of 0.5 μg/mL in HBSS was used for the actin stain. CellTracker Green CMFDA dye was used at a concentration of 10 μM. Hoechst was used at a concentration of 0.5 μg/mL for nuclear staining. Trypsin-EDTA (0.05%, 10 minutes at 37 ℃) was used to dissociate cells. All staining were performed for 1 hour at 37 ℃.

2.2.3 Fluorescence microscopy

Cells were fixed in 4% paraformaldehyde (Sigma) and then permeabilized with 0.1% triton-X-100 (Sigma). Cells were then incubated in the primary antibody or the phalloidin, CellTraker

Green (CTGreen) and Hoechst label for an hour at 37℃, followed by PBS washes and then, for samples tagged with a primary antibody, a secondary antibody incubation for another hour, washed again and then imaged. Microscopy was performed at room temperature using an Olympus IX-81 inverted fluorescence microscope and images were acquired using an Olympus UPlanFL 10x NA 0.13 and Olympus LCPlanFL 40x NA 0.60 objective lens, and an Orca CCD (Hamamatsu, Bridgewater, NJ, model C10600) camera using MetaMorph Software. Additional images were acquired using an Olympus FV10 Confocal microscope, an Olympus OPLFLN 40X O NA 1.3 objective lens, and Olympus FV10-ABW Software. Images were processed using ImageJ (version 1.43u for Windows; National Institutes of Health) and Photoshop (Adobe) to prepare the final figures [127-129]. Images were brightness/contrast enhanced and fluorescent colors were added for clarity. Relative nuclear and overall plakoglobin intensities were quantified by ImageJ, with values normalized to the signal (100%) at untreated control. Imaging conditions were taken identical and analyses were done in the raw fluorescence images.

2.2.4 Assessment of apoptosis using a TUNEL assay

Keratinocytes were grown to full confluence in 35 mm culture dishes, and then were grouped into three conditions: (1) untreated controls, which were cultured in ker-sfm media, (2) trypsinized, which were treated with a Trypsin-EDTA solution, suspended in ker-sfm media and transferred to 35 mm suspension culture dishes, or (3) dispase-lifted, which were treated with dispase, resuspended in ker-sfm medium and transferred to 35 mm suspension culture dish as an intact cell sheet. An *in situ* cell death detection kit (Roche Diagnostics, Basel, Switzerland) that measures TdT-mediated dUTP nick end labeling (TUNEL) was used in the apoptosis assays according to the manufacturer's instructions.

2.2.5 Dispase-based cell sheet lifting assay

A dispase-based lifting assay was performed to test cell sheet, and thus cell-cell adhesive, strength, adapted from similar protocols [76,130-132]. Cells grown to full confluence in 35 mm culture dishes were treated with 1 mL dispase at a concentration of 2.4 units/mL in HBSS and incubated at 37 ℃ for approximately 30 minutes or until the monolayer lifted from the dish as an intact cell sheet. The cell sheets were then suspended in ker-sfm media for zero, one or two days prior to the lifting assay. Cell sheets were carefully transferred to 50 mL tubes containing 6ml of ker-sfm media, then vortexed at a fixed setting at 10 second intervals. The earliest time for which the cell sheet was completely disrupted, as assessed visually, was recorded for each sheet. Please refer to the published protocols [76,130-132] for more technical details.

2.2.6 Caspase inhibition assay

To determine whether the apoptosis is caspase-dependent, cells were treated with a general caspase inhibitor Z-VAD-FMK at a final concentration of 20 μM (BD Pharmingen, San Diego, CA). Keratinocytes were grown to full confluence in 35 mm culture dishes, and then were grouped into three conditions: untreated controls, which were cultured in ker-sfm media; dispase-lifted, which were cells suspended as an intact cell sheet; and trypsinized, which were treated with a Trypsin-EDTA solution, suspended in ker-sfm media and transferred to 35 mm suspension culture dishes. DMSO was used as a vehicle control. The TUNEL assay was used to determine the apoptosis rate as described.

2.2.7 siRNA knockdown and overexpression of plakoglobin

Two Silencer® Pre-designed siRNA for plakoglobin (siRNA sequence 5’-3’: GGGCAUCAUGGAGGAGGAUtt; CCAUCGGCUUGAUCAGGAAtt), a negative control siRNA (Invitrogen) and an overexpression vector pCMV6-XL5 (OriGene, Rockville MD) were

used to assess the effects of inhibition and overexpression of plakoglobin on cell survival. Cells were transfected with siRNA using Lipofectamine 2000 (Invitrogen). Briefly, transfection was performed using 100 pmol siRNA oligomer or 100 pmol DNA plasmid and 6 μL Lipofectamine 2000 for each sample in a 35 mm dish. Alternatively, cells were trypsinized 4 days after transfection, then suspended in ker-sfm media in 35 mm suspension culture dishes for one additional day, after which the apoptosis rate of transfected cells were analyzed using the TUNEL assay as described.

2.2.8 Immunoblotting

Cells were lysed with RIPA buffer (Sigma) and total protein concentration was determined by Bradford assay (Sigma). Soluble fractions containing equal amounts of total protein were separated using SDS polyacrylamide gel electrophoresis and transferred onto PVDF membranes (Millipore, Billerica, MA). Immunoblotting was performed using mouse anti-human antibodies diluted in TBS with 1% w/v BSA and 0.1% v/v Tween-20 (Sigma) at the following dilutions: anti-Plakoglobin 1:2000, anti-GAPDH 1:1,000, and horseradish peroxidase conjugated goat anti-mouse secondary antibody 1:1,000. Blots were developed with ECL (Perkin Elmer, Waltham, MA) and imaged using a FUJI imaging unit (Fujifilm, Stamford, CT). Relative plakoglobin intensity in immunoblotting images was quantified by ImageJ, with values normalized to GAPDH of each matching blot lane and the signal (100%) at untreated control.

2.2.9 Statistical analysis

Data are expressed as the mean ± SD compared by ANOVA and post-hoc. A value of $p < 0.05$ was considered significant, with each group having sample sizes $n \geq 3$.

2.3 Results

2.3.1 Losing cell-substrate and cell-cell contact results in actin reorganization

Immortalized human keratinocytes were divided into three treatment groups: control (C), which were confluent cells maintained in a cell culture dish, dispase-lifted (D), which were cells that were grown to confluence and then lifted as an intact cell sheet, so that cells maintained cell-cell contact but lost cell-substrate contact, and trypsinized (T), which were cells that were grown to confluence, trypsinized and then maintained in suspension dishes as single cells so that the cells had neither cell-cell nor cell-substrate contact.

When performing the dispase-lifting assay, the cell sheets showed contraction immediately on separation from the substrate, followed by further contraction one day after separation from the substrate (Figure 2.1 A). A second day of incubation yielded no significant further contraction. When adhering to the substratum, cells generate stress fibers and adhesion plaques, which allow cells to maintain their spread morphology. To determine (1) the extent of actin reorganization during trypsinization or dispase lifting and (2) whether dispase lifting affects cell spreading, control, dispase-lifted and trypsinized cells were stained for actin immediately after enzyme treatment (i.e., at zero days). Control cells exhibited cortical localization of actin as well as stress fibers through the interior of the cells (Figure 2.1B). Dispase-lifted cells in the floating sheet exhibited primarily cortical localization of actin, and displayed clearly smaller in-plane cross-sectional areas compared to control cells, suggesting that spreading was reduced on separation from the substrate, consistent with the contraction observed in the whole cell sheet. Trypsinized cells exhibited primarily diffuse staining with no consistent localization of actin

within the cell, indicating a nearly complete disruption of actin organization within the cell. Thus, both dispase-lifting and trypsinization alters actin distribution within the cell.

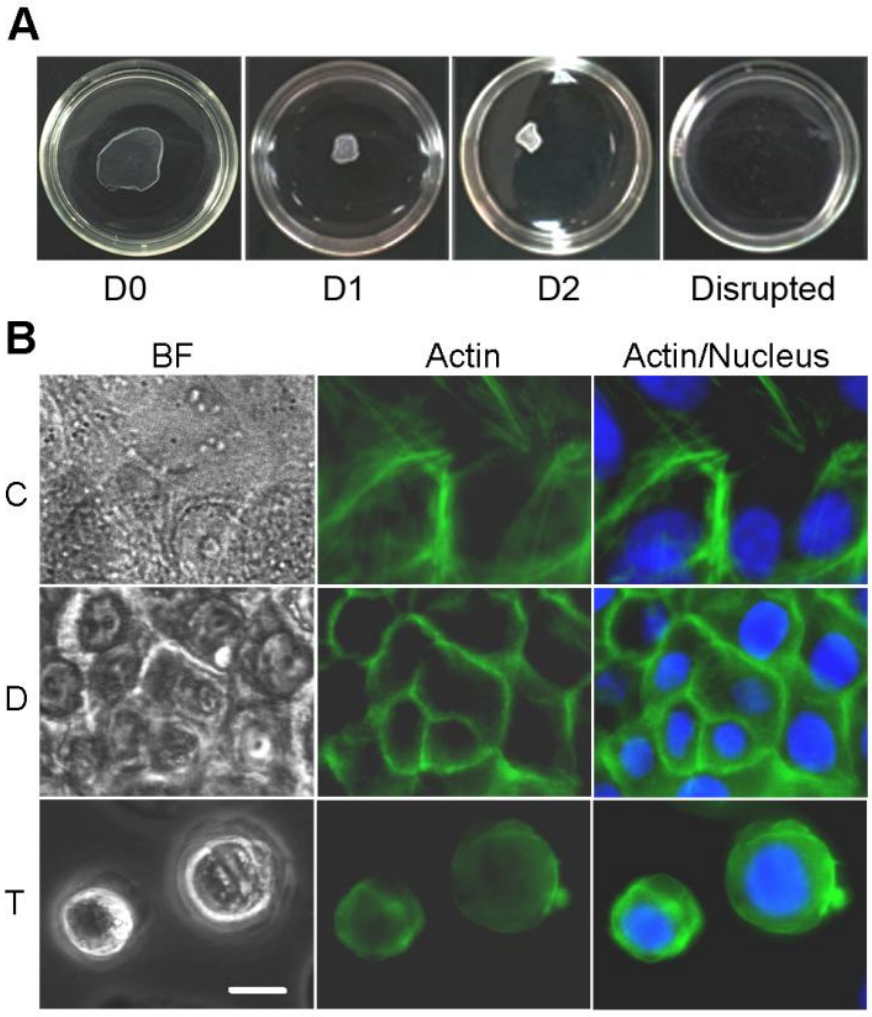

Figure 2. 1 Loss of cell-substrate and cell-cell contact results in reorganization of actin cytoskeleton.

(A) Images of dispase-lifted cell sheets at zero, one and two days post-dispase-lifting and disrupted by the mechanical shear test in 35 mm dishes. (B) Immortalized human keratinocytes were divided cells into three treatment groups: control (C), confluent cells that maintained in a cell culture dish, had both cell-cell and cell-substrate contact; dispase-lifted (D), confluent cells

that lifted as an intact cell sheet, maintained cell-cell contact but lost cell-substrate contact, and trypsinized (T), cells that trypsinized and suspended as single cells, had neither cell-cell nor cell-substrate contact. Representative images of bright field (left panels), actin stain (middle panels), and actin merged with nucleus stain (right panels) in untreated control cells (top panels), dispase-lifted cell sheet (middle panels), and trypsinized cells (bottom panels) show attenuation or loss of non-junctional stress fibers in the dispase-lifted cell sheet and loss of actin organization in the trypsinized cells. Further, cells in the dispase-lifted cell sheet shrunk in the horizontal plane upon release from the substrate. Green: actin, Blue: nucleus. Scale bar: 10 μm.

2.3.2 Cell-cell adhesion strength increases on loss of cell-substrate contact

Because dispase-lifted cell sheets maintain actin at cell-cell junctions, we next assessed whether cell-cell adhesion is affected by culturing the cell sheets in suspension. To quantify the relative cell-cell adhesion strength of the dispase-lifted cell sheets, a mechanical shearing test, adapted from similar protocols [76,130-132], was performed and the amount of time necessary to disrupt the dispase-lifted cell sheet was recorded, with increased disruption time indicating increased cell-cell adhesion strength. Cell-cell adhesion strength increased significantly from day zero to day one post dispase-lifting, but no further from one to two days post dispase-lifting. Specifically, shorter disruption times were measured from day zero sheets (immediately post dispase lifting) compared to sheets lifted and kept in suspension for one and two days post dispase-lifting ($p<0.01$, day zero versus day one; $p<0.05$, day zero versus day two, Figure 2.2A). There was no significant difference in cell-cell adhesion strength between day one and day two ($p>0.05$),

suggesting that after loss of cell-substrate contact, there is fast, but not immediate, reinforcement of cell-cell adhesion strength.

Next, we confirmed that the change in adhesion strength of the dispase-lifted cell sheets is independent of post-confluence effects. Because enhanced cell sheet strength may arise from post-confluence effects, such as overcrowding, cells grown to confluence but maintained while attached to the cell culture dish rather than dispase-lifted, to one day and two days after the typical dispase-treatment target time, were used in the same shearing test protocol. There was no difference in post-confluence cell-cell adhesion if the cells are maintained on a substrate; thus, the reinforcement is due to loss of cell-substrate adhesion and not post-confluence factors (Figure 2.2B, $p>0.05$).

Because cell sheets are capable of maintaining cohesion to at least two days after lifting from the substrate, we next examined the apoptotic rate of cells cultured in suspension, with and without cell-cell contact, compared to control cells.

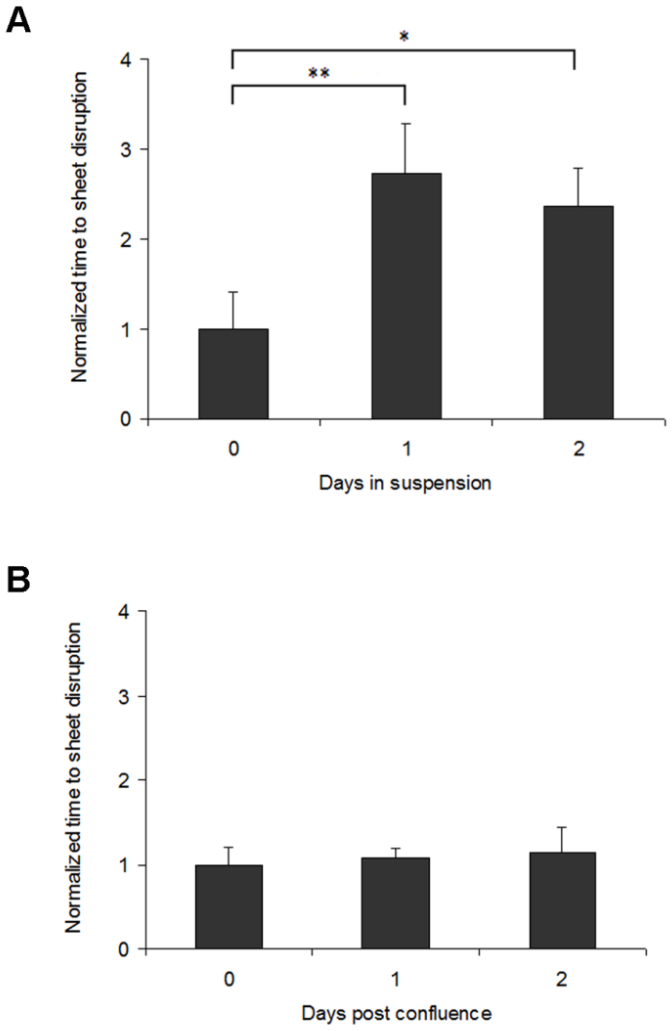

Figure 2. 2 Cell-cell adhesion strength increases on loss of cell-substrate contact.

(A) Quantification of the strength of cell sheets suspended for zero, one or two days post dispase-lifting. Cell-cell adhesion strength increases significantly from zero to one day, but not from one to two days post dispase-treatment. The y axis represents relative time to sheet disruption, i.e. sheet strength, with values normalized to the time (100%) at zero days. (B) The change in strength of the suspended cell sheets is independent of post-confluence effects. *$p<0.05$ and ** $p<0.01$ relative to the control at zero days.

2.3.3 Cell-cell contact suppresses apoptosis in the absence of substrate adhesion

Cells were assayed for apoptosis at three time points: immediately, one and two days post treatment (C0, C1 and C2 for control cells, D0, D1and D2 for cells in dispase-lifted sheet and T0, T1, and T2 for trypsinized, suspended single cells, respectively). Immediately after treatment, the number of apoptotic cells remains statistically unchanged (Figure 2.3A, apoptosis percentages: 0.65% for control at C0, 1.73% for dispase at D0, and 3.00% for trypsinization at T0, $p>0.05$). After one day post treatment, a significant percentage of trypsinized cells were apoptotic, whereas controls cells remained overwhelmingly viable (apoptosis percentages: 1.12% for control at C1, 6.40% for dispase at D1, and 48.7% for trypsinization at T1, $p<0.01$, C1 versus T1). The dispase lifted cells did not exhibit statistically significantly increased apoptosis at one day ($p>0.05$, C1 versus D1).

After two days post treatment, an even higher percentage of trypsinized cells were positive for apoptosis (Figure2. 3A, apoptosis percentages: 0.61% for control at C2, 8.17% for dispase at D2, 75.60% for trypsinization at T2, $p<0.01$, C2 versus T2). Again, the dispase lifted cells did not exhibit increased apoptosis compared to controls ($p>0.05$, C2 versus D2).

To determine whether the apoptosis is caspase-dependent, cells were treated with a general caspase inhibitor Z-VAD-FMK (ZVAD). DMSO was used as a vehicle control. Keratinocytes were grown to full confluence, and then were grouped into three conditions: controls (C); dispase-lifted (D), and trypsinized (T) of which dispase-lifted and trypsinized cells were suspended for one day, with each group consisting of untreated, DMSO-treated and ZVAD-treated cells. There were no significant differences within the three treatments of the control and dispase groups. Cells trypsinized and suspended for one day exhibited increased apoptosis

(Figure 2.3B, $p<0.005$ versus control in normal media, $p<0.001$ versus control in DMSO-supplemented media). Cells dosed with ZVAD exhibited increased apoptosis ($p<0.05$) but with only a marginal increase in the actual apoptotic rate (from 3.24 % to 15.42 %). Compared to trypsinization in normal media or in DMSO-supplemented media, ZVAD dosing significantly reduced apoptosis ($p<0.01$).

The results from trypsinization are consistent with previous work [6] indicating cells require some form of contact maintain viability. However, our data demonstrate that cells do not need to be attached to, or allowed to spread on, a substrate to remain viable, so long as there is some degree of cell-cell contact. Further, these data show that apoptosis resulting from loss of contact is mainly, but not totally, caspase-dependent. Because of previous data implicating plakoglobin as a key signaling molecule in ARVC models, we next examined the role of plakoglobin in suppressing apoptosis in the absence of cell-substrate adhesion.

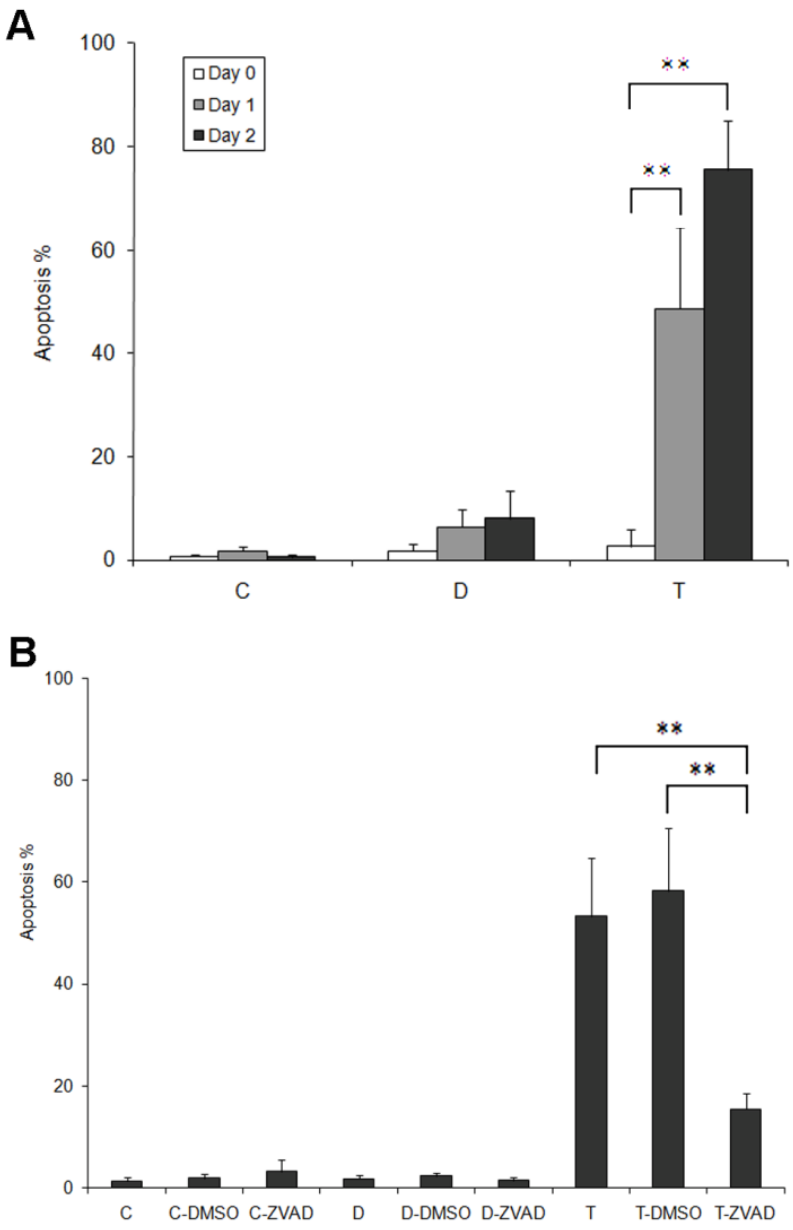

Figure 2. 3 Cell-cell contact suppresses cell death.

(A) Percentage of cells undergoing apoptosis analyzed at zero, one and two days post treatments for cells left as untreated control (C group), treated with dispase and suspended as cell sheets (D group), or trypsinized and suspended as single cells (T group). Trypsinized cells, lacking both cell-substrate and cell-cell contact, exhibited significantly increased apoptosis after one day post

treatment. (B) The general caspase inhibitor Z-VAD-FMK (ZVAD) significantly reduced apoptosis in trypsinized single cells. Keratinocytes were grouped into three broad groups: untreated controls (C group, lane 1-3), dispase-lifted and suspended as sheets for one day (D group, lane 4-6), and trypsinized and suspended as single cells for one day (T group, lane 7-9). DMSO was used as a vehicle control. ** $p<0.01$.

2.3.4 Plakoglobin translocates to cytoplasm and nucleus after loss of cell–cell contact

Plakoglobin is thought to play a major role in various signaling and structural processes including cardiac and skin cohesion, tumor metastasis and the Wnt-catenin regulatory pathway. To examine the localization of plakoglobin in cells in our three treatment groups (control, dispase-lifted and trypsinized), we performed immunofluorescence staining immediately upon treatment (zero days) and at 24 hours post treatment (one day). Control (untreated) cells exhibited primarily junctional localization of plakoglobin (Figure 2.4A). Dispase-lifting did not appear to significantly affect plakoglobin distribution. In contrast, trypsinized cells clearly exhibited diminished plakoglobin localization at the cell boundary and increased localization of plakoglobin in the cell cytoplasm, suggesting loss of junctional plakoglobin.

The percentage of plakoglobin overlapping the nuclei were quantified from the confocal immunofluorescence images (Figure 2.4B, percentages of PG in nuclei: 22.8% for C0, 21.8% for D0, 24.6% for D1, 19.9% for T0, and 52.1% for T1). There was substantially more plakoglobin overlapping the nuclei in cells trypsinized and suspended for one day ($p<0.01$ for C0 versus T1, $p<0.01$ for T0 versus T1).

CellTracker Green, a cell-permeant, nonspecific fluorescent dye, was used to confirm the nuclear translocation of plakoglobin (Figure 2. S1A). Similar quantification analysis indicated that there were no significant differences for the amount of CellTracker Green in nucleus within the five groups (Figure S1B). Thus, this result demonstrates that plakoglobin, but not CellTracker Green, translocates to nucleus after loss of cell-cell contact.

Western blot analysis shows expression level of plakoglobin in dispase-lifted cell sheets increase significantly from zero to one day post dispase-lifting, but decreases again from one to two days (Figure 2.4C). Increase in plakoglobin expression above baseline likely correlates to the increase in cell-cell adhesion (Figure 2.2A), but apparently a limit is reached so that the decrease in plakoglobin from days one to two is not significantly associated with a decrease in cell-cell adhesion.

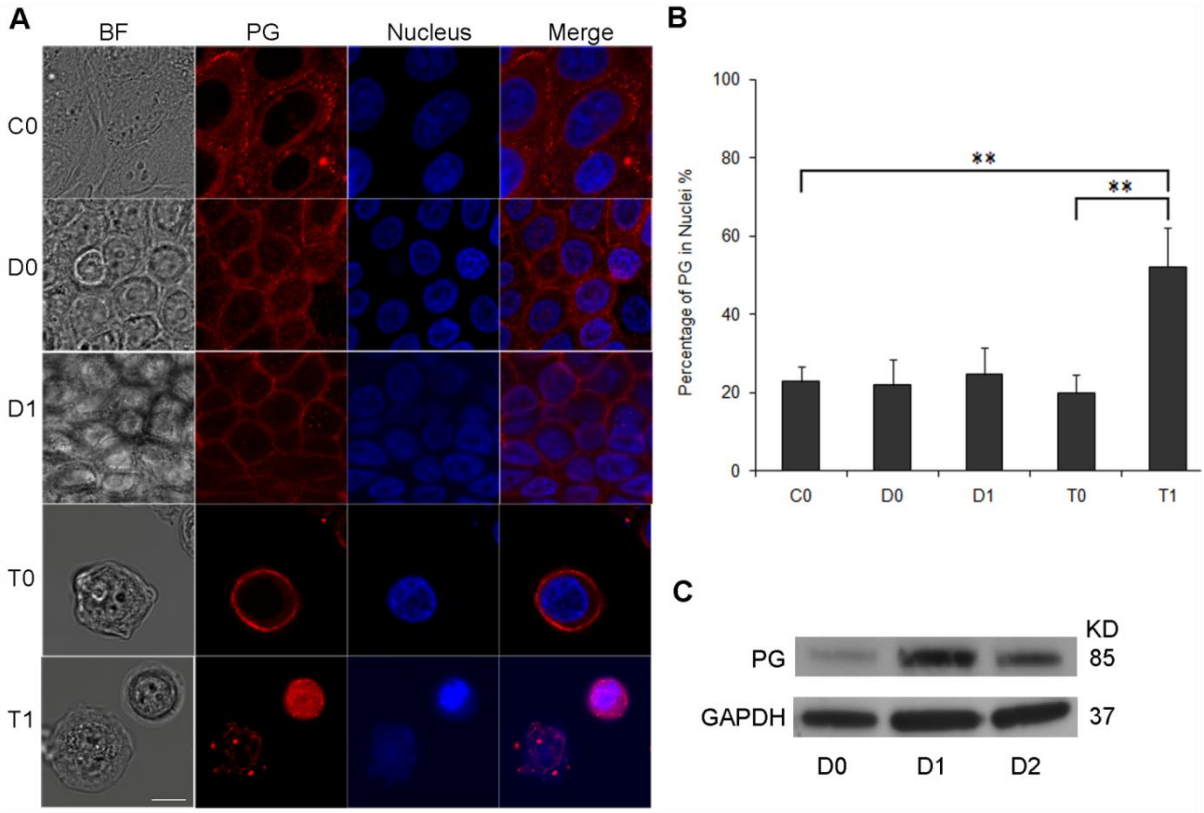

Figure 2. 4 Plakoglobin translocates to the cytoplasm and nucleus after loss of cell–cell contact.

(A) Plakoglobin localization was assessed using confocal fluorescence microscopy. Keratinocytes were either untreated (C0), treated with dispase and suspended as cell sheet for zero or one days (D0 and D1) or trypsinized and suspended as single cells for zero or one day (T0 and T1). Shown are images of bright field (left panels), plakoglobin stain (second left panels), nuclear stain (second right panels) and plakoglobin merged with nuclear stain (right panels) in untreated control cells (top row), dispase-lifted cell sheet (second and third rows), and trypsinized cells (fourth and fifth rows). Plakoglobin was shown predominantly localized to cell junctions in control cells (C0) and the floating cell sheets (D0 and D1). In contrast, plakoglobin exhibited a more diffuse localization into the cytoplasm once cell-cell adhesion was lost (T0), and translocated significantly into the nuclei at one day post trypsinization (T1). Red: plakoglobin (PG), Blue: nucleus. Scale bar: 5 μm. (B) Quantification of the percentage of plakoglobin in nuclei, showing elevated nuclear plakoglobin in cells trypsinized for one day. ** $p<0.01$. (C) Western blot analysis of dispase-lifted and suspended cell sheets shows plakoglobin level increases significantly from zero to one day post dispase-lifting, but not from one to two days post dispase-lifting. GAPDH was used as a loading control.

2.3.5 Suppression of plakoglobin inhibits apoptosis in trypsinized cells

To determine whether plakoglobin plays a role in the apoptotic pathway, RNA interference was used to suppress plakoglobin expression. Immunofluorescence images of plakoglobin knockdown four days after siRNA transfection demonstrated diminished plakoglobin expression throughout the cell (Figures 2.5A and 2.5B, $p<0.005$); transfection with the negative control

vector showed no significant difference ($p>0.05$). The strength of the cell sheet transfected with siRNA against plakoglobin decreased significantly compared to the untransfected control (Figure 2.5C, $p<0.01$); transfection with the negative control vector showed no significant difference ($p>0.05$), which correlates well with the changes of plakoglobin level shown in Figure 2.5A and 2.5B.

To determine whether plakoglobin is involved in the apoptotic pathway, cells were transiently transfected with siRNA against plakoglobin or a negative control vector. A CMV-driven plakoglobin vector was used to restore plakoglobin expression. Western blot analysis (Figure 2.5D and 2.5E) four days post transfection shows a decrease in plakoglobin level with siRNA transfection and a slight increase in plakoglobin level with plakoglobin overexpression. Relative plakoglobin level was normalized to untreated control set as 100%, with 30.7% for plakoglobin siRNA knockdown ($p<0.001$). The relative plakoglobin level in the cells transfected with the negative control siRNA (102.3%) was similar to the untreated control ($p>0.05$). Transfection with CMV-driven plakoglobin led to an increase in plakoglobin level (111.0% for CMV-driven plakoglobin alone, 117.3% for CMV-driven plakoglobin vector and negative control vector co-transfection, $p>0.05$ versus untreated control for both cases). Co-transfection with siRNA for plakoglobin and the CMV-driven plakoglobin vector resulted in a significant increase in plakoglobin level compared to transfection with siRNA alone (63.8% for CMV-driven plakoglobin and plakoglobin siRNA co-transfection, $p<0.01$ versus untreated plakoglobin siRNA alone). However, co-transfection still exhibited decreased plakoglobin level compared to untreated controls ($p<0.01$), likely due to the overpowering nature of the siRNA.

Next, we assessed the effects of plakoglobin on the apoptotic rate of cells transfected with siRNA for plakoglobin, the negative control vector, the CMV-driven plakoglobin vector, or

combinations thereof. Cells were trypsinized four days post transfection, then suspended for an additional day. As shown in Figure 5F, there was a significant decrease in the percentage of cells undergoing apoptosis in the cells suppressing plakoglobin, suggesting that even partial inhibition of plakoglobin is sufficient to rescue approximately half the cells (48.2% apoptosis for untreated control, 24.3% apoptosis for plakoglobin siRNA knockdown, $p<0.0005$). The percentage of cells undergoing apoptosis in the cells transfected with the negative control siRNA (45.2%) was similar to the untreated control ($p>0.05$). Transfection with CMV-driven plakoglobin led to a marginal increase in cell death (61.1% apoptosis for CMV-driven plakoglobin alone, 60.6% apoptosis for CMV-driven plakoglobin vector and negative control vector co-transfection, $p>0.05$ versus untreated control for both cases). Co-transfection with siRNA for plakoglobin and the CMV-driven plakoglobin vector resulted in a significant increase in apoptosis rate compared to transfection with siRNA alone (36.2% apoptosis for CMV-driven plakoglobin and plakoglobin siRNA co-transfection, $p<0.05$ versus untreated plakoglobin siRNA alone). However, co-transfection still exhibited decreased apoptotic rate compared to untreated controls ($p<0.05$), likely due to the overpowering nature of the siRNA. The changes in apoptosis rate are well correlated with the relative expression level of plakoglobin showed in Figure 2.5D and 2.E. These apoptosis experiments were repeated with a second siRNA against plakoglobin, with similar results.

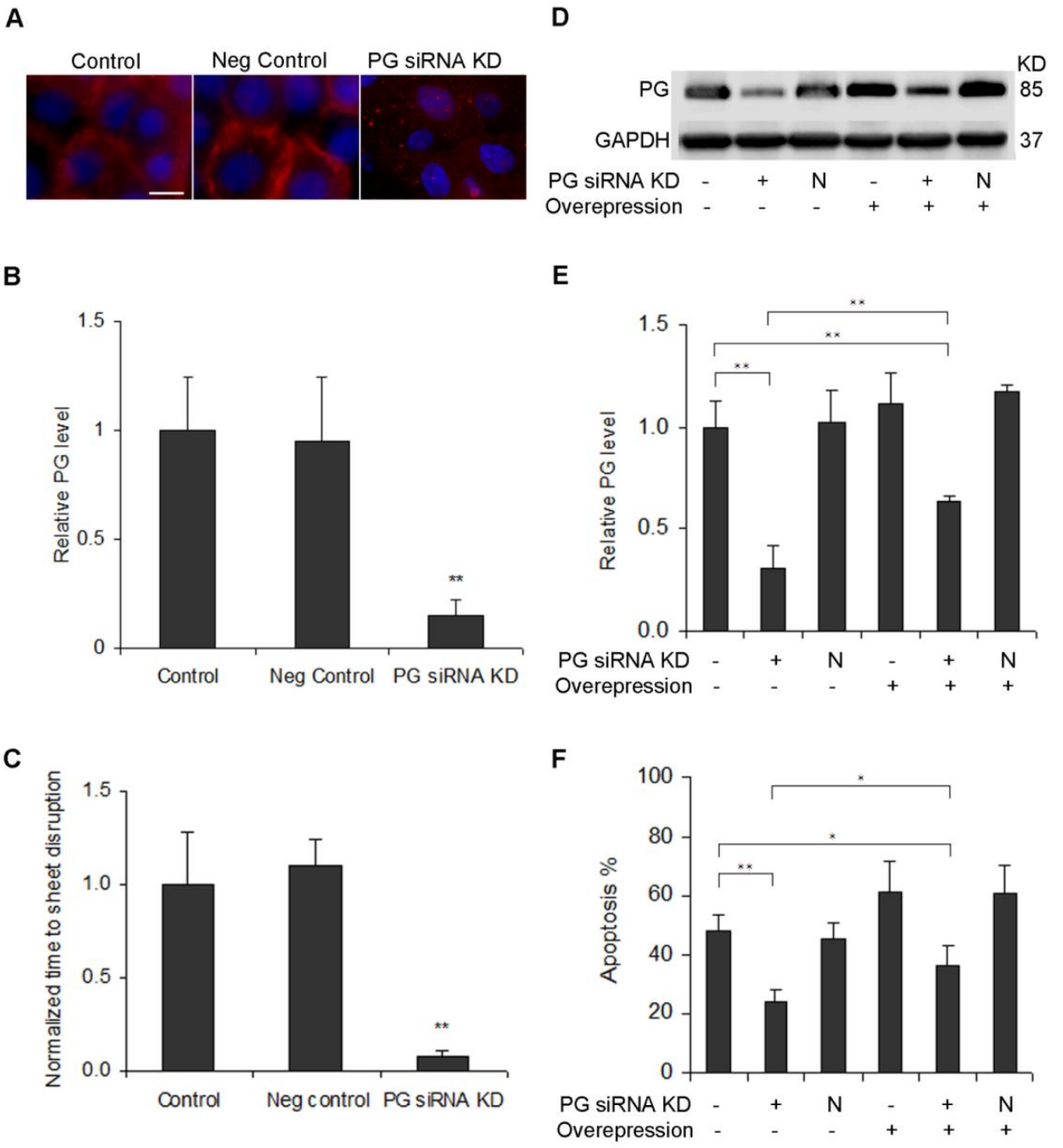

Figure 2. 5 Plakoglobin is a key regulator of the apoptotic pathway.

(A) Immunofluorescent images of untreated control (left) and plakoglobin knockdown four days after transfection with siRNA (right). Green: plakoglobin, Red: Nucleus. Scale bar: 10 um. (B) Quantification of relative plakoglobin levels based on fluorescence images. The y axis represents

relative plakoglobin intensity, with values normalized to the untreated control. (C) Quantification of the strength of cell sheet transfected with siRNA for plakoglobin (PG siRNA KD) and a negative control (Neg control). Cell sheets were dispase-lifted four days after transfection. The y axis represents relative time to sheet disruption, i.e. sheet strength, with values normalized to the untreated control. (D) Western blot analysis of plakoglobin four days after transfection with or without siRNA for plakoglobin (PG siRNA KD), a negative control (N), or plakoglobin overexpression (Overexpression). GAPDH was used as a loading control. (E) Quantification of relative plakoglobin level in each western blot lane. The y axis represents relative plakoglobin intensity, with values normalized to the untreated control. (F) Apoptosis rate of cells transfected with siRNA for plakoglobin, negative control (N), or plakoglobin overexpression vector. Cells were trypsinized four days after transfection, and then suspended for one day, after which the TUNEL assay was performed. * $p < 0.05$ and ** $p < 0.01$.

2.4 Discussion

Cell apoptosis is induced by trypsinization, but not dispase-lifting, suggesting that cell-substrate interactions, and spreading of cells, are not the ultimate regulators of cell viability. Further, cohesive cell sheets lacking adhesive substrates maintain or reinforce the junctional localization of actin and plakoglobin. Suppression of endogenous plakoglobin protected cells from trypsinization-induced apoptosis, suggesting that plakoglobin deficiency reduces cell susceptibility to apoptosis.

Cell-matrix interactions have been widely used as a standard model system for studying cellular adhesion. Cell attachment and spreading on the extracellular matrix (ECM) through integrins and focal adhesions were found to govern cell vitality [6,133-135]. We show that in the absence of cell-ECM/substrate interactions and active spreading, intercellular junctions become a major control mechanism. One possible reason that cell junctions are so important is that junctions are vital information processing centers where clustered molecules can exchange biochemical and mechanical information among adjacent cells. When those regulatory and signaling molecules connect and communicate along the integrated adhesion site-cytoskeleton networks, individual cells may contribute to tissue-wide decision-making by becoming part of a 'global' network, even if there is no ECM.

Most, if not all, adhesion sites likely contribute to cell regulation. Provided that properly organized cytoskeleton networks form and are anchored at adhesion sites, either cell-ECM adhesion or cell-cell adhesion is sufficient to maintain cell viability. Isolated cells resulting from trypsinization and cells that were allowed to attach, but prohibited from spreading via micropatterned islands [6], induced apoptosis. In both cases, cell spreading is highly restricted or

nonexistent, and the cytoskeleton is likely disorganized, which render the cell vulnerable. In the case of the dispase-lifted cell sheet, cell spreading is also highly restricted, and a significant part of the internal cytoskeleton is disrupted, but the death rate is extremely low. Thus, we suggest that it is not cell spreading itself, but organized adhesion site-cytoskeleton organization that controls cell life and death.

There is emerging evidence that plakoglobin may participate in the Wnt/LEF/TCF signaling pathway [65,136,137]. Plakoglobin has the capacity to translocate to the nucleus and regulate Wnt signaling by competing with β-catenin, affecting β--catenin localization, accumulation and/or function [66,138]. Given the relative ubiquity of plakoglobin in a broad variety of tissues, it is likely that our conclusion that cell junctions are key to cell fate regulation can be generalized to all contacting cells in multicellular organisms, with perhaps different junctional proteins participating in those tissues lacking plakoglobin. Indeed, it is possible that other junctional proteins, including other desmosomal proteins, may participate in similar, perhaps overlapping, regulatory pathways. We note that this study focuses on keratinocytes, but since keratinocytes are normally adherent, our results are likely general, and we have preliminary evidence that other cell types exhibit similar behavior. Additionally, other studies are consistent with these results.

Almost all tumor cells originate in the epithelium and metastasize as single cells [139]. The vast majority of tumor cells that make their way into bloodstream die off quickly, usually within a few hours of leaving the tumor [139]. Expression levels of plakoglobin is often reduced or absent in invasive cancer cells [140-145], which likely result in weakened cell-cell adhesion and enhanced migratory capacity [10,131]. However, we show here that plakoglobin may have a more vital role – cells that detach and enter the bloodstream with reduced plakoglobin may be

protected from apoptotic effects, and thus lead to enhanced metastatic capabilities. Our findings could provide an additional mechanism underlying the poorer prognosis associated with tumors expressing diminished plakoglobin [146-149].

Many adhesion defect diseases, such as pemphigus vulgaris (PV) and arrhythmogenic right ventricular cardiomyopathy (ARVC) are thought to be caused in part by alterations in cell junctions. The mechanisms behind these diseases are a source of active investigation but may rely on the fact that diminished cell-cell adhesion leads to increased susceptibility of cell separation, leading to altered junctional protein localization and possibly the engagement of apoptotic pathways. For example, models of ARVC have been shown to exhibit nuclear plakoglobin localization, increased apoptosis and altered cell-cell adhesion [63,76]. Thus we show here a unifying mechanism for this class of disease, which may eventually be expanded to include muscular dystrophy and other adhesion defect conditions.

Tissue formation depends critically on the ability of cells to form specific contacts with each other [8]. During development, cell-cell interactions are likely far more important than cell-substrate interactions, given the relatively isolated environment of the embryo. In fact, culturing stem cells to induce specific differentiation sometimes requires using a hanging drop method, both to eliminate a hard adhesive substrate and to provide a more three-dimensional environment for differentiation [150]. Understanding the mechanism underlying cell-cell interactions is vital, but difficult, due to the intricacies working with suspended cell masses. Our study represents an important first step towards explaining how cells communicate in a more realistic environment compared to the commonly used *in vitro* tools. As such, this approach may be a useful supplement to the growing work in developing three-dimensional scaffolds using novel materials.

This study demonstrates that cell junctions are a fundamental control mechanism in governing cell life and that junctional protein plakoglobin is a key regulator of this process. These findings could have significant implications for understanding cell adhesion, modeling disease progression, developing therapeutics and improving the viability of tissue engineering protocols. Furthermore, this study laid the groundwork for future characterization and manipulation of viable cell sheets for cell sheet engineering purpose. The recent development of cell-sheet tissue engineering has generated a need for a systematic characterization of cell-cell interactions in cell sheets to better mimic and condition them for *in vivo* applications. Though promising, the technique is currently limited by the fragility and shrinkage of the sheets as well as the lack of information regarding the characteristics of such sheets [151]. Direct experimental methods for understanding and improving the cell sheets' biomechanical properties, such as cell-cell adhesion, mechanotransduction, and other baseline cellular properties are essential for further development of these sheet constructs. However, comprehensive *in vitro* experimental data are still lacking due to lack of suitable experimental methods. Our enzyme-based cell sheet lifting method offers a novel way to study cell junctions when substrate interactions are no longer dominant, enable us to further develop and apply novel *in vitro* method for characterizing how junctional proteins may modulate cellular responses, such as cell sheet biomechanics and tissue integrity, which are currently not well-studied but critical for future clinical applications.

2.5 Supplemental figure

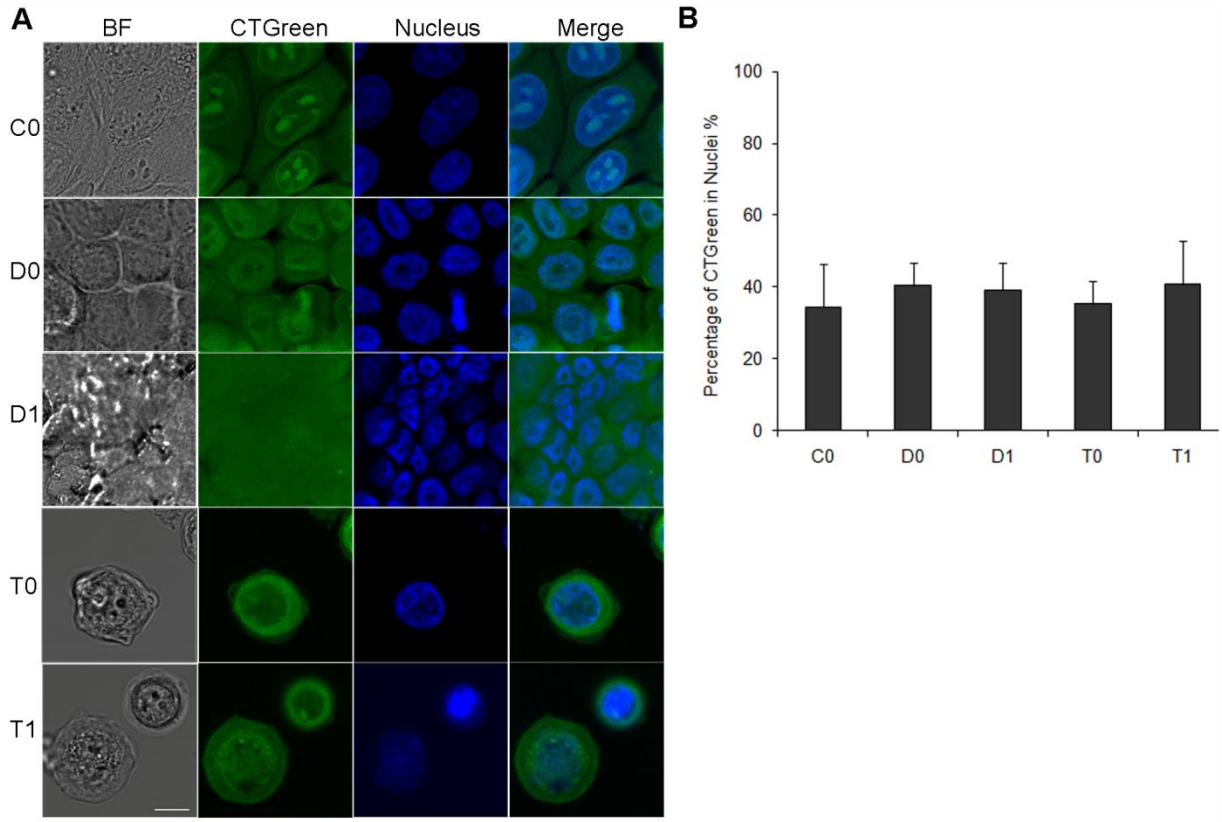

Figure 2. 6 Supplement Figure S1. CellTracker Green doesn't translocate to the cytoplasm and nucleus after loss of cell–cell contact. (A) CellTracker Green (CTGreen) localization was assessed using confocal fluorescence microscopy. Keratinocytes were either untreated (C0), treated with dispase and suspended as cell sheet for zero or one days (D0 and D1) or trypsinized and suspended as single cells for zero or one day (T0 and T1). Shown are images of bright field (left panels), CTGreen stain (second left panels), nuclear stain (second right panels) and CTGreen merged with nuclear stain (right panels) in control cells (top row), dispase-lifted cell sheet (second and third rows), and trypsinized cells (fourth and fifth rows). Green: CTGreen, Blue: nucleus. Scale bar: 5 μm. (B) Quantification of the percentage of CTGreen in nuclei, showing no significant difference of CTGreen location within the groups.

Chapter 3 Characterization of partially-lifted keratinocyte cell sheets

3.1 Introduction

The recent development of cell-sheet tissue engineering has generated a need for a systematic characterization of cell-cell interactions in cell sheets to better mimic and condition them for *in vivo* applications. Rather than using conventional three-dimensional scaffolds for tissue reconstruction, an approach using thermo-responsive polymeric surfaces that facilitate the non-invasive harvest of cultured cells as intact tissue sheets was developed [37]. Such cell sheets have been generated for a wide variety of laminar tissues, such as skin, heart, corneal and renal components [84,104,105]. Additionally, cell sheet tissue engineering bears a striking resemblance to the embryonic cell sheet building machinery. In early development, the rearrangement and deformation of the substrate-free cell sheet in blastoderm and later in blastopore involves a series of precisely orchestrated morphogenetic episodes [119,152]. The parallels between tissue morphogenesis and tissue engineering suggest that force homeostasis across cell-cell junctions not only govern blastoderm and blastopore formation, but also may play crucial roles in regulating mechanical strength of the cell sheet constructs for tissue engineering purposes.

Currently, cell sheets are fragile and are typically handled by external supports [151]. Direct experimental methods for understanding and improving the sheets' biomechanical properties, such as cell-cell adhesion, mechanotransduction, and other baseline cellular properties are essential for further development of these sheet constructs. However, comprehensive *in vitro* experimental data are still lacking due to lack of suitable experimental methods. First, research in cell sheet engineering primarily focuses on biological or chemical

cues; comparatively little is known about mechanical cues. In particular, how mechanical cues may regulate, or be regulated by, the cytoskeleton remain incompletely resolved. Since components such as actin are responsible for certain mechanoresponses as well as for cell processes such as migration, contraction and adhesion, it is imperative that their role be examined in more detail [12,33,153-157]. Second, most studies are done in adherent cells which may primarily maintain cell-substrate interactions and as a result, likely introduce mixed responses into the readouts. Thus, the roles of key junctional proteins in desmosomes, adherens junctions, etc. are not well-characterized. However, recent studies have demonstrated that such junctional proteins regulate a variety of processes such as viability and migration [10,11,158]. Third, most cell sheets are generated for immediate use and not conditioning - without supporting scaffolds, these sheets are too fragile to endure *in vitro* handling or significant manipulation. Further, when no external support was used, the detached cell sheets size can shrink by 90%, which significantly impairs the sheet's ability to provide sufficient coverage in the tissues being repaired [151]. Therefore, it is desirable to develop a novel method to generate mechanically conditioned and unshrunk substrate-free, scaffold-free cell sheets. A recent study on characterizing the mechanics of cultured cell monolayers has begun to shed light on this topic [43]. Despite this excellent work, our knowledge of underlying mechanisms regarding how cell-cell junctions and cytoskeleton regulate cell sheet mechanical properties, and more importantly, the capability to mechanically condition the cell sheet for tissue engineering purposes remain poor.

The viability study in Chapter 2 laid the groundwork for future characterization and manipulation of viable cell sheets for cell sheet engineering purpose. Our enzyme-based cell sheet lifting method offers a novel way to study cell junctions when substrate interactions are no

longer dominant, enable us to further develop novel *in vitro* method for characterizing how junctional proteins may modulate cellular responses, such as cell sheet biomechanics and tissue integrity, which are currently not well-studied but critical for future applications. To address two of the major challenges in current cell sheet engineering constructs, fragility and shrinkage, it is desirable to develop a method to generate mechanically strong and unshrunk substrate-free, scaffold-free cell sheets. In this study we developed a novel method to generate partially-lifted cell sheets which can be manipulated in a way similar to adherent cells. This simple yet powerful tool enables us to investigate the effects of mechanical conditioning on cell sheet properties, and permits direct comparison of physiological parameters between lifted cells and their adherent controls, side-by-side. We hypothesized that lifted cells would exhibit changes to the distribution of cytoskeletal and junctional proteins, with reinforcement occurring at cell-cell contacts via mechanotransduction. We further hypothesized that mechanical conditioning would enhance such reinforcement, as well as lead to greater cohesion in the lifted cells. To test this hypothesis, we characterized cellular actin and junctional reinforcement, and evaluated cell sheet strength and cohesion, to assess changes in cell properties when cell-cell interactions dominate. We found that our hypotheses are generally supported, but that there is a limit to reinforcement via mechanical conditioning.

Keratinocytes were chosen for this study in part due to the ease with which they can be manipulated, existing interest in keratinocyte cell sheet cohesion for dermal tissue engineering and in part because they exhibit strong cell-cell interactions, including desmosomes. These results represent a first systematic examination of mechanical conditioning on cells with primarily intercellular interactions. These findings suggest that cytoskeleton and tightly associated intercellular junctions may be crucial for unlocking the potentials for cell sheet

engineering, which has emerged as a promising approach to reconstructing various types of laminar tissues, such as skin, myocardium, cornea, and vascular systems, etc. without using any biodegradable materials [159-161]. Of particular interest is cardiac sheet engineering. Due to existing similar junctional structures between epidermal and cardiac tissues and strong interest in characterizing cell sheet properties for cardiac sheet engineering, this study also provide a solid foundation for extend partial-lifting technique to cardiac sheet engineering.

3.2 Methods

3.2.1 Cell culture

Immortalized human keratinocytes (N/TERT-1) were maintained as described elsewhere [11,126]. Briefly, cells were seeded on 0.005" thick silicone sheeting (SMI, Saginaw, MI) in a 100 mm diameter custom-made stretch device chamber, expanded and propagated in keratinocyte serum-free media (abbreviated ker-sfm, media and supplements from Invitrogen, Carlsbad, CA, unless otherwise stated), supplemented with rEGF (0.2 ng/mL) and BPE (25 μg/mL), $CaCl_2$ (0.4mM, Sigma, St. Louis, MO), and penicillin/streptomycin. To grow cells to high confluence, cells were switched to a medium consisting of a 1:1 mixture of ker-sfm and a medium DF-K, the latter consisting of a 1:1 mixture of DMEM and Ham's F-12, supplemented with rEGF (0.2 ng/mL) and BPE (25 μg/mLl), L-glutamine (1.5 mM) and penicillin/streptomycin.

3.2.2 Antibodies and reagents

Unless otherwise noted, reagents were purchased from Invitrogen/Life Technologies (Carlsbad, CA). Primary mouse monoclonal antibodies anti-plakoglobin (γ-Catenin) and anti-GAPDH (Novus Biologicals) were used for immunoblotting at 1:1000 dilutions. Immunofluorescence staining was performed using the monoclonal anti-plakoglobin anti-β-tubulin (Sigma, St. Louis, MO), anti-pan Cytokeratin, antibody (PCK-26, Sigma) and monoclonal Anti-Keratin 5/8 antibody (C50, sc-8021, Santa Cruz Biotechnology), monoclonal anti-Keratin 14 antibody (LL001, sc-53253, Santa Cruz Biotechnology) antibodies as the primary and Alexa Fluor 594 goat anti-mouse IgG as the secondary antibody (all at 1:1000 dilutions). Alexa Fluor 488 conjugated phalloidin at a concentration of 0.5 μg/mL in HBSS was used for actin staining. Hoechst was used at a concentration of 0.5 μg/mL for nuclear staining. All staining was

performed for 1 hour at 37℃.For cytoskeleton toxin disruption, Cytochalasin D (cytoD, Sigma) was used to disrupt actin at 3 μM for 1 hour at 37℃, and Y-27632 was used to inhibit ROCK at 10 μM for 1 hour at 37℃ right after sheet lifting. Nocodazole (noco, Sigma) was used to disrupt the microtubules at 10 μM for 1 hour at 37℃. Acrylamide (acryl, Sigma) was used to disrupt keratin filaments at 10 mM for 4 hours at 37℃.

3.2.3 Fluorescence microscopy

Cells were fixed in 4% paraformaldehyde (Sigma) and then permeabilized with 0.1% triton-X-100 (Sigma). For plakoglobin-nucleus co-staining, cells were incubated in the monoclonal anti-plakoglobin primary antibody and Hoechst together for an hour at 37℃, followed by PBS washes and then a secondary antibody incubation for another hour, washed again and then imaged. For actin-nucleus co-staining, cells were incubated in the phalloidin and Hoechst together for an hour at 37℃, followed by PBS washes and then imaged. For plakoglobin-actin-nucleus triple-staining, cells were incubated in the monoclonal anti-plakoglobin primary antibody, the phalloidin and Hoechst together for an hour at 37℃, followed by PBS washes and then a secondary antibody incubation for another hour, washed again and then imaged. Microscopy was performed at room temperature using an Olympus FV10 Confocal microscope, an Olympus OPLFLN 40X O NA 1.3 objective lens, and Olympus FV10-ABW Software. Images were processed using ImageJ (version 1.43u for Windows; National Institutes of Health) and Photoshop (Adobe) to prepare the final figures [127-129]. Imaging conditions were taken identical and analyses were done in the raw fluorescence images. Images were brightness/contrast enhanced and fluorescent colors were added for clarity. Relative actin or plakoglobin intensities were quantified by ImageJ, with values normalized to untreated control (i.e. unstretched, unlifted cells) signals. The percentage of actin or plakoglobin signal at the

junctions was calculated as signal intensity at the junctions divided by the total signal intensity of the whole cells [74,76].

3.2.4 Dispase-based partial-lift method

Cells grown to full confluence were treated with dispase at a concentration of 2.4 units/mL in Hanks Buffered Saline Solution inside the custom-made PDMS mold (with inner diameter 10 mm), and incubated at 37 ℃ for 20 minutes or until the monolayer lifted from the chamber as an intact sheet. Cells outside the PDMS mold remained adhered to the substrate. Thus, this plating is considered a partially-lifted culture, where the cells within the PDMS mold form a lifted cell sheet that was dissociated from the substrate but were attached at the periphery to cells that remain plated.

3.2.5 Cell viability assay

Cell viability was assessed using a Live-Dead staining assay[162]. Briefly, for nuclear staining, Hoechst (0.5 μg/mL) and Propidium Iodide (2 μg/mL) were added to cells. After staining for 5 minutes at 37 ℃, cells were washed with HBSS and examined under the microscope immediately. Death rate is calculated as the ratio of positive Propidium Iodide over Hoechst stained nuclei. Viability rate is calculated as 1-Death Rate.

3.2.5 Cyclic stretch and mechanical tests

Partially lifted cell sheets were subjected to equiaxial cyclic stretch for 4hr at 5% strain and 1 Hz before staining using a custom equiaxial stretching device (with uniform strain fields, as previously described [163]) maintained in a cell culture incubator. Tensile test assays were performed using an Instron ElectroPlus E1000 All-Electric Test Instrument (Instron, Norwood, MA). Briefly, a 2cm-wide and 10cm long strip of the membrane containing both adherent and

lifted cells was cut off and then immediately mounted to the test instrument. The mounted membrane was stretched at a speed of 1 mm per second and the maximum sheet strain before failure was measured. Strain was calculated as the ratio of the change in length to the original length ($e=\Delta L/L_0$). A previously-established shear test protocol was performed to test cell sheet cohesion, and thus cell-cell adhesive strength [11,76,131,164]. A second custom equiaxial stretch apparatus, referred to as the microscope stage-top stretch apparatus, was used for simultaneous stretching and imaging. This device consisted of a moving plate that is moved vertically by a microactuator against a ring-shaped piston that generates uniform strain on the membrane. A microscope objective can fit within the piston to image the membrane, and this device was used to measure strains of the cell sheets, and to verify that cells in the lifted regions were subject to the same strain as cells that remain attached. Nuclei were labeled using a Hoechst stain and imaged during stretch. Nuclei centroids were tracked in multiple fields of view and their coordinate positions were determined using an automated particle-tracking Matlab program as previously described [165,166]. The paired lengths between multiple randomly picked nuclei in the stretched versus unstretched represented the same field were measured.

3.2.6 siRNA knockdown

Silencer® Pre-designed siRNA for plakoglobin (5’-3’: GGGCAUCAUGGAGGAGGAUtt), a negative control siRNA (Invitrogen) were used assess the effects of plakoglobin knockdown on cell sheet cohesion. Additionally, two Silencer Pre-designed siRNA for keratin 5 (5’-3’: GCAUGUCUCUGACACCUCAtt; GGAGAGUAGUCUAGACCAAtt), two Silencer Pre-designed siRNA for keratin 14 (5’-3’: GCCGAGGAAUGGUUCUUCAtt; GGACAUGGAUGUGCACGAUtt), and a negative control siRNA (Invitrogen) were used to assess the effects of keratin 5 and keratin 14 knockdown on cell sheet contraction and cell sheet

cohesion. Cells were transfected using Lipofectamine 2000 (Invitrogen), according to the manufacturer's instructions. Cells were harvested and analyzed four days after transfection.

3.2.7 Immunoblotting

Total protein concentration was determined by Bradford assay (Sigma). Soluble fractions containing equal amounts of total protein were separated using SDS polyacrylamide gel electrophoresis and transferred onto PVDF membranes (Millipore, Billerica, MA). Immunoblotting was performed using mouse anti-human antibodies at the following dilutions: anti-Plakoglobin 1:2000, anti-GAPDH 1:1,000, and horseradish peroxidase conjugated goat anti-mouse secondary antibody 1:1,000. Blots were developed with ECL reagents (Perkin Elmer, Waltham, MA) and imaged using a FUJI imaging unit (Fujifilm, Stamford, CT). Relative plakoglobin intensity in immunoblotting images was quantified by ImageJ, with values normalized to GAPDH of each matching blot lane and the signal of the untreated control.

3.2.8 Statistical analysis

Data are expressed as mean $\pm$ SD and analyzed by ANOVA. A value of $p < 0.05$ was considered significant, with each group having sample sizes $n \geq 3$.

3.3 Results

3.3.1 Generation of partially-lifted cell sheets

To examine and manipulate cell sheets that have minimal or no interaction with substrates, we developed a method to generate partially-lifted cell sheets. Table 3.1 summarized the partial-lift techniques explored for this study. Confluent human keratinocyte monolayers plated on a flexible silicone membrane were lifted by dispase inside a PDMS mold gently placed atop part of the culture area. Cells outside, and under, the PDMS mold remained attached to the membrane (Figure 3.1A). The lifted cell region inside the mold thus consisted of a cell sheet that engaged mostly cell-cell interactions, yet was available for immunofluorescence staining and microscopy, and importantly, could be mechanically conditioned due to their attachment to cells that remain attached to the substrate. To confirm effectiveness of the PDMS mold in making an un-leaking well and determine whether cells in the lifted region were no longer significantly interacting with the substrate, a nucleus stain was first performed across the whole monolayer, followed by partial lift with dispase and actin stain with phalloidin inside the mold. Only cells inside the PDMS mold, i.e. lifted cells, were stained with phalloidin, the cells under and outside the mold remain un-stained. This result confirmed that the PDMS mold has the ability to contain the dispase and/or phalloidin within the mold and the attached cells under PDMS were not torn off. Cells in the lifted region displayed a morphology consistent with fully detached cell sheets, exhibiting actin primarily at cell-cell junctions (Figure 3.1B) [12]. The attached cells (top half) of the nucleus stain image is a little out of plane, further confirms that the attached cells under PDMS were not torn off, and suggests the detachment of cells inside the well (bottom half). To further microscopically verify the detachment of the cells inside the PDMS mold, about 75% of the perimeter of the lifted region was purposely cut open along the PDMS mold border. The

lifted region was clearly not attached to the substrate as it was easily shifted around and significantly contracted overtime, unlike the regions that remained attached.

To verify that cells in the lifted regions were subject to the same strain as the controls, we used a custom-made microscope stage-top stretch apparatus which is capable of simultaneous stretching and imaging. The partially lifted sheets were imaged, stretched to 9% and imaged again. Nuclear centroids were tracked and their coordinate positions were determined using a Matlab program. The changes in lengths between nuclei, normalized to the baseline lengths (i.e., the strains) were measured. The representative images showed measurements of changes in length between three randomly picked nuclei. No significant differences between the lifted sheets (8.5% ± 1.1%) and controls (8.8% ± 1.4%) were observed ($p>0.05$, $n=3$, Figure 3.1C). Other strains (from 0% to 12%) displayed similar results (higher strain data was presented as differences are likely to be clearer at higher strains).

To ensure that neither lifting, nor the application of cyclic stretch would lead to cell death, viability assays were applied to cells under four conditions: lifted or attached, and following cyclic stretch or unstretched. Cyclic mechanical stretch was performed using an equiaxial stretch device for 4 hr at 5% strain and 1 Hz. Cells were effectively 100% viable, with no significant differences among the four tested conditions (Figure 3.1D). A viability test was also done on cells located under the PDMS mold with similar results, indicating that the application of the mold did not significantly damage the cells underneath it.

Table 3. 1Development and evaluation of partial lift techniques for keratinocyte sheet

Technique	Method	Results& Comments
Partial lift: Inside PDMS ***	A small PDMS mold is placed on top of the large cell monolayer; dispase is then added inside the mold	Pros: Only sheet inside PDMS lifted Cons: PDMS mold may slide and damage monolayer
Partial lift: Vacuum **	A small area of the cell monolayer is vacuumed (from outside) to form a well; dispase is then added to the well	Pros: Only sheet inside well lifted Cons: 1) cells inside well are unevenly deformed during lifting; 2) technically difficult to form a stable well in incubator
Partial lift: Gravity **	A small area of the cell monolayer is forced to form a well helped by gravity or magnet (from outside) ; dispase is then added to the well	Pros: Only sheet inside well lifted Cons: 1) cells inside well are unevenly deformed during lifting
Whole lift followed by partial reattachment *	The cell monolayer is lifted by dispase; then suspends in minimum amount of growth medium	Pros: Part of the sheet reattached Cons: 1) whole sheet contracts after lifting; 2) only part reattached; 3) hard to control reattachment
Whole lift followed by partial reattachment: Collagen *	The cell monolayer is lifted by dispase; then suspends in another collagen partially pre-coated membrane with minimum amount of growth medium	Pros: Part of the sheet reattached Cons: 1) whole sheet contracts after lifting; 2) only part of the sheet reattached
Whole lift followed by partial reattachment: Collagen-sheet-collagen sandwich *	The cell monolayer is lifted by dispase; then place on top of another collagen partially pre-coated membrane, seal periphery with additional collagen to form a collagen-sheet-collagen sandwich	Pros: Part of the sheet reattached Cons: 1) whole sheet contracts after lifting; 2) only part of the sheet reattached
Whole lift followed by partial reattachment: Fibronectin (FN) *	The cell monolayer is lifted by dispase; then suspends in another fibronectin partially pre-coated membrane with minimum amount of growth medium	Pros: Part of the sheet reattached Cons: 1) whole sheet contracts after lifting; 2) only part of the sheet reattached
Whole lift followed by partial	The cell monolayer is lifted by dispase; then place sheet on top of	Pros: Part of the sheet reattached

reattachment: FN-sheet-FN sandwich *	another fibronectin partially pre-coated membrane, seal periphery with additional fibronectin to form a FN-sheet-FN sandwich	Cons: 1) whole sheet contracts after lifting; 2) only part of the sheet reattached
Whole lift followed by partial reattachment: temperature-responsive substrates transfer to elastic membrane *	Cells monolayer grown on temperature-responsive substrates (Up-Cell dish) is lifted after switching to room temperature. The cell sheet is then transferred to a fibronectin pre-coated membrane, and suspends in minimum amount of growth medium	Pros: Part of the sheet reattached Cons: 1) whole sheet contracts after lifting; 2) only part of the sheet reattached
Temperature-responsive substrates on elastic membrane *	Cells monolayer grown on temperature-responsive substrates (Up-Cell dish) that is cut and placed on a fibronectin pre-coated elastic membrane is lifted after switching to room temperature	Pros: Only sheet on Up-Cell dish lifted Cons: 1) un-level surface; 2) fragile sheet along the Up-Cell dish and membrane periphery

* Good, ** better, *** best. Ranking was based solely on actual results.

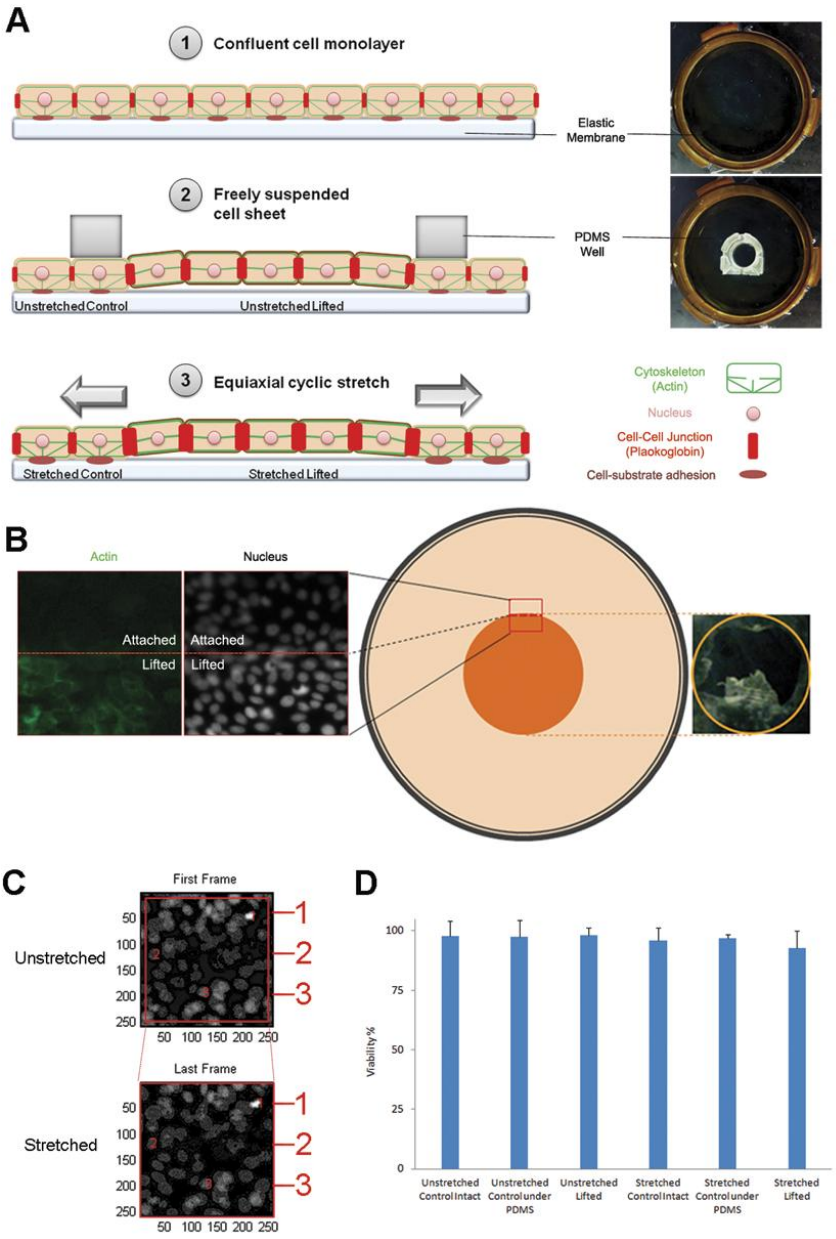

Figure 3. 1 Generation of partially-lifted cell sheets.

(A) Schematic illustration (side-view) of the partially-lifted cell sheet (1) before lifting, (2) after lifting, and (3) subject to cyclic stretch. Confluent keratinocyte monolayers were completely lifted by dispase inside the PDMS mold leaving the lifted region freely suspended; cells outside the mold remained adhered to the substrate. Changes in actin (green) and plakoglobin (red)

indicate anticipated changes in relative levels of the respective proteins in response to stretch. (B) Schematic illustration (middle, top-view), and enlarged fluorescent actin stain and nucleus stain images (left) on the border of the partially lifted cell sheet. Nucleus stain was performed across the whole monolayer, partial lift and actin stain were performed inside the PDMS well. Only lifted cells inside the well were stained, the cells under & outside the well remain un-stained. This result confirmed that the PDMS well has the ability to contain the dispase and/or phalloidin within the well and the attached cells under PDMS were not torn off. Right image shows a partially torn cell sheet with apparent contraction (purposely torn only for showing, with three edges detached to assess contraction and attachment to the substrate). These images also provide evidence to confirm the effectiveness of dispase lifting. (C) Nuclei tracking was used to verify that lifted sheets were subject to the same strain as controls. The representative images show changes in length between pairs of three randomly picked nuclei centroids. No significance difference is observed between the attached and lifted sheets. (D) Viability testing show that cells are effectively 100% viable, with no significant differences among the six tested conditions (0% unstretched control and 5% strain). Please refer to Figure 3.S1 for additional viability tests at 3%, 10% and 20% strains.

3.3.2 Stretch induces reinforcement of lifted cell sheet cohesion

We next assessed whether mechanical conditioning can significantly alter biomechanical properties such as cell-cell adhesion strength. We chose to use stretch for mechanical conditioning since stretch is a well-known potent stimulus for various functions, such as growth, remodeling, gene expression and is relevant for skin. Interestingly, the effects of stretch conditioning on cell-cell adhesion of lifted sheets have not been directly measured. Two tests

were used to assess cell-cell adhesion strength: (1) a tensile test which consisted of slowly stretching the cell sheet uniaxially until the sheet (or membrane) breaks, and (2) a shear test which consisted of removing and shearing the lifted region and measuring the shearing time until the sheet fragments. The former represents a measure of the maximum strain of the cell sheet and the latter represents a measure of overall cell sheet cohesion (the overall strength). Both tests were carried out on lifted sheets stretched at 3, 5, 10 and 20% strains for either four or twenty-four hours, and compared to matched unstretched lifted sheets (for clarity, while the tensile test involves stretching, further references using the term "stretch" refer to mechanical conditioning, while the tensile test will be referred to by name). Mechanical conditioning at 3% and 5% strain resulted in a 68% and 60% increase in maximum sheet extension before failure in the tensile test at 4 hours (Figure 3.2A), and a 77% and 87% increase in sheet shearing time (Figure 3.2C) at 4 hours, respectively. Similarly, mechanical conditioning at 3% and 5% strain resulted in a 73% and 82% increase in maximum sheet extension before failure in the tensile test at 24 hours (Figure 3.2B), and a 112% and 93% increase in sheet shearing time (Figure 3.2D) at 24 hours, respectively. However, increasing strain to 10 and 20% resulted in no significant increase in cell-cell adhesion strength, and in fact at 24 hours, this strength actually decreased compared to unstretched controls for 20% strain. These results quantitatively demonstrate that mechanical stretch regulates sheet mechanical properties when cell-cell interactions dominate.

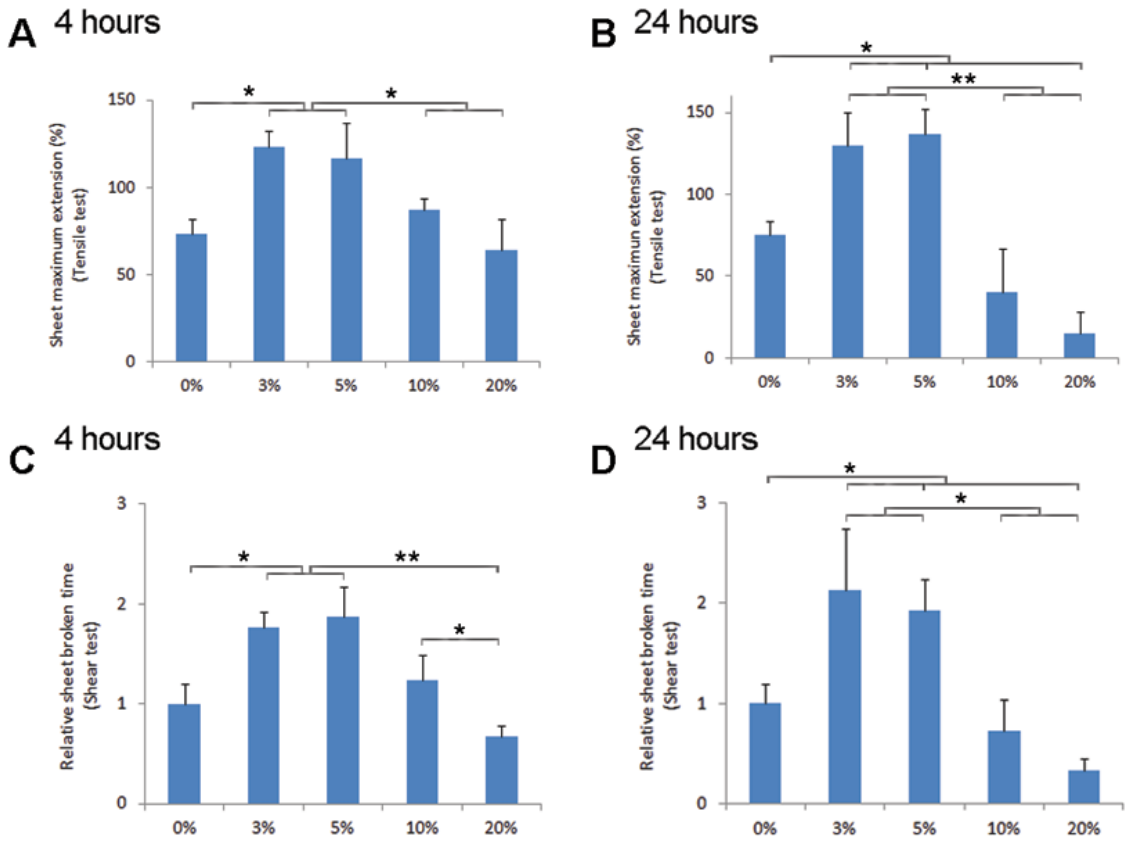

Figure 3. 2 Stretch induces reinforcement of substrate-free sheets strength and cohesion.

(A) The tensile tests show that stretch at 3% and 5% strain resulted in a significant increase in maximum sheet extension before failure at (A) 4 hours and (B) 24 hours, normalized to unstretched controls respectively. However, increasing strain to 10 and 20% resulted in no significant increase in maximum sheet extension, and in fact at 24 hours, it actually decreased compared to unstretched controls for 20% strain. The shear tests show significant increase in sheet cohesion strength or sheet broken time after stretch at (C) 4 hours and (D) 24 hours, normalized to unstretched controls respectively. Similarly, increasing strain to 10 and 20% resulted in no significant increase in cell-cell cohesion strength, but decrease compared to unstretched controls for 20% strain at 24 hours.

3.3.3 Actin distribution is significantly altered in lifted cell sheets

Since cell-cell adhesion is increased with mechanical conditioning, we next examined actin expression, working from previous data showing that the actin cytoskeleton is an essential contributor to cell sheet cohesion [12]. To determine the changes to actin expression and distribution in mechanically conditioned cell sheets, we stained cells under four different experimental conditions – attached or lifted; and with or without cyclic mechanical stretch conditioning. Unstretched attached cells generated stress fibers throughout the cell. After losing cell-substrate contact, the lifted cells lost cytoplasmic stress fibers and exhibited primarily cortical localization of actin at cell-cell contact regions (Figure 3.3A, top row).

In response to cyclic stretch, adhering cells exhibited stronger overall staining for actin, while cells in the lifted regions exhibited stronger cortical staining of actin (Figure 3.3A, bottom row). Quantification of the fluorescence signal at cell-cell junctions showed that the percentage of cortical actin was significantly increased from 39% to 60% after being lifted, or to 52% after being stretched while attached (Figure 3.3B). Stretched, lifted cells exhibited highest percentage of cortical actin at 74%. Stretching and/or lifting lead to significant increases in actin at, or near, cell-cell junctions, which may contribute to increased cell-cell adhesive strength.

We next measured the level of total cellular actin, under the same conditions of lifting and stretching. Western blot analysis revealed that the loss of cell-substrate contact resulted in a 79% decrease in the total expression of actin (Figure 3.3C, 3.3D). Cyclic stretch caused a 55% up-regulation of actin in cells that remained attached; however, actin levels were not significantly altered by stretch in the lifted cells. Thus, for cells in the substrate-free region, both the spatial arrangement and expression level of actin cytoskeleton are significantly altered when

cell-cell interactions dominate. These results suggest that the majority of actin is used for establishing and maintaining components for adhesion to the substrate.

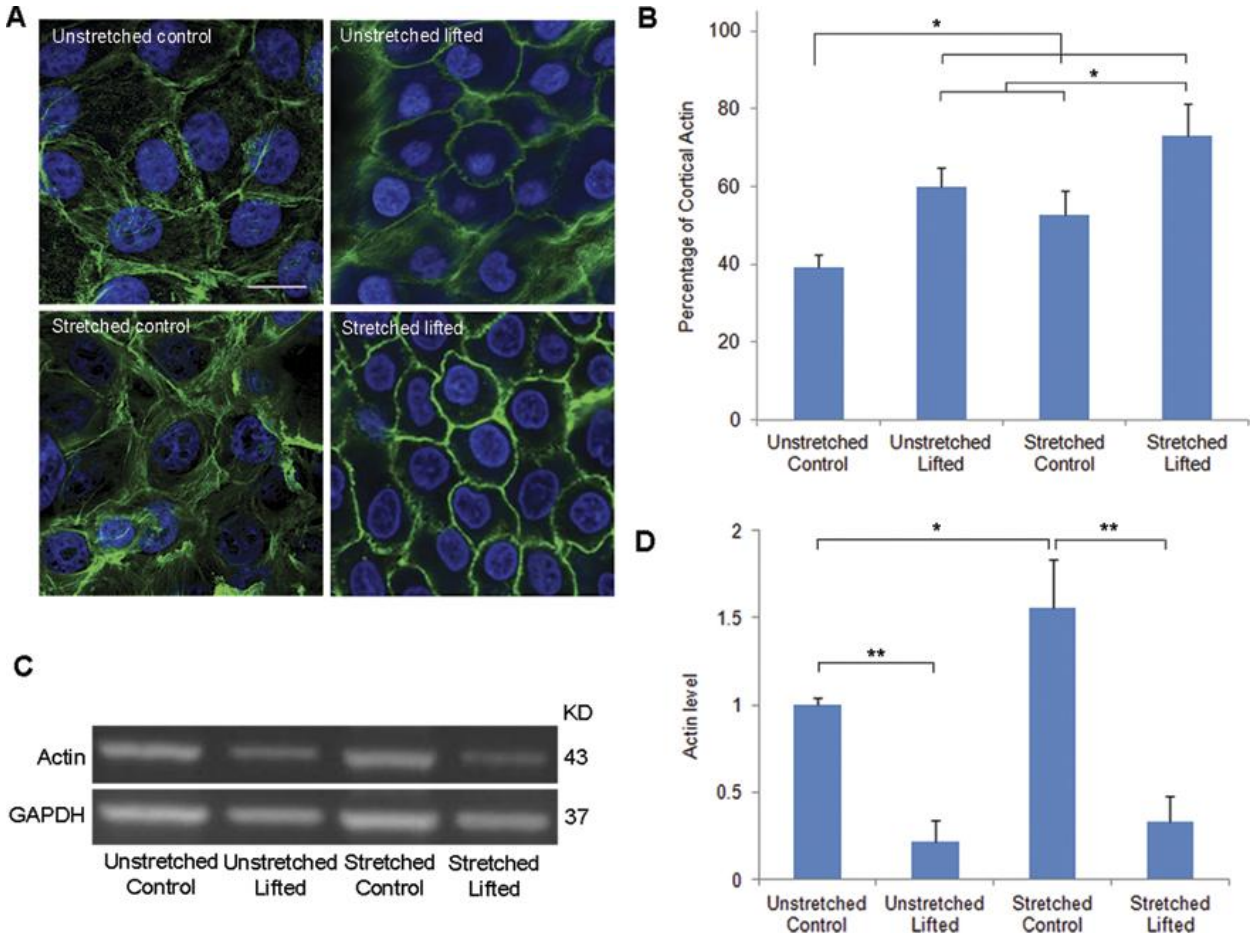

Figure 3. 3 Actin localization and expression is altered in mechanically-conditioned lifted cells.

(A) Fluorescence images of actin in unstretched control cell (top left), unstretched lifted (top right), stretched control (bottom left) and stretched lifted (bottom right) show that the spatial arrangement of the actin cytoskeleton is significantly altered when cells are lifted or mechanically conditioned. Green: actin, Blue: nucleus. Scale bar: 10 μm. (B) Quantification of the percentage of cortical actin, showing highest levels of cortical actin in cells that are both lifted and stretched. (C) and (D) Western blot analysis shows significant upregulation of total cellular actin in response to stretch in adherent, but not lifted, cells. Significant decrease in total

cellular actin occurred after losing cell-substrate adhesion. The y-axis represents relative actin expression level, with values normalized to the unstretched control. GAPDH was used as a loading control. * $p<0.05$, ** $p<0.01$.

3.3.4 Actin or ROCK disruption mechanically weakens lifted cell sheets

Actin-myosin coupling participates in force generation among neighboring cells [33]. To determine whether intact actin or myosin regulates the cohesion of lifted cells, cytochalasin D (CytoD) or Y-27632 (a selective inhibitor of the Rho-associated kinase ROCK) was used to disrupt those processes, respectively. Each type of disruption substantially altered actin distribution in lifted cells, leading to diffuse distribution of actin throughout the cell (Figure 3.4A). Tensile and shear testing showed that disruption of either actin or myosin interactions weakened lifted sheet maximum strain (Figure 3.4B, a 71% and a 50% reduction, respectively) as well as sheet cohesion (Figure 3.4C, a 60% and a 56% reduction, respectively). The increased fragility of the lifted cells was apparent when mechanical conditioning led to significant tears in the lifted region before any measurements could be made. These results confirm the importance of actin and myosin interactions in maintaining cell sheet strength and cohesion, and provide the first quantitative data of ultimate mechanical strain for cell-cell adhesion under these treatment conditions.

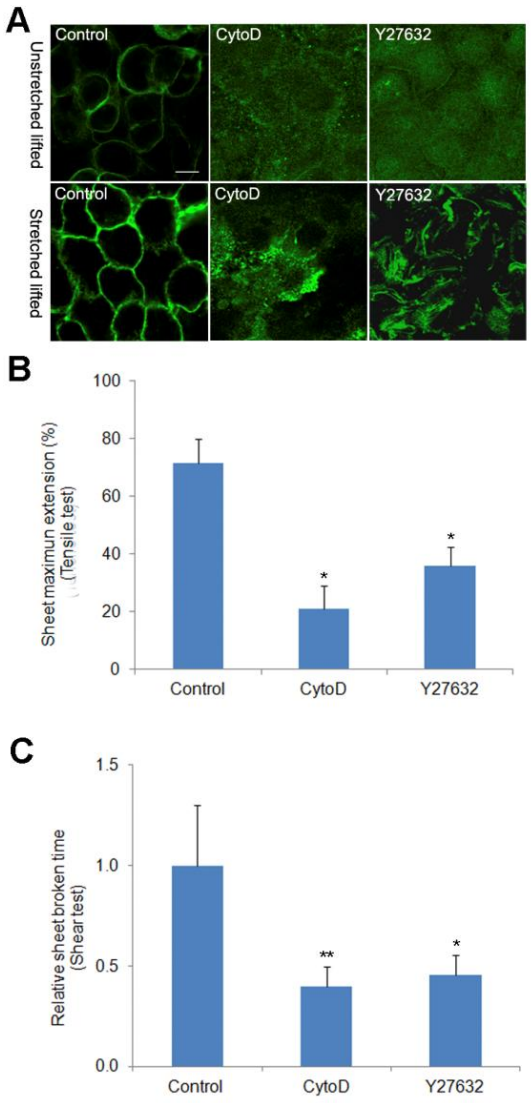

Figure 3. 4 Actin or actin-myosin disruption weakens lifted cell sheet strength and cohesion.

(A) Fluorescence images of actin-stained lifted sheets, in unstretched control (top left), unstretched CytoD treated (top middle), and unstretched Y27632 treated (top right), stretched control (bottom left), stretched CytoD treated (bottom middle), and stretched Y27632 treated (bottom right). Scale bar: 10 μm. (B) Tensile tests shows that treatments with CytoD or Y2763 lead to significant reductions in maximum sheet strain before failure. (C) Shear tests shows significant diminishments in sheet cohesion with treatment of CytoD or Y27632. *$p<0.05$, **$p<0.01$ compared to the matched untreated control.

3.3.5 Plakoglobin expression is significantly altered in lifted cell sheets

One of the major functions of certain cell-cell junctions is to glue cells together and connect the cytoskeletons of adjacent cells [8,9,11,29,71]. Plakoglobin, a key molecular constituent that resides in both adherens junctions and desmosomes, is essential for maintaining cellular viability in substrate-free conditions [11]. Further, plakoglobin exhibits stretch induced upregulation under conventionally plated conditions [75,76]. Plakoglobin was thus examined using the same four conditions as actin to assess its role in modulating cell properties when cell-cell interactions dominate. After losing cell-substrate contact, the lifted cells exhibited primarily junctional localization of plakoglobin, which appears to colocalize with actin (Figures 2.5A and 2.5B). After cyclic stretch for 4 hr at 5% strain and 1 Hz, adhering cells significantly increased plakoglobin throughout the cell. Stretched lifted cells exhibited enhanced junctional immunoreactive signal, again appearing to colocalize with actin (Figure 5A and 5B). The percentage of plakolgobin's immunoreactive signal at the junctions was significantly increased from 62% in unstretched control cells to 89% after being lifted, or to 85% after being stretched while remaining attached (Figure 3.5C). Stretched lifted cells exhibited the highest percentage of junctional plakoglobin at 98 % (Figure 3.5C).

Western blot analysis (relative to unstretched, unlifted cells) revealed that lifting cells resulted in a 42% decrease in the total expression level of plakoglobin (Figure 3.5D and 3.5E). Cyclic stretch led to a 17% upregulation of plakoglobin in attached cells. After lifting, cyclic stretch led to a 53% upregulation of plakoglobin (Figure 3.5D and 3.5E), or an increase of 166% when compared to the unstretched, lifted cells. Thus, for cells in the lifted region, both the spatial arrangement and expression level of plakoglobin are significantly altered, but with differences from actin. While both total actin and plakoglobin expression dropped significantly on lifting,

plakoglobin remains significantly mechanoresponsive, while actin's sensitivity is considerably diminished.

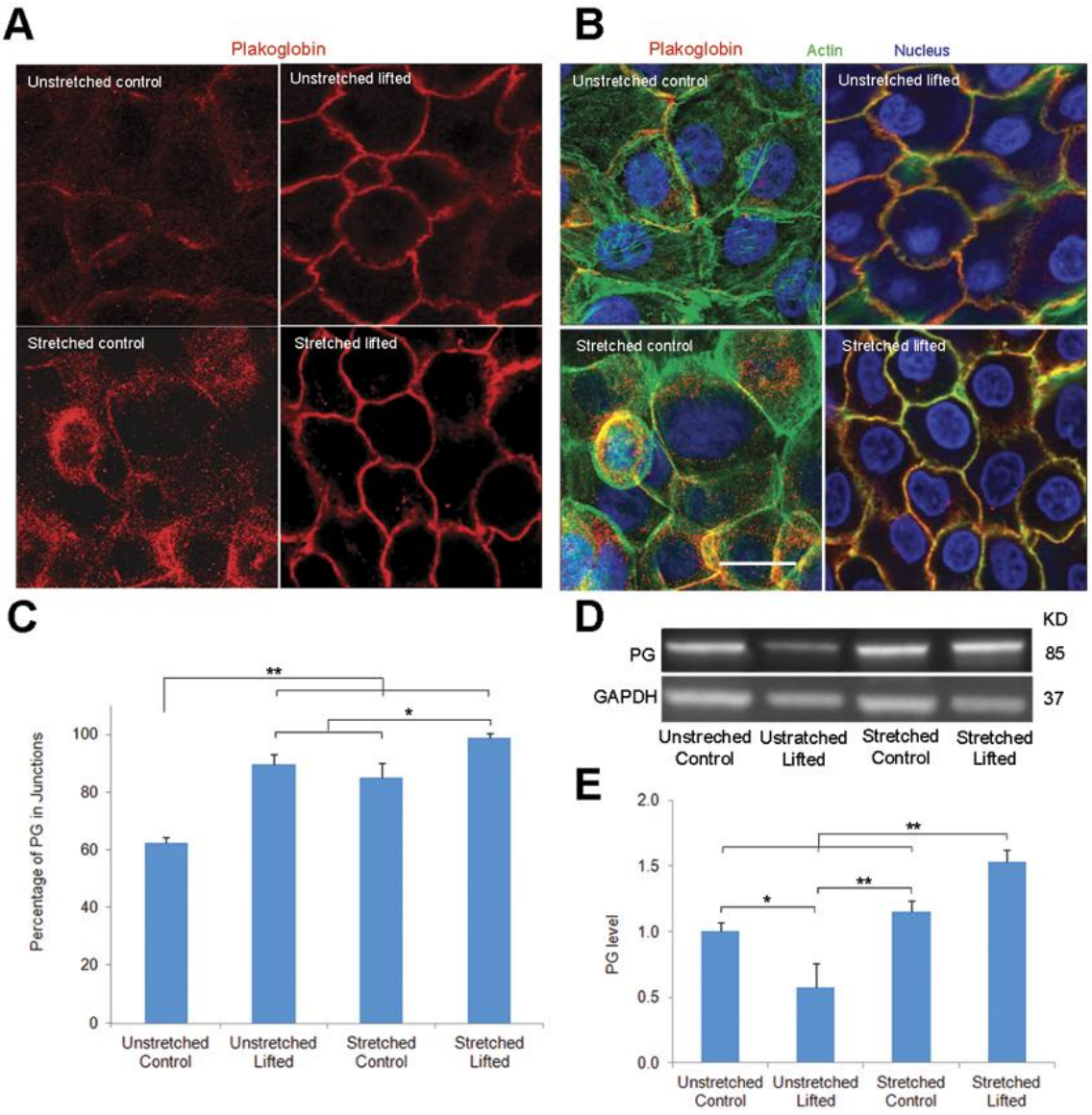

Figure 3. 5 Plakoglobin localization and expression is significantly altered in lifted cells.

Immunofluorescence images are shown of (A) plakoglobin and (B) triple staining for plakoglobin, actin and nuclei in unstretched control (top left), unstretched partial-lifted (top right), stretched control (bottom left) and stretched, partial-lifted (bottom right) cells. Partially-

lifted sheets were subjected to cyclic stretch for 4hr at 5% strain and 1 Hz before staining. Red: Plakoglobin (PG), Green: actin, Blue: nucleus. Scale bar: 10 μm. (C) Quantification of junctional plakoglobin reveals elevated junctional accumulation in both lifted and stretched cells. (D) and (E) Western blot analysis shows significant reduction of total cellular plakoglobin when cell-substrate adhesion was lost, while cyclic stretch caused substantial up-regulation of plakoglobin, especially in the lifted cells. * $p<0.05$, ** $p<0.01$.

3.3.6 Plakoglobin knockdown mechanically weakens lifted cell sheets

Due to the responsiveness of plakoglobin in lifted cells, RNA interference was next used to determine the role of plakoglobin in regulating sheet cohesion. Bright field images of lifted cells acquired four days after plakoglobin knockdown demonstrated small tears in the cell sheets, while stretched lifted sheets exhibited significant tears (Figure 3.6A). Immunofluorescence staining showed diminished plakoglobin expression in both unstretched and stretched cases. To confirm the effects of siRNA knockdown, western blot analysis of siRNA transfection was performed. Lifted cells transfected with plakoglobin siRNA displayed a 77% reduction of plakoglobin expression level relative to cells transfected with negative control siRNA (Figure 3.6B and 3.6C). Stretch caused a 57% up-regulation of plakoglobin expression level. Interestingly, even with plakoglobin knockdown, stretch induced a nearly threefold increase in plakoglobin expression.

Next, tensile tests and shear tests were performed to evaluate the mechanical strength and cohesion of the siRNA transfected sheets. Mechanical tests were performed on unstretched lifted sheets with plakoglobin siRNA knockdown and compared to matched untreated lifted sheets.

Similar to actin disruption, plakoglobin siRNA knockdown led to more fragile sheets (a 96% reduction in maximal strength, Figure 3.6D, and an 87% reduction in sheet cohesion, Figure 3.6E). The tears in mechanically conditioned sheets precluded tensile testing or cohesion measurements. These results further confirm the importance of junctional plakoglobin in maintaining sheet mechanical properties, but also provide support for the notion that mechanical forces directly regulate cell-cell junctional dynamics.

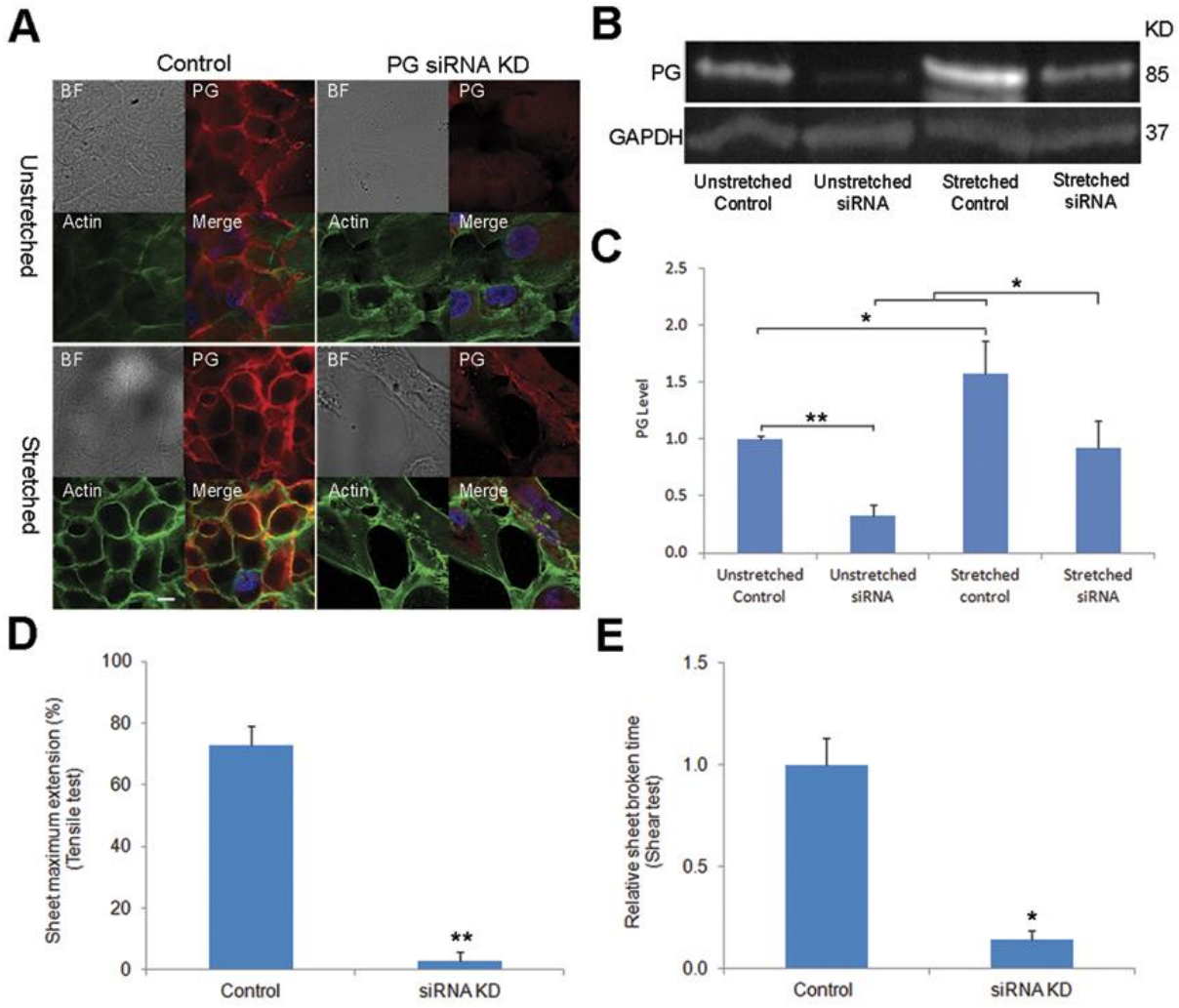

Figure 3. 6 Plakoglobin RNA interference weakens mechanical strength and cohesion of the substrate-free sheets.

(A) Bright field and immunofluorescent images of plakoglobin, and fluorescent images of actin in unstretched control (top left), unstretched plakoglobin siRNA knockdown (top right), stretched control (bottom left) and stretched PG siRNA knockdown (bottom right) in lifted cells. Red: plakoglobin (PG), green: actin, blue: nucleus. Scale bar: 10 μm. (B) Western blot analysis of plakoglobin four days after transfection (PG siRNA KD). GAPDH was used as a loading control. (C) Quantification of relative plakoglobin level in each western blot lane, with values normalized to the untreated control. Western blot analysis shows significant reduction of total cellular plakoglobin with siRNA knockdown. Stretch significantly increased plakoglobin expression levels compared to their respective unstretched controls. Both (D) Tensile test measuring ultimate broken strain and (E) shear test measuring cell-cell adhesion strength show siRNA knockdown of plakoglobin significantly weakened the lifted sheets' cohesion. *$p<0.05$ and **$<p<0.01$ compared to the matched untreated control.

3.4 Discussion

In this study we developed a novel enzyme-based, noninvasive harvest method to generate partially-lifted substrate-free cell sheets which can be manipulated and assayed. Experimentation on these partially lifted cell sheets provide critical information on cell-cell interactions, which have numerous downstream applications in tissue engineering, investigation of certain genetic and autoimmune diseases, as well as embryonic development and cell and tissue mechanics.

This study primarily focused on the characterization of cell-cell junction in cells without substrate and very limited extracellular matrix support. We demonstrated that when cell-cell interactions dominate, the basic physiology of cells is significantly altered. Intercellular junctions may be mechanically-sensitive signaling hubs that participate in mechanotransduction [167,168]. Our data are consistent with the notion that the cell's ability to convert physical perturbations into signaling cascades is based on the integrity of the junctional-cytoskeletal linkages [8,9,11,29,71]. Moreover, stretch is a well-known potent stimulus for many cell functions [29,167]. Upon stretching, applied physical force may stiffen the intercellular junctional-cytoskeletal network through mechanical strain-stiffening [169,170] or signaling-mediated reinforcement [4,157]. Therefore, force-induced junctional assembly and accumulation can serve as a self-protective mechanism and dissipate mechanical stress across intercellular junctions/cytoskeletal network more effectively. We hypothesize that when cell-cell interactions dominate and are subject to stretch stimuli, increased tension at intercellular junctions leads to recruitment of junctional components, leading to further enhancement of junctional tension in a positive mechanosensory feedback loop [171,172]. Previously characterized elevated intercellular contraction, junctional reinforcement and increased cohesion are consistent with this hypothesis [11,12].

Further, understanding cell-cell interactions is important for generating strategies for conditioning cell sheets or other constructs for tissue engineering purposes, or at least to define some limitations of cell-sheet engineering. Thus, results from the characterization of how different cytoskeletal components contribute to cell sheet cohesion and contraction have broad application. To determine the contribution of different parts of the cytoskeleton to cell sheet mechanics, we assessed the changes to the cytoskeleton from dispase lifting as well as from pharmaceutical or siRNA-based disruption of each of the major cytoskeletal components. Consistent with the idea that the intermediate filaments contribute to tissue strength, we show that keratins are at least as important as actin in establishing cell sheet cohesion, even though actin clearly localizes to cell-cell junctions, whereas microtubules and intermediate filaments appear less prominent at these junctions. Disruption of microtubules also diminishes cell sheet strength, suggesting that all components of the cytoskeleton likely play significant roles in establishing cell sheet cohesion. While increased cell sheet fragility may also be due to cell rupture (similar to what is observed in blistering diseases), the role of the cytoskeleton remains vital to keeping the cell sheet whole.

In this study we show that all components of the cytoskeleton are important for regulating the properties of the cell sheet, but that in particular the intermediate filaments, which are generally not well-studied, play a significant role in maintaining cell sheet cohesion and potentially in regulating cell sheet contraction. Thus, optimization of cell sheet engineering may benefit from manipulation of all three components of the cytoskeleton, such as via mechanical conditioning. Additionally, our previous work in Chapter 2 suggests that cell sheet contraction is a mechanism for parts of the cell cytoskeleton to reinforce cell-cell junctions [11]. Combined with our previous work in Chapter 2 and another cytoskeleton study [36], we can propose the

following for tissue-engineering applications. If cells sheets are initially too fragile for use, extended incubation in suspension will yield improved cohesion at the cost of usable area for the tissues being repaired. Alternatively, if cell sheet cohesion is extremely strong, then pretreatment with either actomyosin-, actin- or keratin-disrupting compounds will yield increased area at the cost of increased fragility. Microtubule disruption yields increased fragility without a corresponding preservation in cell sheet size and thus is likely not useful to creating larger, stronger sheets. Thus, mechanical conditioning the partially lifted cell sheet may provide a solution to generate stronger and meanwhile non-contracted cell sheet.

For tissue engineering purposes, this study demonstrates that it is possible to mechanically precondition dissociated cell sheets. If the monolayer is intended for transplantation (by patching, for example) into tissues, then such preconditioning may alleviate fragilities associated with dissociation from the monolayer [36,104,151,173]. As far as we know, the partial-lift method represents the first technique for achieving this goal since current work is primarily limited to simple, short-term manipulations [43]. We additionally demonstrate that because the lifted cells exhibit vastly different physiologies, in terms of total cellular content of actin and plakoglobin (and likely other proteins), pre-lifting the cells may offer an opportunity for the cells establish a new, different distribution of junctional proteins, prior to use. We offer the partial lift method as one that achieves theses advantages by allowing the cell sheet to remain attached at edges to neighboring cells, which maintains a cellular environment friendly to the lifted cells, prevents significant contraction associated with full dissociation, and permits a variety of chemical and mechanical manipulation, although obtaining mechanical readouts, such as via optical tweezers or AFM, are challenging. This method is also suited for studies of cellular physiology for development [31,118], where substrates play a reduced role during key junctures,

as well as diseases where cell-cell interactions are altered [45,48]. Thus this study provides a method to engineer tissues by mimicking environments where cell-cell interactions need to be tuned or tested.

Cell sheet engineering offers a potential method for reconstructing well-organized cell-dense tissues *in vitro,* and meanwhile avoiding the potential scaffold-associated limitations. So far several cell sheet harvesting approaches have been developed. For example, one approach using modified thermo-responsive polymeric surfaces [84,104,105]; however, two drawbacks for this technique are high cost of preparing the modified surface and long cell sheet harvesting time, which typically takes an hour. Another approach used magnetic beads [174]; however, this technique requires peptide-conjugated magnetite cationic liposomes coating, a magnetic field and potential dose-dependent detrimental effect on cell proliferation and metabolism [175]. Another approach used electrochemical desorption of self-assembled monolayer of alkanethiol; however, the desorbed alkanethiol molecules may remain bound in the cell membrane proteins of the detached cells [176]. Here we present a cell sheet harvesting technique using dispase, a proven rapid, effective and gentle protease, which has been used for separating intact epidermis from the dermis and intact epithelial sheets in culture from the substratum, in which it selectively cleaving the basement membrane zone region while preserving the viability of the epithelial cells [177]. Studies using human keratinocytes showed that dispase removes the lamina densa, rich in type IV collagen, but preserves the type VII collagen-containing anchoring fibrils and the epidermal cells [130,177,178]. Another study using collagenase treatment showed that that cytoskeleton and fibronectin matrix of human periodontal ligament cells was maintained in the cell sheet after 2 hours long collagenase treatment, resulting in the formation of a detached and shrunken cell sheet [179]. On the other hand, Lim et al. have reported the disruption of several

ECM molecules ultrastructure with increasing duration of dispase incubation [180]. Thus, the effects on dispase treatment on ECM structure dependent on cell-type and incubation time, and suitability of the enzyme for detaching a particular cell line should be determined empirically. Our dispase-based partial-lift technique takes as little as 15 minutes, resulting in a human keratinocyte cell sheet with selectively cleaved ECM. Additional tests have showed that our cell sheet has the ability of re-plantation on another culture surface or living tissue and the maintenance of sheet structure (data not shown). Thus, our dispase-based partial-lift scaffold-free cell sheet harvesting approach has the advantage of being biocompatible, easily applicable, rapidly collectable and stretchable. The novel technique is desired for building *in vivo*-like constructs for tissue engineering applications.

In conclusion, we show that the partial-lift method results in cells sheets that engage primarily intercellular interactions, and demonstrate that lifted cells respond by altering their baseline behavior while remaining sensitive to mechanical conditioning. These findings suggest that cytoskeleton and tightly associated intercellular junctions may be crucial for unlocking the potentials for cell sheet engineering, which has emerged as a promising approach to reconstructing various types of laminar tissues, such as skin, myocardium, cornea, and vascular systems, etc. without using any biodegradable scaffolds. Of particular interest is heart tissue regeneration. Further, this study provide a solid foundation for extend partial-lifting technique to heart tissue regeneration, in part due to existing strong interest in characterizing and improving cell sheet properties for cardiac sheet engineering, and in part because they exhibit similar and strong cell-cell interactions, including desmosomes.

3.5 Supplemental figure

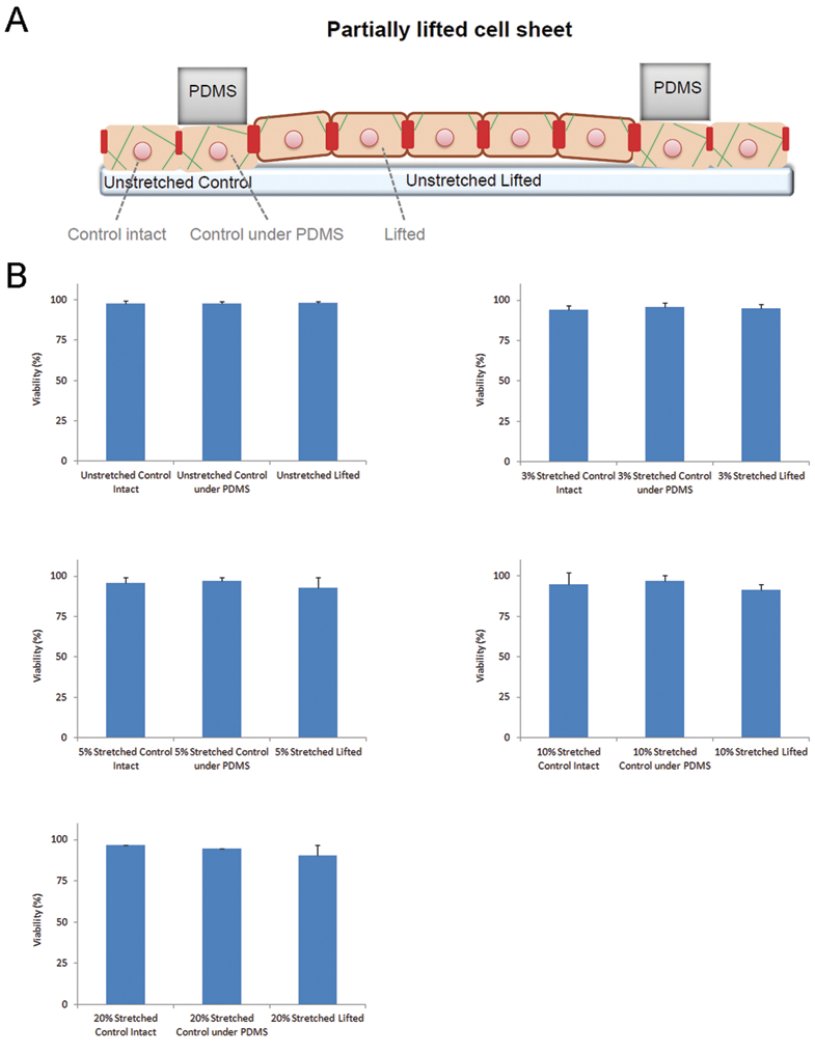

Figure 3. 7 Supplemental Figure S1 Additional viability tests of partially-lifted cell sheets.

(A) Schematic illustration (side-view) of the partially-lifted cell sheet. Cells were divided to three categories: control intact cells, control cells under PDMS mold and lifted cells. Diagram not to scale (there is more than one cell under the PDMS mold). (B) Viability testing show that all cells at 0% unstretched control, 3% strain, 5% strain, 10% strain and 20% strain are effectively 100% viable, independent of their plating location, with no significant differences among the tested conditions.

Chapter 4 Characterization of partially-lifted cardiomyocyte cell sheets

4.1 Introduction

Heart disease, including myocardial infarction (MI) and congestive heart failure (CHF), is currently the leading cause of death in the USA and is rapidly becoming one of the leading causes of global mortality [90,91]. Though recent studies have demonstrated that there is limited regeneration potential in the adult heart, the turnover capability of the heart itself after MI cannot compensate for the large-scale tissue and contractile function loss [92,93]. Heart transplantation is still the gold standard for treating CHF [96], but its benefits are limited by donor scarcity and further complicated by the need for lifelong immuno-suppression therapy [97,98]. Consequently, there exists a need for alternative and innovative strategies.

Cardiac cell sheet tissue engineering has recently emerged as a promising therapeutic option for the repair of damaged heart tissue [109,110]. This technique uses cultured cells detached from substrates without the disruption of intercellular junctions that are critical for myocardial adhesive strength, excitation-contraction coupling and mechanotransduction [59,60,72,181,182]. Furthermore, cardiac cell sheet engineering may allow for the development of cardiac tissues without the use of external biomaterial scaffolds. However, scaffold-free cardiac sheets are mechanically fragile, typically requiring heterogeneous external supports such as chitin membranes, or stacking of multiple sheets [109,110,151]. It remains to be seen whether a single scaffold-free cardiac sheet can withstand mechanical forces required to function as cardiac muscle under *in vitro* biomimetic physiological condition. Further, when no external support was used, the detached cardiac sheets size shrank by 90% and ceased spontaneous beating [151]. Though shrinking may lead to stronger cell sheets, as indicated in our previous

work in Chapter 2 and other studies [11,12], it also significantly impairs the sheet's ability to provide sufficient coverage in the cardiac tissues being repaired. Therefore, it is desirable to develop a novel method to generate mechanically conditioned and minimally shrunk substrate-free, scaffold-free cardiac cell sheets.

Such a method must rely on mechanisms by which cardiac sheet biomechanical properties are regulated. Recent work has emphasized the critical roles that cell-cell junctional proteins play in regulating cell sheet mechanics, in conjunction with the actin cytoskeleton [8,9,11,29,71]. The heart is a dynamic organ that requiring cardiomyocytes to be mechanically durable and capable of sensing, transducing and converting a variety of environmental signals [72]. Cardiomyocytes are connected by intercalated discs which are composed mainly of an amalgamation of typical desmosomal and fascia adherens proteins [183-185]. Mutations in these proteins, notably plakoglobin, have been reported lead to diseases characterized by increased tissue defects and fragility, particularly in skin and cardiac tissues that are constantly subject to mechanical stimuli [8,9,22,46,48,60,61]. Furthermore, cardiac muscle functionality relies on the correct assembly of myofibrils, which are composed of tandem arrays of sarcomeres and closely associated with intercalated discs [186]. Abnormalities in actin cytoskeletal dynamics are associated with many pathological disorders such as myofibrillar myopathies [187]. These studies suggest that force homeostasis across the cardiac cell junctions-cytoskeleton network may play key roles in regulating biomechanical and physiological properties of the cardiac cell sheets. Therefore, there is a need for a systematic characterization of cardiac cell-cell junctions and closely associated sarcomeric actin filaments. However, our knowledge regarding how these protein complexes regulate cardiac sheet mechanical properties, such as cell-cell adhesion

strength, calcium signaling, mechanotransduction and other baseline cellular properties, remains poor.

Externally applied mechanical stretch is an extrinsic cue that induces intrinsic changes in cell size and gene expression [188-191]. Application of mechanical stimuli has been demonstrated to be an attractive strategy for tissue engineering mechanically functional cardiac tissues [111-115]. However, previous studies were generally performed in adherent cell models which maintain cell-substrate interactions and as a result, may introduce mixed responses into the readouts. The study in Chapter 3 has showed that externally applied mechanical stretch improved the biomechanical properties of a substrate-free keratinocyte sheet. It remains to be seen whether similar mechanical conditioning can improve the biomechanical properties of a substrate-free cardiac sheet.

The keratinocyte study in Chapter 3 provides a solid foundation for extend partial-lifting technique to cardiac sheet engineering. Our aim here is to extend this technique to cardiomyocytes for eventual application to cardiac tissue repair, and to assess commonalities and differences between the different cell types treated with this technique. However, cardiomyocytes do not form as robust a monolayer as keratinocytes, and fragment very easily upon dissociation. Further, cardiac myocytes have additional functional requirements, such as maintenance of robust calcium responses, which must be examined We hypothesize that in regions of primarily cell-cell contact, cardiac myocytes will respond to mechanical stretch by reinforcing junctional proteins and increasing cell-cell adhesion strength. Further, myocyte calcium responses and rheological properties will be enhanced by mechanical stimuli. To our knowledge, this study presented a first systematic examination of mechanical conditioning on cardiac cells with primarily intercellular interactions. Moreover, this partial-lift technique

enables us to generate mechanically strong, minimally shrunk substrate-free cardiac sheets with enhanced beating and calcium signaling functionality.

4.2 Methods

4.2.1 Isolation and culture of neonatal rat cardiomyocytes

Unless otherwise noted, media, supplements and reagents were purchased from Invitrogen (Carlsbad, CA). Neonatal rat cardiomyocytes were isolated from 1-day-old Wistar rat pups (Charles River, Wilmington, MA) following a protocol approved by the committee on animal care at Columbia University. Briefly, the pups were decapitated, their hearts extracted and placed in a dish containing HBSS (Cellgro, Manassas, VA) supplemented with 10 units/mL penicillin and 10 μg/mL streptomycin. The hearts were then minced, collected and subjected to a series of enzyme digestion (10 minutes each at 37℃, 75 rpm in shaking water bath) with trypsin (0.14%) and pancreatin (0.22mg/mL, Sigma) in HBSS. After digestion, the cells were then pooled and resuspended in M199 culture medium supplemented with 10% Newborn Calf Serum (NCS), plated in a culture-treated flask for further enrichment (3 hours at 37℃, 1% CO_2 incubator). After 3 hours, the supernatant containing cardiomyocytes were passed through a 40 μm filter to remove debris, harvested and maintained in M199 culture medium supplemented with 10% NCS and 10 units/mL penicillin/streptomycin. Bromodeoxyuridine (BrdU, 100 μM; Sigma-Aldrich) was added to the growth medium to minimize proliferating fibroblasts and progenitor cells [192,193]. The isolated cardiomyocytes were seeded at a density of 1.5 x 10^6 cells per PDMS mold.

Pre-coating of elastic membrane. A custom-made 28mm x 12mm PDMS mold was placed on 0.005" thick silicone sheeting (SMI, Saginaw, MI) pre-installed in a 100 mm diameter custom-made stretch device chamber (Figure 4.1). The membrane area inside the PDMS mold were pre-coated with type I collagen (0.2 μg/mL, BD Biosciences, Bedford, MA) for 30 minutes at room

temperature. The PDMS mold was then washed with HBSS and sterilized using an ultraviolet lamp overnight before cell seeding.

4.2.2 Antibodies and reagents

The primary mouse monoclonal antibodies anti-plakoglobin (γ-Catenin) and anti-GAPDH (Novus Biologicals) were used for immunoblotting. Immunofluorescence staining were performed using mouse anti-plakoglobin, anti-cardiac troponin I (Biodesign), anti- sarcomeric α-actinin (Sigma) and anti-pan cadherin (Sigma) IgG as the primary antibodies and Alexa Fluor 594 goat anti-mouse IgG as the secondary antibody (all at 1:1000 dilutions). Alexa Fluor 488 conjugated phalloidin at a concentration of 0.5 μg/mL in HBSS was used for the actin stain. Hoechst was used at a concentration of 0.5 μg/mL for nuclear staining. All staining was performed for 1 hour at 37 ℃ on day 4 post seeding.

4.2.3 Fluorescence microscopy

Cells were fixed in 4% paraformaldehyde (Sigma) and then permeabilized with 0.1% triton-X-100 (Sigma). For plakoglobin-nucleus co-staining, cells were incubated in the monoclonal anti-plakoglobin primary antibody and Hoechst together for an hour at 37 ℃, followed by PBS washes and then secondary antibody incubation for another hour, washed again and then imaged. For actin-nucleus co-staining, cells were incubated in the phalloidin and Hoechst together for an hour at 37 ℃, followed by PBS washes and then imaged. For plakoglobin-actin-nucleus triple-staining, cells were incubated in the monoclonal anti-plakoglobin primary antibody, the phalloidin and Hoechst together for an hour at 37 ℃, followed by PBS washes and then a secondary antibody incubation for another hour, washed again and then imaged. Microscopy was performed at room temperature using an Olympus FV10 Confocal microscope, an Olympus OPLFLN 40X O NA 1.3 objective, and Olympus FV10-ABW Software. Images were processed

using ImageJ (version 1.43u for Windows; National Institutes of Health) and Photoshop (Adobe) to prepare the final figures [127-129]. Imaging conditions were identical for each experiment and analyses were done using the raw fluorescence images. Relative actin or plakoglobin intensities were quantified by ImageJ, with values normalized to untreated control (i.e. unstretched, unlifted cells) signals. The percentage of actin or plakoglobin signal at the junctions was calculated as signal intensity at the junctions divided by the total signal intensity of the whole cells [74,76]. Images were brightness/contrast enhanced and fluorescent colors were added for clarity for presentation, after analysis was completed.

4.2.4 Dispase-based partial-lift method

To facilitate dispase lifting and minimize sheet rupture, on day 3 after seeding (one day prior to dispase lifting), a static pre-stretch (20%, 37℃ for 24 hours) was added to the neonatal rat cardiomyocytes cultivated inside the PDMS mold. On day 4 post seeding, to stop actomyosin contraction [194] and facilitate dispase lifting while minimizing the tearing of the sheet, the cell monolayer within the PDMS mold was pre-treated with blebbistatin (2 μL, at a final concentration of 10 μM in culture medium, Sigma) prior to dispase lifting (30 minutes, 37℃). After aspirating the blebbistatin media off the cells, the PDMS mold was gently removed and then immediately re-placed perpendicularly on top the cell monolayer, so that only the center portion of the monolayer would be lifted, while the edges of the monolayer, underneath and outside the PDMS mold, would remain attached to the membrane. The part of the cell monolayer inside the PDMS mold was then treated with dispase (0.5 mL at a concentration of 1 units/mL in M199 medium) supplemented with blebbistatin (0.5 μL, at a final concentration of 10 μM) at 37℃ for 3 minutes until the monolayer lifted from the elastic membrane. This new partial lift method significant conserves cells, which is important for cardiomyocytes due to their limited

regeneration potential. Moreover, the shape of lifted region is slightly different from the keratinocytes lifting method, and is more closely related to the normal longitudinal and radial strains of left ventricular deformation. The unique square-shaped lift cardiomyocyte sheet is bordered by adherent cardiomyocytes at left and right side; the open edges on upper and lower sides facilitate access of dispase and manipulation.

4.2.5 Mechanical tests and cyclic stretch

A previously-established shear test protocol that was developed in our group for keratinocyte study and other groups performed to test cell sheet cohesion, and thus cell-cell adhesive strength [11,76,131,164].Tensile tests were performed using an Instron ElectroPlus E1000 All-Electric Test Instrument (Instron, Norwood, MA). Strain was calculated as the ratio of the change in length to the original length ($e=\Delta L/L_0$) and the maximum sheet strain or extension before failure was measured. Cardiomyocytes were subjected to equiaxial cyclic stretch at 5 or 20% strains for either two or six hours at 1 Hz using a custom equiaxial stretching device (with uniform strain fields, as previously described [163]) maintained in a cell culture incubator. Unless otherwise noted, partially lifted cardiac sheets were subjected to equiaxial cyclic stretch for 2 hours at 20% strain and 1 Hz.

4.2.6 siRNA knockdown of plakoglobin

A Silencer® Pre-designed siRNA for plakoglobin (5'-3': GGGCAUCAUGGAGGAGGAUtt), a negative control siRNA (Invitrogen) were used. Cells were transfected using *Trans*IT-siQUEST (Mirusbio, Madison, WI), according to the manufacturer's instructions. Transfection was performed using 50 pmol siRNA oligomer or 50 pmol DNA plasmid and 3 µl *Trans*IT-siQUEST for each sample in the PDMS mold. On day 3 after transfection (i.e. one day prior to dispase lifting), cells were pre-stretched (20%static stretch, 37℃) for 24 hours. On day 4 after

transfection, cells were lifted, cyclically stretched (when applicable) and then harvested and analyzed for experimentation.

4.2.7 Immunoblotting

Cells were lysed with RIPA buffer (Sigma) and total protein concentration was determined by Bradford assay (Sigma). Soluble fractions containing equal amounts of total protein were separated using SDS polyacrylamide gel electrophoresis and transferred onto PVDF membranes (Millipore, Billerica, MA). Immunoblotting was performed using mouse anti-human antibodies diluted in TBS with 1% w/v BSA and 0.1% v/v Tween-20 (Sigma) at the following dilutions: anti-Plakoglobin 1:1000, anti-actin 1:1000, anti-GAPDH 1:1,000, and horseradish peroxidase conjugated goat anti-mouse secondary antibody 1:1,000. Blots were developed with ECL (Perkin Elmer, Waltham, MA) and imaged using a FUJI imaging unit (Fujifilm, Stamford, CT). Relative plakoglobin intensity in immunoblotting images was quantified by ImageJ, with values normalized to GAPDH of each matching blot lane and then to the signal at untreated control.

4.2.8 Calcium signaling

Three days after cardiomyocyte seeding (i.e. one day prior to dispase lifting and Fluo-3 AM treatment), cells were pre-stretched (20% static stretch, 37℃) for 24 hours to facilitate dispase lifting and minimize sheet rupture. Four days after seeding, 10 μM Fluo-3 AM (an indicator of $[Ca^{2+}]_i$ or Ca^{2+} transients signal intensity, excitation at 485 nm, emission at 520 nm) was added to cells cultivated in M199 culture medium for 1 hour in a cell culture incubator (37℃, 1% CO_2) before dispase lifting. Before fluorescence measurements, cells were washed in M199 media to remove any dye that is non-specifically associated with the cell surface, and then incubated for a further 30 minutes to allow complete de-esterification of intra cellular AM esters. Fluorescence signals were recorded using an Orca CCD camera (Hamamatsu, Bridgewater, NJ, model

C10600), an Olympus LUCPLFLN 40X NA 0.75 objective, at a rate of 16 frames per second using MetaMorph Software at room temperature. Images of fluorescence intensity were processed using ImageJ. Relative changes in $[Ca^{2+}]_i$ were calculated as differences between signal peak to signal base [195,196].

4.2.9 Particle-tracking microrheology

Three days after cardiomyocyte seeding, cells were pre-stretched (20% static stretch, 37℃) for 24 hours to facilitate dispase lifting and minimize sheet rupture. Particle-tracking microrheology was used to measure local viscoelastic properties of cardiomyocyte cytoplasm according to a previously established technique [166]. Briefly, 1 μL fluorescent beads of 0.5 μm in diameter at or working concentration 1.5 x 10^7 beads/mL (1:50,000 dilution, Bangslabs, Fishers, IN) were added to the culture medium and then enter the cells via endocytosis. These beads were embedded in the viscoelastic cytoplasm and their properties are extracted from the thermal fluctuation subsequently tracked by digital fluorescence video-microscopy. The mean-square-displacement (MSD) of the bead's trajectory was used to quantify its amplitude of motions over different time scales [197-199]. Fluorescence signals were recorded using an Orca CCD camera (Hamamatsu, Bridgewater, NJ, model C10600), an Olympus LUCPLFLN 40X NA 0.75 objective, at a rate of 16 frames per second using MetaMorph Software at room temperature. The storage modulus G′ and (B) loss modulus G″ were calculated according to a previously published protocol [166].

4.2.10 Statistical analysis

Data are expressed as mean ± SD and compared by ANOVA and post-hoc. Normality tests are used to determine if a data set is well-modeled by a normal distribution. A value of $p < 0.05$ was considered significant, with each group having sample sizes $n \geq 3$.

4.3 Results

4.3.1 Generation of partially-lifted cardiac cell sheets

In this study we further refined the partial-lift technique to apply to cardiomyocytes. Table 4.1 summarizes the partial-lift techniques explored for this study. Based on the advantages of disadvantages of each method in the keratinocyte study in Chapter 3, we repeated several proven effective methods and further developed additional methods specifically suitable for cardiomyocytes. A confluent rat neonatal cardiomyocyte monolayer plated on a flexible silicone membrane was selectively lifted by dispase inside a PDMS mold gently placed atop part of the culture area. Cells outside and under the PDMS mold remained attached to the membrane (Figure 4.1A). Thus, this novel technique enabled us to generate a partially-lifted minimally shrunk cardiac cell sheet.

To ensure that neither PDMS mold, enzyme lifting, nor the application of cyclic stretch would lead to cell death, viability assays were applied to cells under six conditions: lifted, attached outside the PDMS or attached under the PDMS, and following cyclic stretch or unstretched. Cyclic mechanical stretch was performed using an equiaxial stretch device for 2 hr at 20% strain and 1 Hz. Cells were nearly 100% viable, with no significant differences among the six tested conditions (Figure 4.1B; Unstretched control intact 92.5 % ± 6.5%, Unstretched control under PDMS 91.1 % ± 6.8%, Unstretched lifted 93.7 % ± 3.2%, Stretched control intact 92.5 % ± 5.7%, Stretched control under PDMS 90.7 % ± 4.5%, Stretched lifted 88.7 % ± 7.2%). Additional stretch tests were performed to validate the cells in the lifted regions were subject to the same strain as cells that remain attached according to a previously published protocol [165,166].

Table 4. 1 Development and evaluation of partial lift techniques for cardiac sheet

Technique	Method	Results& Comments
Partial lift: Inside PDMS *	Cardiac cells seeded and monolayer formed inside PDMS mold that is placed on top of the membrane; the same mold is then re-placed perpendicularly on top the cell monolayer	Pros:(1) Only sheet inside PDMS lifted; 2) maintain spontaneous beating Cons: Fragile sheet
Partial lift: Inside PDMS Blebbistatin**	Cardiac cells seeded and monolayer formed inside PDMS mold; supplemented with blebbistatin before and/or during and/or after dispase lifting inside the same PDMS mold	Pros: Only sheet inside PDMS stronger lifted sheet Cons: 1) Spontaneous beating stopped; 2) bleb need to present all the time
Partial lift: Inside PDMS Static pre-stretch **	Cardiac cells seeded and monolayer formed inside PDMS mold; subject to 20% static pre-stretch for 24hr prior to dispase treatment inside the same PDMS mold	Pros: Only sheet inside PDMS lifted; 2) maintain beating; 3) sheet mechanically stronger than un-prestretched; 4) suitable for assays that require beating Cons: Without blebbistatin, sheet may shrink and rupture
Partial lift: Inside PDMS Cyclic pre-stretch *	Cardiac cells seeded and monolayer formed inside PDMS mold; subject to cyclic 20% stretch for 24hr at 1 Hz prior to dispase treatment inside PDMS mold	Pros: Only sheet inside PDMS lifted; 2) maintain spontaneous beating Cons: Cyclic pre-stretch tears sheet
Partial lift: Inside PDMS Static pre-stretch + Blebbistatin ***	Cardiac cells seeded and monolayer formed inside PDMS mold; subject to 20% static pre-stretch for 24hr prior to dispase treatment; supplemented with blebbistatin before, during and after dispase treatment	Pros: Only sheet inside PDMS lifted; 2) maintain spontaneous beating; 3) sheet mechanically stronger than un-prestretched and un-bleb treated control Cons: beating stopped and thus unsuitable for certain assays
Temperature-responsive substrates on elastic membrane *	Cardiac ell monolayer grown on temperature-responsive substrates (Up-Cell dish) that is cut and placed on membrane is lifted after switching to room temperature	Pros: Only sheet on Up-Cell dish lifted; 2) maintain beating Cons: 1) un-level surface and 2) extremely fragile sheet along the Up-Cell dish periphery

* Good, ** better, *** best. Ranking was based solely on actual results.

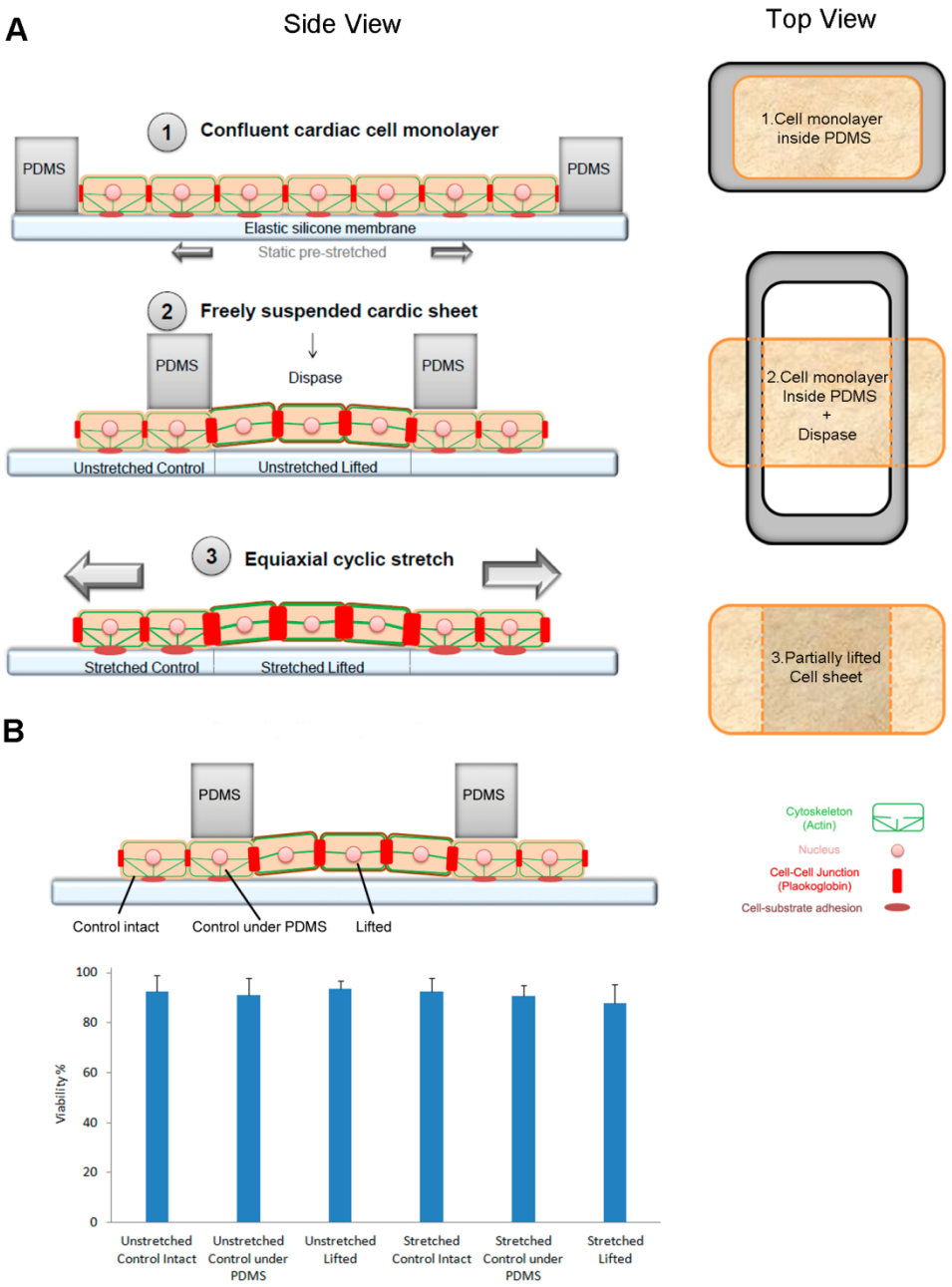

Figure 4. 1 Generation of partially-lifted cardiac sheets.

(A) Schematic illustration of the partially-lifted cardiac sheet (1) before lifting as a confluent monolayer, (2) after lifting as a partially, freely suspended cell sheet, and (3) subject to cyclic stretch. Confluent cardiomyocyte monolayers were statically pre-stretched, then lifted by dispase

inside the PDMS mold, leaving the lifted region freely suspended; cells outside the mold remained adhered to the elastic membrane. Changes in actin (green) and plakoglobin (red) indicate anticipated changes in relative levels of the respective proteins in response to lift and/or stretch. (B) Viability testing show cells are effectively near 100% viable, with no significant differences among the six tested conditions.

4.3.2 Stretch induces reinforcement of lifted cardiac cell sheet cohesion

Scaffold-free cardiac sheets are generally mechanically fragile, typically requiring heterogeneous external supports or stacking of multiple sheets [109,110,151]. It remains to be seen whether a single scaffold-free cardiac sheet can withstand mechanical forces and more importantly, if mechanical forces can been utilized to improve the functionality of engineered cardiac sheets [75,123,124]. It has been demonstrated that externally applied mechanical stretch can induce intrinsic changes in junctional gene expression and remodel cell-to-cell communication in cultured cardiomyocytes [111-115,188-191]. However, previous studies were generally performed in adherent cell models which maintain cell-substrate interactions and as a result, may introduce mixed responses into the readouts.

We assessed whether mechanical conditioning, or cyclic stretch, can significantly improve biomechanical properties such as cell-cell adhesion strength. Tensile tests and shear tests, developed in the keratinocyte study in Chapter 3, were used to assess cardiac cell-cell adhesion strength. Both tests were carried out on lifted cardiac sheets stretched at 5 or 20% strains for either two or six hours at 1 Hz, and compared to matched unstretched lifted cardiac sheets. Mechanical conditioning at 5% strain for 2 hours resulted in no significant increase in

cell-cell adhesion strength in both tests (Figure 4.2). However, increasing time to 6 hours resulted in a 54% increase in maximum sheet strain before failure in the tensile test (Figure 4.2A), and a 107% increase in sheet shearing time (Figure 4.2B). Further, mechanical conditioning at 20% strain for 2 hours resulted in a 71% increase in maximum sheet strain before failure in the tensile test (Figure 4.2A), and a 114% increase in sheet shearing time (Figure 4.2B). These results quantitatively demonstrate that mechanical stretch can significantly improve cardiac sheet mechanical properties when cell-cell interactions dominate. Unless otherwise noted, all following mechanical stretch studies used the fast and effective 2 hours, 20% strain and 1 Hz protocol.

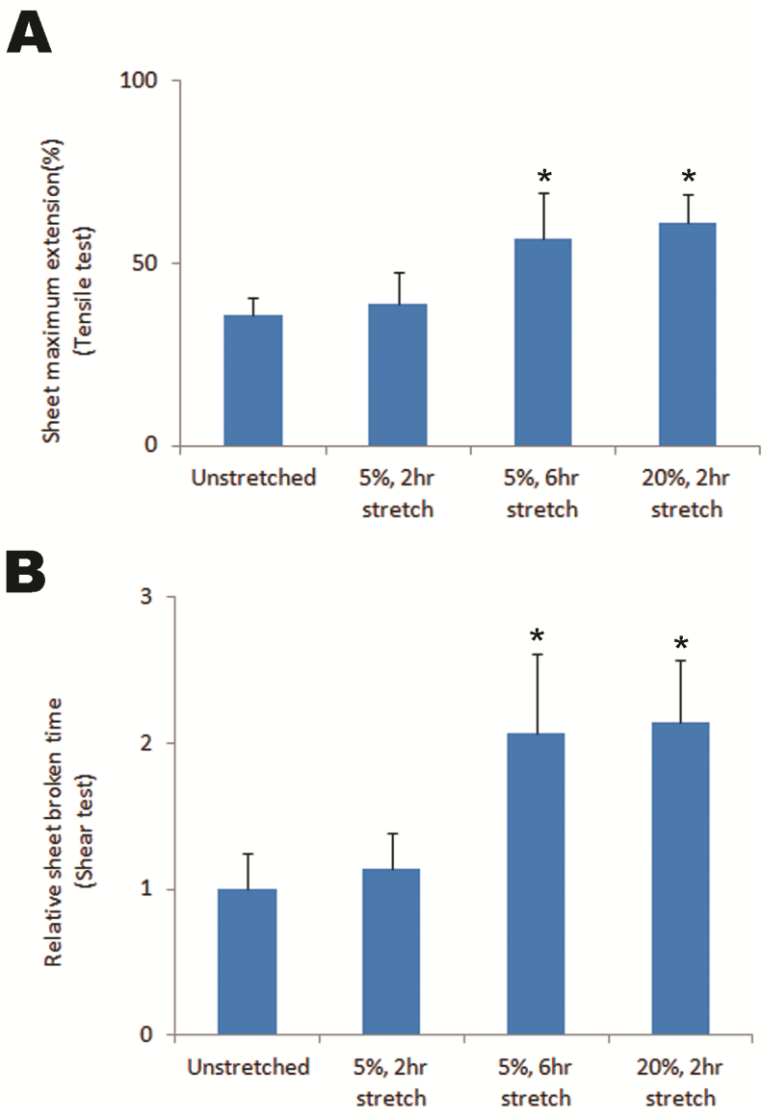

Figure 4. 2 Stretch induces reinforcement of lifted cardiac sheets cohesion.

(A) The tensile tests show that stretch at 5% strain 1 Hz for 6 hours (but not 2 hours) or 20% 1 Hz for 2 hours resulted in a significant increase in maximum sheet strain before failure. (B) The shear tests show at 5% strain 1 Hz for 6 hours (but not 2 hours) or 20% 1 Hz for 2 hours resulted in a significant increase in sheet cohesion strength, normalized to matched unstretched lifted sheets. * $p<0.05$.

4.3.3 Actin is altered in lifted cardiac sheets and is critical for sheet cohesion

Since cell-cell adhesion strength is increased with mechanical conditioning, we next examined expression of sarcomeric actin filaments, which is closely associated with intercalated discs consisting of mixed-type cell-cell junctions [183-185]. Our previous study showed that the actin cytoskeleton is an essential contributor to cell sheet cohesion [12]. To determine the changes to actin expression and distribution in mechanically conditioned cardiac cell sheets, we stained cells under four different experimental conditions – attached or lifted; and with or without cyclic mechanical stretch conditioning. Unstretched attached cells displayed sarcomeric actin filaments throughout the striated cardiac cells (Figure 4.3A, top left). After losing cell-substrate contact, the lifted cardiac cells maintained striated sarcomeric cytoarchitecture (Figure 4.3A, top middle). In response to cyclic stretch, both adhering and lifted cardiac cells exhibited brighter overall striation compared to their unstretched counterparts (Figure 3A, bottom left and middle). Moreover, the cardiomyocytes maintained their striated sarcomeric cytoarchitecture integrity after either detaching from the substrate or stretching, at least for short period of time [186]. These results suggest that mechanical stretch can influence the development of the sarcomeric structure in neonatal cardiomyocytes even without attachment to the substrate.

To determine whether intact actin regulates the cohesion of lifted cardiac sheets, we next used cytochalasin D (CytoD) to disrupt actin. Actin disruption substantially altered actin distribution in lifted cells, leading to disorganized sarcomeric cytoarchitecture and diffuse distribution of actin throughout the cell (Figure 4.3A). We next measured the level of total cellular actin. Western blot analysis revealed that the loss of cell-substrate contact resulted in a

41% decrease in the total expression of actin (Figure 4.3B, 4.3C). Cyclic stretch caused a 29% up-regulation of actin in cells that remained attached; however, actin levels were not significantly altered by stretch in the lifted cells. Thus, for cells in the substrate-free region, both the spatial arrangement and expression level of actin cytoskeleton are significantly altered when cell-cell interactions dominate. In general, compared with adult human keratinocytes in Chapter 3, rat neonatal cardiomyocytes display changes in a similar pattern, although the changes in cardiac sheets are smaller than those in keratinocytes. However, a notable difference is a majority of cytoplasmic actin structures in keratinocytes is lost on lifting, which resulted in a 79% decrease in the total expression of actin level (Figure 3.3). In comparison, only 41% decrease in the total expression of actin level was observed in cardiomyocytes and a majority of sarcomeric actin structures maintained, at least during the 6 hours study period.

Tensile and shear tests showed that disruption of actin significantly reduced the maximum strain of the lifted cardiac sheet (Figure 4.3D, a 63% reduction) as well as sheet cohesion (Figure 4.3E, a 79% reduction). The increased fragility of the lifted cardiac cells was apparent when mechanical conditioning led to significant tears in the lifted region, and both tests showed nearly complete maximum strain reduction (Figure 4.3D, 95%) and sheet cohesion reduction (Figure 4.3E, 96%). These results confirm the importance of actin in maintaining cardiac cell sheet strength and cohesion, and provide the first quantitative data of ultimate mechanical strain for cell-cell adhesion in cardiomyocytes under these treatment conditions.

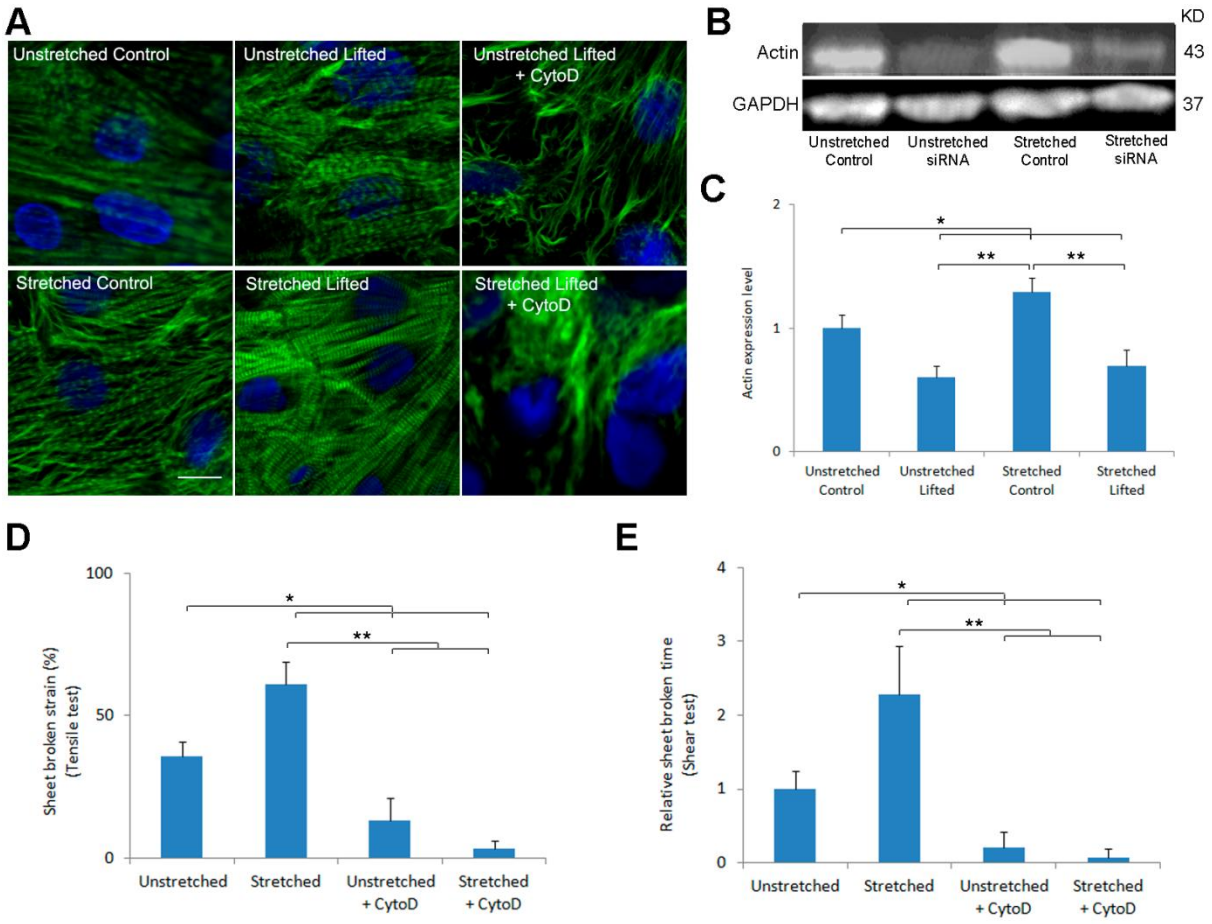

Figure 4. 3 Actin is altered in lifted cardiac sheets and is critical for sheet cohesion.

(A) Fluorescence images of actin in unstretched control cell (top left), unstretched lifted (top middle), unstretched CytoD treated (top right), and stretched control (bottom left) and stretched lifted (bottom middle) and stretched CytoD treated (bottom right) show that the spatial arrangement of the actin cytoskeleton is significantly altered when cells are lifted or mechanically conditioned. Actin disruption by CytoD weakens lifted cell sheet cohesion. Green: actin, Blue: nucleus. Scale bar: 20 μm. (B) Western blot analysis shows mechanical stretch resulted in a small but non-significant up-regulation of actin in both adherent and lifted cells. Significant decrease in total cellular actin occurred after losing cell-substrate adhesion. The y-axis represents relative actin expression level, with values normalized to the unstretched control.

GAPDH was used as a loading control. (C) Tensile tests show that treatments with CytoD lead to significant reductions in maximum sheet strain before failure. (D) Shear tests show significant diminishments in sheet cohesion with treatment of CytoD. *$p<0.05$, **$p<0.01$.

4.3.4 Plakoglobin distribution is significantly altered in lifted cardiac sheets

Since we previously showed that keratinocyte cell-cell adhesion strength is increased with mechanical conditioning and plakoglobin is an essential contributor to cell sheet cohesion [12], we next examined plakoglobin's role in modulating cardiac cell sheet biomechanical properties. Cyclic stretch resulted in significant changes in the expression and distribution of plakoglobin (Figures 4.4A and 4.4B). After losing cell-substrate contact, the lifted cardiomyocytes exhibited enhanced junctional localization of plakoglobin (Figures 4.4A and 4.4B, top right). The percentage of plakoglobin's immunoreactive signal at the junctions was significantly increased from 25% in unstretched attached cells to 55% after being lifted, or to 56% after being stretched while remaining attached (Figure 4.5C). Stretched lifted cells exhibited the highest percentage of junctional plakoglobin at 72 % (Figure 4.4C).

Western blot analysis (relative to unstretched, unlifted cells) revealed that lifting cells resulted in a 66% decrease in the total expression level of plakoglobin (Figure 4.4D and 4.4E). Cyclic stretch led to an 87% upregulation of plakoglobin in attached cells. After lifting, cyclic stretch led to a non-significant 14% decrease of plakoglobin when compared to the unstretched, unlifted cells, or a significant increase of 153% when compared to the unstretched, lifted cells (Figure 4.5D and 4.5E). Thus, for cells in the lifted region, both the spatial arrangement and expression level of plakoglobin are significantly altered, but with differences compared to actin.

While both total actin and plakoglobin expression dropped significantly on lifting, plakoglobin remains significantly mechanoresponsive, while actin's sensitivity is considerably diminished. Additional study on cadherins (shown in supplemental study) showed that changes of cadherins regarding spatial arrangement and expression level are generally similar to plakoglobin, though unlike plakoglobin, the additional gain of junctional localization of cadherins for stretched lifted cardiomyocytes is not significant compared to the either stretched or lifted cardiomyocytes. These results suggest that as an extrinsic mechanical cue, cyclic stretch can induce intrinsic changes in junctional proteins, either in adherent or lifted cardiomyocytes.

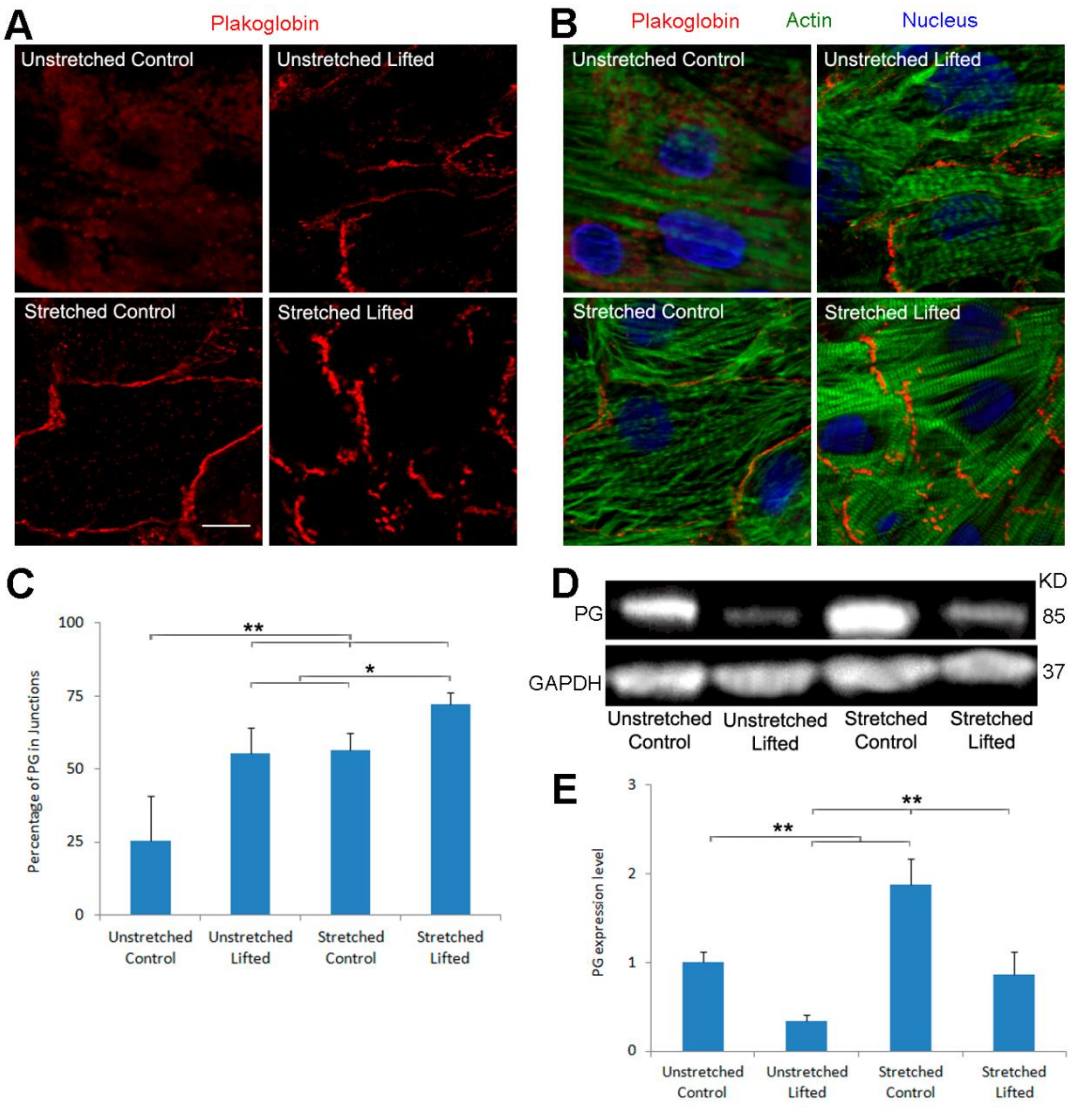

Figure 4. 4 Plakoglobin is significantly altered in lifted cardiac sheets.

Immunofluorescence images are shown of (A) plakoglobin (PG) and (B) triple staining for plakoglobin, actin and nuclei in unstretched control (top left), unstretched partial-lifted (top right), stretched control (bottom left) and stretched, partial-lifted (bottom right) cells. Partially-lifted sheets were subject to cyclic stretch for 2hr at 20% strain and 1 Hz before staining. Red: PG, Green: actin, Blue: nucleus. Scale bar: 20 μm. (C) Quantification of junctional PG reveals elevated junctional accumulation in both lifted and stretched cells. (D) and (E) Western blot analysis shows significant reduction of total cellular PG when cell-substrate adhesion was lost, while cyclic stretch caused substantial up-regulation of PG, especially in the lifted cells. The y-axis represents relative PG expression level, with values normalized to the unstretched control. GAPDH was used as a loading control. * $p<0.05$, ** $p<0.01$.

4.3.5 Plakoglobin RNA interference weakens lifted sheet strength

To further evaluate the adhesive structural role that plakoglobin plays in maintaining cardiac sheet integrity, siRNA transfection was performed to determine whether plakoglobin knockdown could reduce the mechanical strength or cohesion of the lifted cardiac sheets. Similar to actin disruption, plakoglobin siRNA knockdown led to more fragile cardiac sheets (Figure 4.5). The tears in mechanically conditioned cardiac sheets precluded tensile tests or shear tests. These results further confirm the importance of junctional plakoglobin in maintaining cardiac sheet biomechanical properties, but also provide support for the notion that mechanical forces directly regulate cell-cell junctional dynamics, as witnessed in the cases of plakoglobin-related

embryonic lethal death and ARVD, where inactivation of the plakoglobin results in either embryonic lethality or sudden death due to cardiac rupture [22,200].

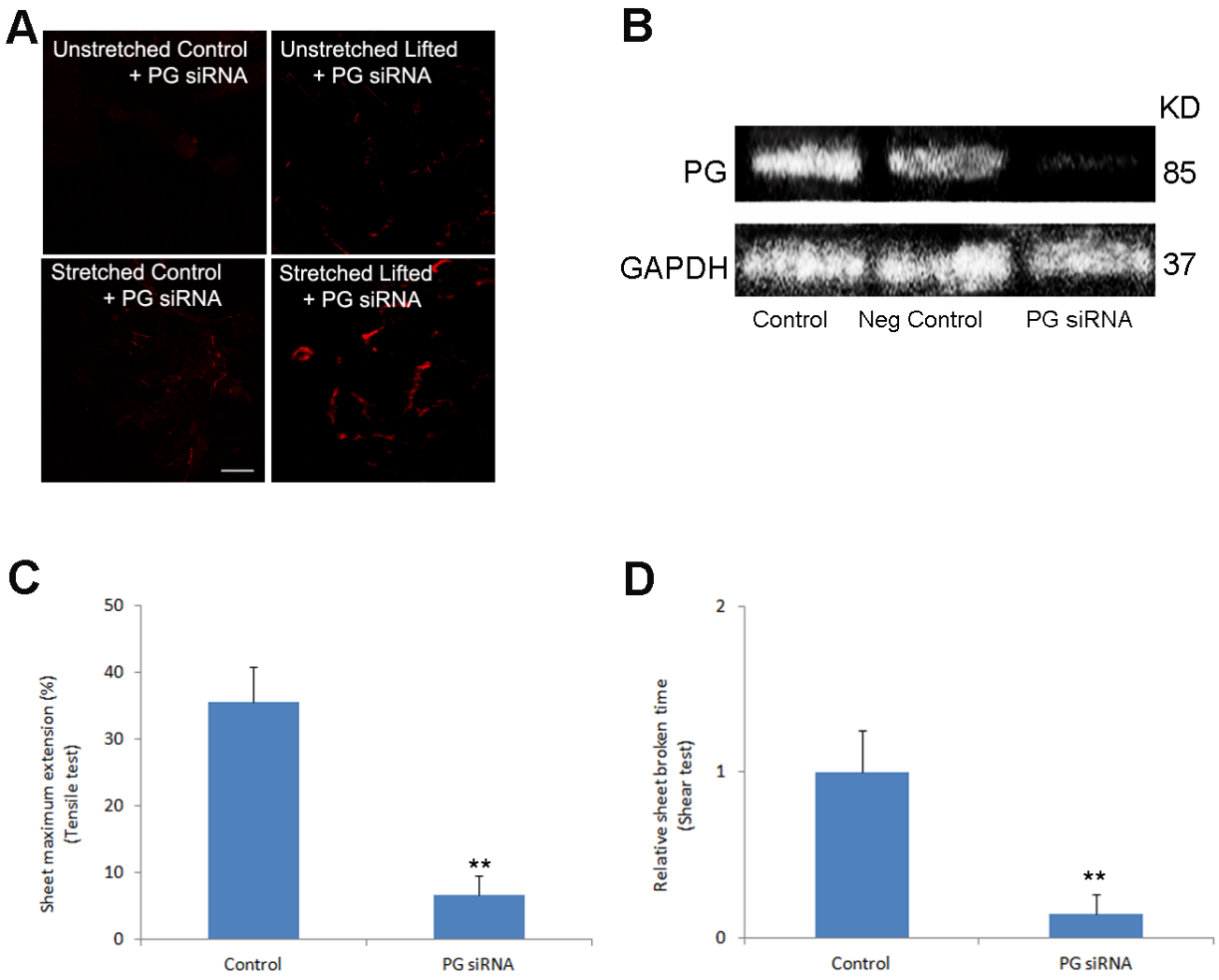

Figure 4. 5 Plakoglobin RNA interference weakens lifted cardiac sheet strength.

(A) Immunofluorescence images of PG with siRNA knockdown in unstretched control (top left), unstretched lifted (top right), stretched control (bottom left) and stretched lifted (bottom right) cells. Scale bar: 20 μm. (B) Western blot analysis shows significant reduction of total cellular PG with siRNA knockdown four days after transfection (PG siRNA). Shown was result from the unstretched control sample. GAPDH was used as a loading control. Both (C) tensile test and (D)

shear test show siRNA knockdown of PG significantly reduce the mechanical strength or cohesion of the lifted cardiac sheets. *$p<0.05$ and **$<p<0.01$ compared to the matched control.

4.3.6 Calcium signaling is enhanced in lifted cardiac sheets

Recent studies demonstrated that cardiac intracellular free Ca^{2+} ($[Ca^{2+}]_i$) is a major mediator of excitation-contraction coupling[201,202] and alterations in $[Ca^{2+}]_{i\ I}$ regulation may contribute to cardiac mechanical dysfunction and arrhythmogenesis [203,204]. Thus, it is imperative to have a clear and relatively quantitative understanding of how ($[Ca^{2+}]_i$ changes in the substrate-free cardiac sheets and how mechanical forces may affect ($[Ca^{2+}]_i$ handling. Cells were pre-loaded with Fluo-3 AM (an indicator of $[Ca^{2+}]_i$ or Ca^{2+} transients signal intensity) before dispase lifting and imaging. After losing cell-substrate contact, the lifted cardiomyocytes exhibited a significant 54% increase in $[Ca^{2+}]_i$ (Figures 4.6 A and 4.6C, peak - base). For comparison purpose, cardiomyocytes cultivated on rigid tissue culture dishes displayed similar enhanced $[Ca^{2+}]_i$ pattern, though at a much smaller scale, after being detached from the substrate (Figures 4.6 B, bottom).

Next, we showed that mechanical conditioning resulted in a significant 109% increase of $[Ca^{2+}]_i$ for adhering cells compared to unstretched adhering cells. The results are in agreement with other studies showing that various mechanical stimuli could enhance $[Ca^{2+}]_i$ uptake [201,205]. Interestingly, for lifted cells, mechanical conditioning resulted in a significant 121% increase of $[Ca^{2+}]_i$ compared to unstretched adhering cells, or a 44% increase compared to unstretched lifted cells, but no significant difference compared to stretched control cells, indicating the gain in calcium handling from stretching and lifting reached a plateau. These

results suggest the substrate-free cardiac sheet maintains its excitation-contraction coupling capability and mechanical stimulation plays important roles on $[Ca^{2+}]_i$ handling.

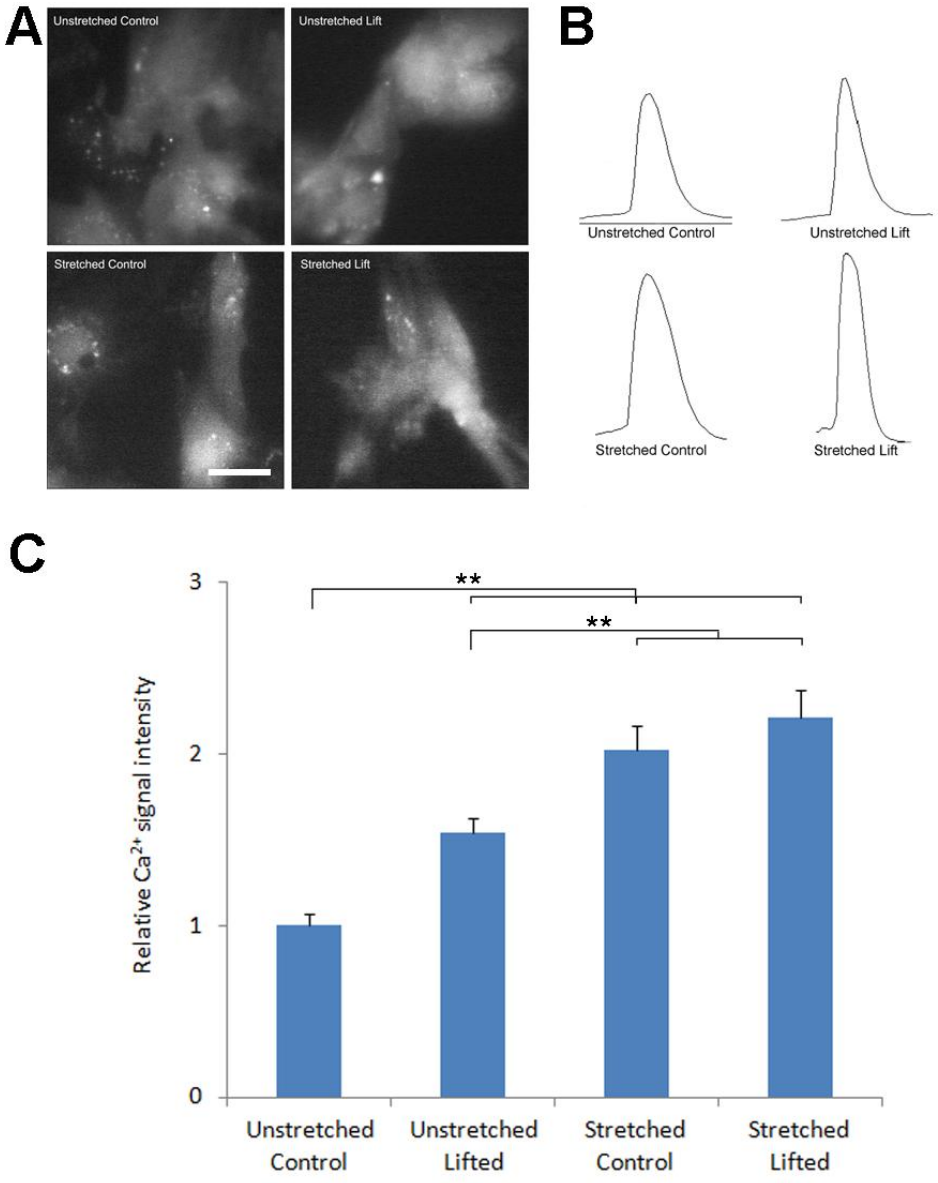

Figure 4. 6 Calcium signaling is enhanced in lifted cardiac sheets.

Representative immunofluorescence images of (A) Ca^{2+} signal and (B) Ca^{2+} transients in unstretched control (top left), unstretched partial-lifted (top right), stretched control (bottom left) and stretched, partial-lifted (bottom right) cells four days after plating. For comparison purposes,

(B) Ca^{2+} transients captured with cardiac cells cultured on stiff substrate at both adherent control and lifted conditions. Scale bar: 20 μm. (C) Quantitative analysis of (A) shows significant increase of relative intracellular free Ca^{2+} ($[Ca^{2+}]_i$) or Ca^{2+} signal intensity (peak - base or maximum - minimum) after lifting from the substrates and mechanical conditioning. **$p<0.01$.

4.3.7 Viscoelastic property is significantly altered in lifted cardiac sheets

Many cellular processes, such as translocation of organelles, are controlled partly by the mechanical deformability or local viscoelastic properties of the cytoplasm [206,207]. A new type of functional microscopy called multiple-particle-tracking microrheology, which measures the local viscoelastic properties of living cells by monitoring the Brownian motion of individual microinjected or endocytosized fluorescent particles, was recently introduced [199]. In most cells, viscoelastic properties of adherent cells are generally dominated by the actin filament cytoskeleton [198]. Here we used this technique to investigate if and how the viscoelastic properties of cardiomyocyte cytoplasm respond to losing cell-substrate contact and mechanical conditioning. After being cyclically stretched, adhering cells showed lower a mean-square-displacement (MSD) compared to the unstretched adherent control (Figures 4.7), suggesting mechanical stretch resulted in a stiffer cytoplasm, which correlates with the finding that mechanical stretch simultaneously resulted in an up-regulation of cellular actin expression level (Figure 4.3). This result is agreement with other studies showing cytoplasmic stiffening response to other types of mechanical conditioning such as fluid flow [208,209]. After detaching from the substrate, the lifted cardiomyocytes exhibited higher MSD compared to the unstretched adherent control, suggesting a softer cytoplasm, which correlates

with the finding that losing cell-substrate contact simultaneously resulted in a down-regulation of cellular actin expression level (Figure 4.3). Moreover, after being cyclically stretched, lifted cardiomyocytes displayed a slightly lower MSD, or a stiffer cytoplasm, compared to the unstretched lifted cells (Figures 4.7). Again, these results are consistent with the finding that cyclic stretch simultaneously resulted in a slight, but non-significant up-regulation of cellular actin expression level to the lifted cardiomyocytes (Figure 4.3). Another point of note is that the lifted cardiomyocytes are both much closer to straight lines than the unlifted cells, suggesting they have more fluid-like behavior, which is what we'd expect with loss of actin and stress fibers. Together, these results help reveal new mechanistic insights concerning cytoplasm viscoelastic property of the partially lifted cardiac sheets, suggest that cells inside the cardiac sheets constantly adapt to changing environmental conditions through coordinated molecular and mechanical responses.

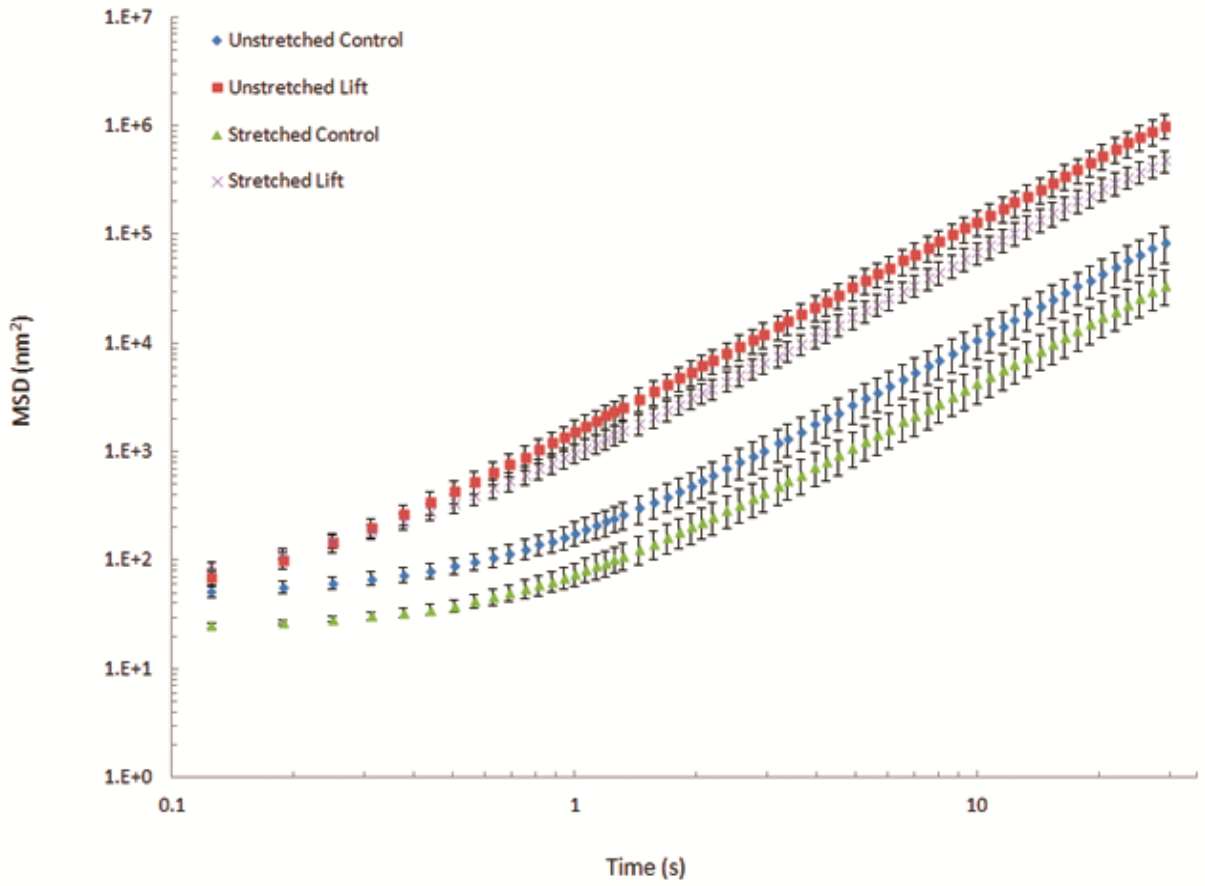

Figure 4. 7 Viscoelastic property is significantly altered in lifted cardiac sheets.

Detaching from the substrate resulted in apparently higher MSD, or softer cytoplasm, compared to the adherent control cells. Mechanical stretching resulted in slight slower MSD, or stiffer cytoplasm, compared to the unstretched control cells. The changes in MSD are consistent with the changes of cellular actin expression level shown in Figure 4.3.

4.4 Discussion

In this study we developed a novel method to generate partially-lifted, mechanically strong and minimally shrunk, substrate- and scaffold-free cardiomyocyte sheets. Experimentation on these partially lifted cell sheets may provide critical information on cell-cell interactions, which have numerous downstream applications in tissue engineering, investigation of certain genetic and autoimmune diseases, and embryonic development and cell and tissue mechanics, particularly for cardiac myocytes.

Examining cell-cell interactions in primary cells for downstream application is challenging. In this study, we demonstrate that it is possible to partially-lift, mechanically condition and perform assays on cardiac myocytes by prestretching the cells and limiting the interface between attached and lifted cells to two lines rather than a perimeter. We further show that in the lifted cardiac sheets, the basic physiology of cardiomyocytes is significantly altered, with diminished intracellular actin and plakoglobin, but elevated actin and plakoglobin at cell-cell junctions, elevated MSD (lower complex modulus) and enhanced calcium signaling. We propose that partial lifting offers a way to mechanically condition cell sheets for tissue engineering purposes, given that mechanical fragility is an ongoing concern in this field. Further, this method offers a robust method to systematically examine cell junctional function in more detail, with minimal cross-talk from cell-substrate interactions. The results confirm our original hypothesis that when cell-cell interactions dominate and are subject to mechanical conditioning, increased tension at intercellular junctions leads to recruitment of junctional components, leading to further enhancement of junctional tension in a positive mechanosensory feedback loop [171,172].

In general, compared with adult human keratinocytes in Chapter 3, rat neonatal cardiomyocytes display changes in a similar pattern regarding cell-cell adhesive strength, actin and plakoglobin expression and distribution, etc., although the changes in cardiac sheets are smaller than those in keratinocytes. These results suggest that to certain degree, actin (and likely other cytoskeletal proteins) and plakoglobin (and likely other junctional proteins) play somewhat similar roles in regulating cell-cell interactions in these two cell types (and likely other cell types). The diminished dynamic response of rat neonatal cardiomyocytes can be attributed to several causes. First, adult cells may have more mature mechanotransductive structures; and second, unlike keratinocytes, cardiomyocytes don't exist by themselves in their native *in vivo* environment; fibroblasts and endothelial cells also play critical roles in supporting the proper functions of cardiomyocytes. Therefore, co-culture of rat neonatal cardiomyocytes, fibroblasts and endothelial cells may enhance the responses and further improve the biomechanical properties of the cardiac sheets.

Plakoglobin was chosen for examination primarily because it can bind to both adherens junctions and desmosomes [33] and is closely associated with sarcomeric actin filaments [183-185]. Moreover, plakoglobin is essential for myocardial functions as shown in plakoglobin-associated cardiac defects [59], Naxos disease or ARVC where malfunction of plakoglobin is thought to contribute to the damages of tissue integrity and mechanical signaling transduction [60,61]. Our data are consistent with the observation that the cardiac cell's ability to convert mechanical perturbations into biological signaling cascades is based on the integrity of the junctional-cytoskeletal linkages [8,9,11,29,71]. From this perspective, intercellular junctions may serve as mechanically-sensitive signaling hubs that participate in mechanotransduction [167,168]. Moreover, stretch is a well-documented stimulus for many cardiac functions including junctional

gene expression and cell-to-cell communication remodeling [111-115,188-191]. When cell-cell interactions dominate, stretch may strengthen the intercellular junctional-cytoskeletal network through mechanical strain-stiffening [169,170] or signaling-mediated reinforcement [4,157]. However, we can't rule out the possibility that this cell-junction related mechanism may not be the only one, or even the cell junctions may play only a passive role – keeping the cells together. There are several mechanisms whereby stretching will lead to mechanotransduction without signaling through cell junctions. For example, ion channels may activate via stretch [210,211].

In the heart, mechanotransduction is necessary for balancing cell and tissue structure and function. The dynamic junctional accumulation of intercellular junctions and the cytoskeleton in response to losing cell-substrate interactions and mechanical stretch suggest that a mechanosensory feedback is involved in junctional and cytoskeletal remodeling. Intercellular junctions have been postulated as mechanically-sensitive molecular signaling hubs that contribute to the process of mechanotransduction [167]. Like roles that focal adhesions play in cell-substrate interactions, intercellular junctions can act as mechanosensors and probe the physical properties of the microenvironment and activate specific signaling pathways within the cells [168]. The ability to convert physical perturbations into discrete signaling cascades is based on the integrity of the intercellular junctions-cytoskeleton syncytium [8,9,11,29,71], which is constantly maintained under certain level of stress, reinforces upon stimulation (as in the cases of losing cell-substrate contact and stretch) and disintegrates upon relaxation (as in the cases of cytochalasin D treatments and plakoglobin RNA interference). Furthermore, one of many responses triggered by mechanical stimulation is cytoskeletal reorganization, closing a feedback loop between mechanosensitivity and structural remodeling as myocytes attempt to reach homeostasis. Therefore, it is reasonable to speculate that upon stretching, increased tension at

intercellular junctions could lead to increased recruitment of junctional components, which in turn would recruit more actin, leading to further enhancement of junctional tension and thus building up a positive mechanosensory feedback loop [171,172]. Figure 4.8A schematically describes the four conditions concerning force balances among neighboring cells and substrates that were investigated in this study. As illustrated in Figure 4.8B, similar to well-studied cell-substrate interactions, we propose that there exists an integrated intercellular junction-cytoskeleton feedback mechanotransduction loop in the lifted cell sheet where cell-cell interactions dominate. First, mechanical forces acting on intercellular junctions activate mechanical sensing processes that lead to mechanical responses. Next, these mechanical cues activate an intracellular signaling cascade and eventually lead to a new state of force homeostasis.

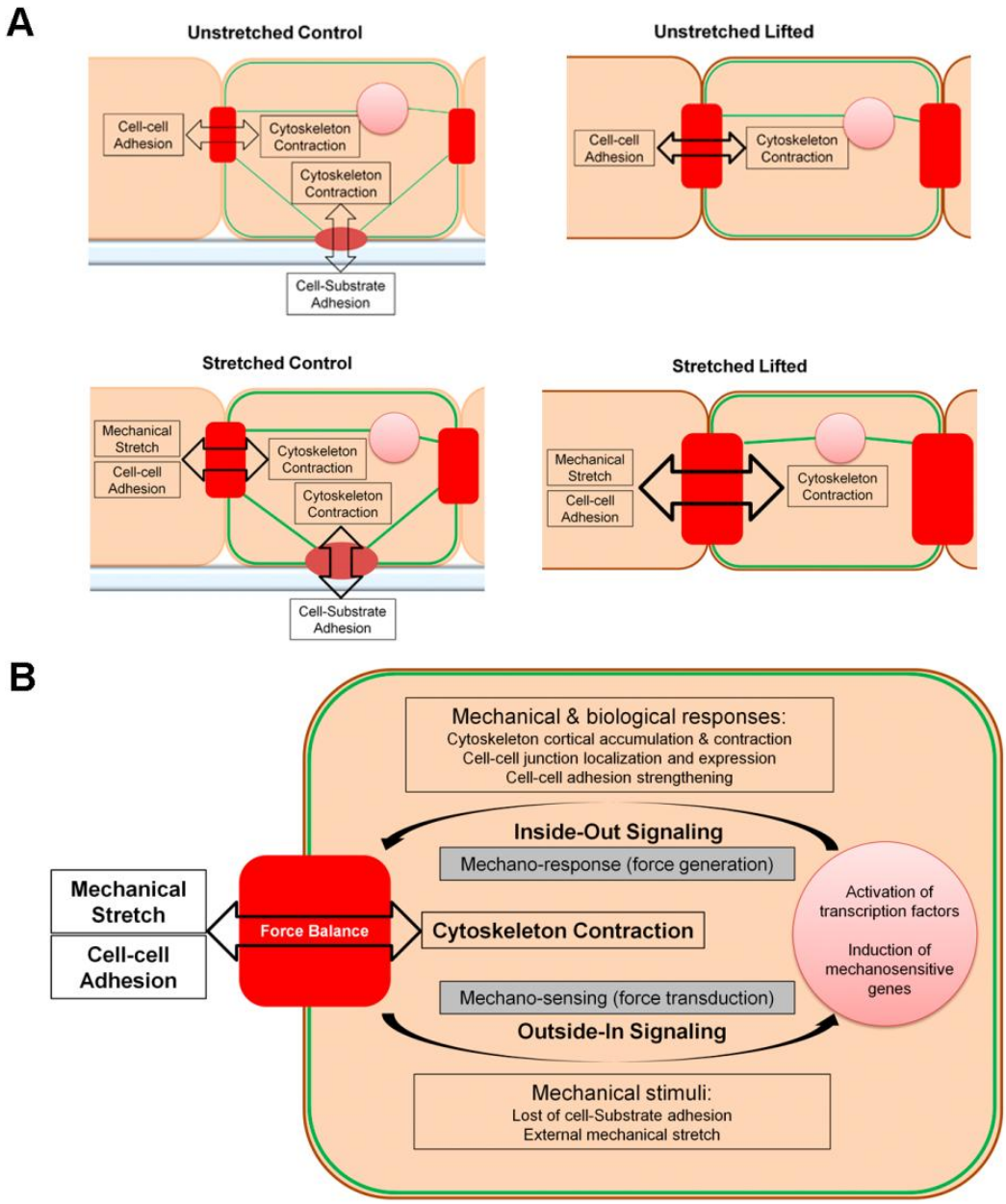

Figure 4. 8 Hypothesized intercellular junction-cytoskeleton mechanotransduction loop in the partially lifted cell sheets.

(A) Schematic illustration of force balances among neighboring cells and substrate in four conditions: unstretched control (top left), unstretched lifted (top right), stretched control (bottom left) and stretched lifted (bottom right). (B) Integrated intercellular junction - cytoskeleton

positive feedback mechanotransduction loop. Mechanical forces trigger biochemical signaling cascades by acting on intercellular junctions and activating mechanical sensing processes that lead to mechanical responses. (1) Outside-In Signaling. Plakoglobin (or other junctional proteins) may act as a surface receptor for forces that tug on cells either by losing cell-substrate adhesion or external mechanical stretch. (2) Inside-Out Signaling. This induces an intracellular signaling cascade, which includes events such as cytoskeleton cortical localization and contraction, intercellular junction localization and expression, and eventually leads to cell-cell adhesion enhancement. During this junction-cytoskeleton mechanotransduction process, the mechanical responses will be felt as a pulling force by the neighboring cell that initiated the cascade, leading to cooperative interactions and achieving a new state of force balance between cells.

For tissue engineering purpose, our novel dispase-based partial-lift cell sheet harvesting approach has the advantage of being biocompatible, easily applicable, rapidly collectable and stretchable compared to currently available cardiac sheet harvesting methods. So far the most popular cardiac sheet harvesting method is using modified thermo-responsive polymeric surfaces [109,110,151]. However, there are several limitations of this technique, including high cost of preparing the modified surface and long cell sheet harvesting time, which typically takes around an hour. More importantly, those cardiac sheets are mechanically fragile, typically requiring heterogeneous external supports such as chitin membranes, polyethylene meshes or stacking of multiple sheets. Another major challenge is cardiac sheet shrinking. When no external support was used, the detached cardiac sheets shrunk to one-tenth of their original size before lifting, which significantly impairs the sheet's ability to provide sufficient coverage [151]. Our novel partial-lift methods successfully addressed these challenges. The dispase is relative cheap and its action on cardiomyocyte sheet takes as little as five minutes. Moreover, dispase primarily targets

type IV collagen in the lamina densa region. In cardiomyocytes, the main ECM proteins are type I and III collagen [212]. Therefore, the ECM-focal adhesions-stress fibers structure is relatively less digested by dispase and cardiomyocytes after detached from culture substrate and thus still maintain their basic functions. Therefore, mechanically conditioning the partially lifted cardiac sheets provides a solution to generate strong, minimally shrunk cardiac sheets with enhanced beating and calcium signaling.

Further work in this area may involve examination of other junctional components, as well as examining the potential roles, if any, for focal adhesion proteins that are dissociated upon lifting. A more thorough analysis of rheological properties and decomposition into the bulk and loss moduli may reveal functional changes within the cardiac cells. Finally, a more comprehensive characterization of the mechanoresponse of lifted cells would be necessary to further develop models of mechanotransduction. The method we developed here can potentially apply to other primary cells and thus offer a new opportunity to study many different aspects of cell biology and biomechanics.

4.5 Supplemental study

4.5.1 Cadherins are significantly altered in lifted cardiac sheets

Cyclic stretch resulted in significantly changes in expression and distribution of fascia adherens junction protein cadherins (Figures 4.S1A and 1B). After losing cell-substrate contact, the lifted cardiomyocytes exhibited enhanced junctional localization of cadherins. The percentage of immunoreactive signal of cadherins at the cell junctions was significantly increased from 62% in unstretched attached cells to 82% after being lifted, or to 83% after being stretched while remaining attached, or to 84% after being lifted and stretched, indicating the gain in junctional localization of cadherins from stretching and lifting reaches a plateau. Western blot analysis (relative to unstretched, unlifted cells) revealed that lifting cells resulted in a 63% decrease in the total expression level of cadherins (Figure 4.S1C and 1D). Stretching led to a 41% upregulation of cadherins in attached cells. After lifting, stretching led to a significant 14% decrease of cadherins when compared to the unstretched, unlifted cells, or an increase of 127% when compared to the unstretched, lifted cells. Thus, for cells in the lifted region, both the spatial arrangement and expression level of cadherins are significantly altered. Overall, the changes of cadherins are similar to plakoglobin, though unlike plakoglobin, the gain in junctional localization of cadherins from stretching and lifting reaches a plateau.

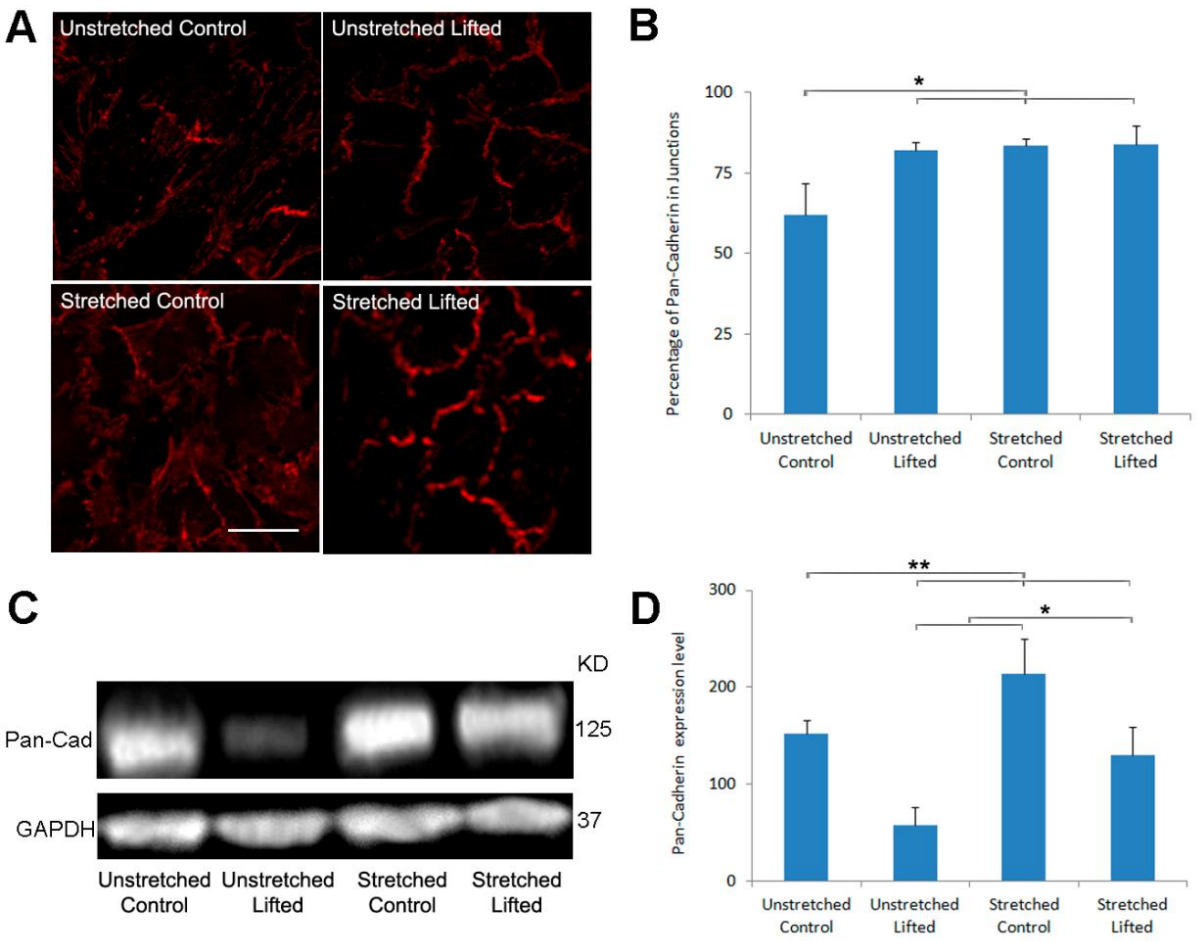

Figure 4. 9 Supplemental Figure S1 Cadherins are significantly altered in lifted cardiac sheets. Immunofluorescence images are shown of cadherins stain in unstretched control (top left), unstretched partial-lifted (top right), stretched control (bottom left) and stretched, partial-lifted (bottom right) cells. Scale bar: 20 μm. (B) Quantification of junctional cadherins reveals elevated junctional accumulation in both lifted or stretched cells, but reaches a plateau in stretched, partial-lifted cells. (C) and (D) Western blot analysis shows significant reduction of total cellular cadherins when cell-substrate adhesion was lost, while stretch caused substantial up-regulation, especially in the lifted cells. The y-axis represents relative cadherins expression level, with values normalized to the unstretched control. GAPDH was used as a loading control. * $p<0.05$, ** $p<0.01$.

4.5.2 Cardiomyocyte bilayer sheets are stronger than monolayer sheets

Here we developed cardiomyocytes (top) and cardiac fibroblasts (bottom) bilayer sheets and measured their mechanical properties using the same mechanical tests for cardiomyocyte monolayer sheets (Figure 4.S2). The unstretched bilayer sheets displayed a near 7 times increases in sheet adhesive strength, suggesting that another supporting cell layer and/or enhanced extracellular matrix secretion, thanks to fibroblasts, is beneficial to cardiac sheet mechanical strength. We speculate that mechanically conditioned bilayer sheets would display even higher adhesive strength.

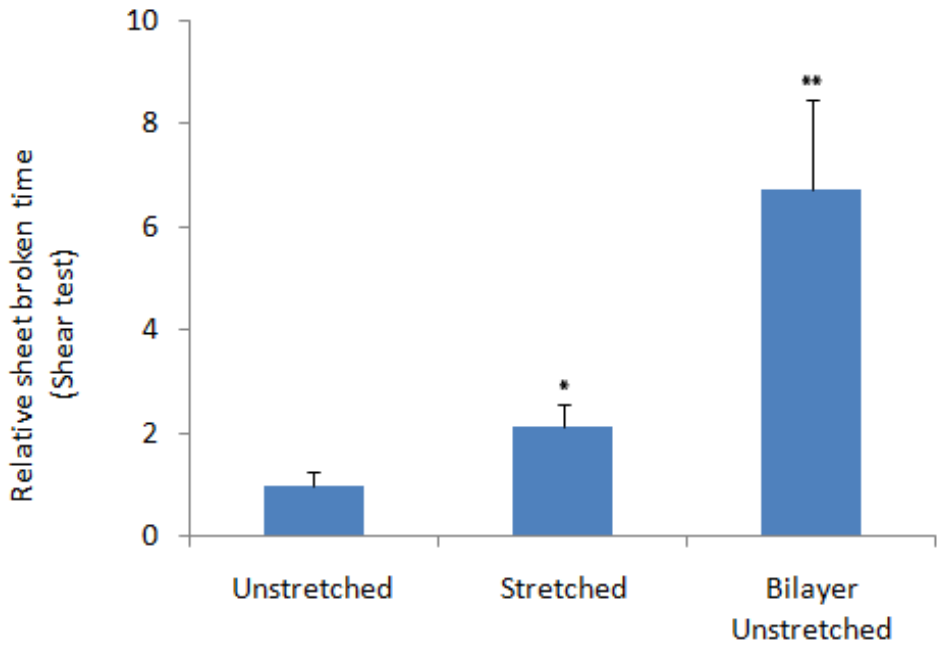

Figure 4. 10 Supplemental Figure S2 Cardiac myocytes and fibroblasts bilayer sheets.

The bilayer sheets are mechanically stronger than cardiomyocyte monolayer sheet.

4.5.3 Cardiomyocyte Markers staining

Immunostaining of specific cardiomyocyte markers, including cardiac troponin I and sarcomeric α-actinin, further validated the identity of isolated cardiomyocytes.

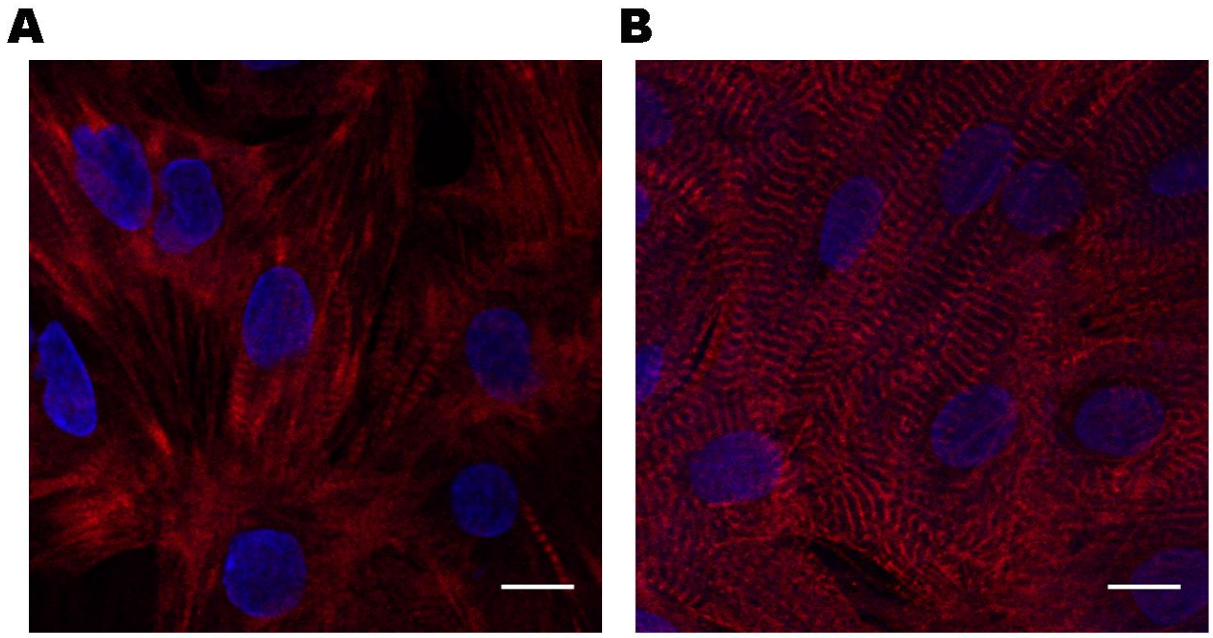

Figure 4. 11 Supplemental Figure S3 Cardiac myocyte markers staining.

(A) Sarcomeric α-actinin and (B) Cardiac troponin I. Scale bar is 10 μm.

4.5.4 Additional microrheology data

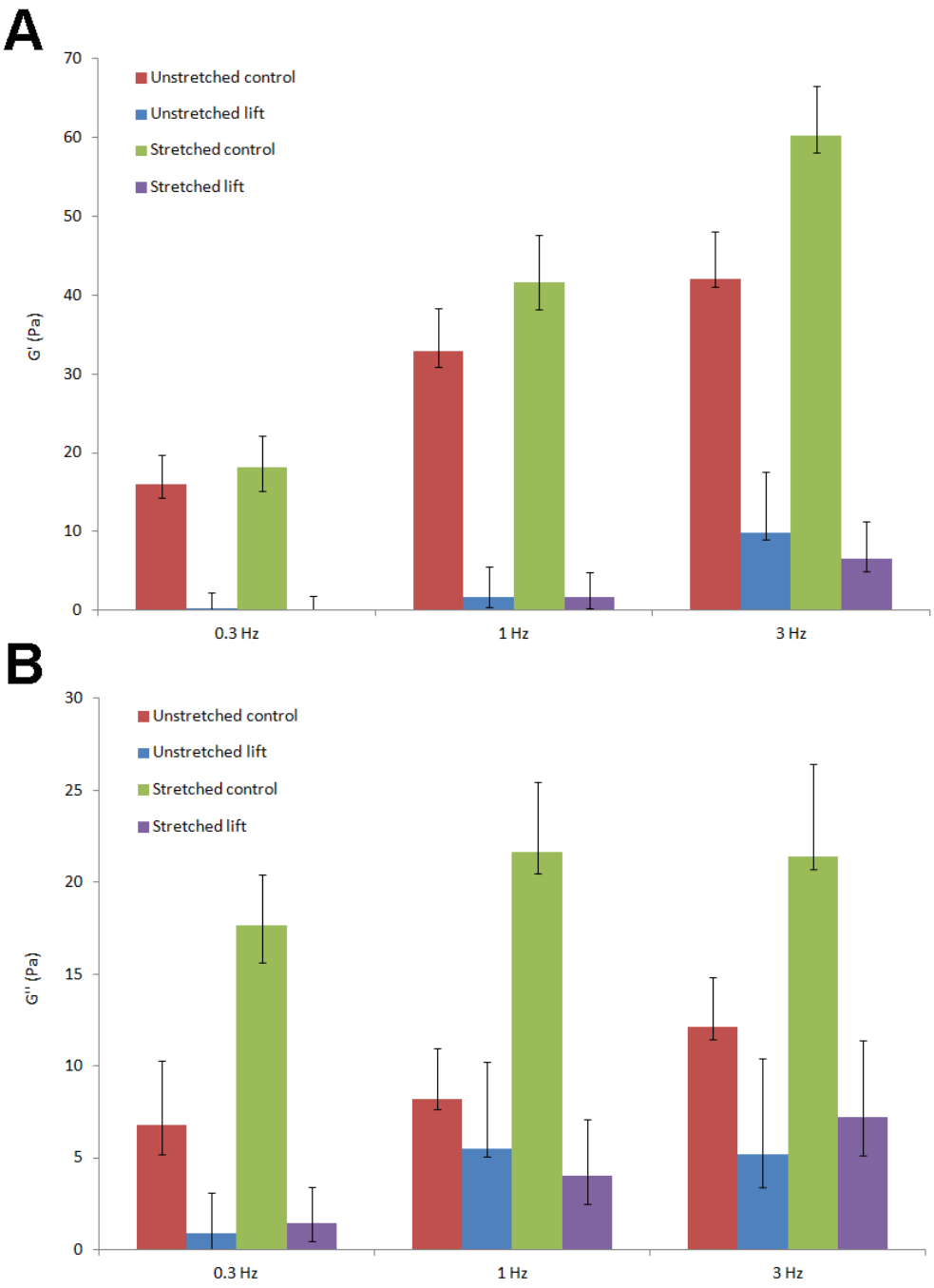

Figure 4. 12 Supplemental Figure S4 Storage modulus G′ and loss modulus G″.

(A) Plot of storage modulus G′ (Pa) vs. frequency (Hz) and (B) loss modulus G″ (Pa) vs. frequency (Hz) for each treatment conditions are compared at three different time lags.

Chapter 5 Summary

Whether adhesion to other cells is important to cell viability is the central question of this study. In Project 1, we show that suspended immortalized human keratinocytes cell sheets with persisting intercellular contacts exhibited significant contraction, junctional actin localization, and reinforcement of cell-cell adhesion strength. Further, cells within these sheets remain viable, in contrast to trypsinized cells suspended without either cell-cell or cell-substrate contact, which underwent apoptosis at high rates. Suppression of plakoglobin weakened cell-cell adhesion in cell sheets and suppressed apoptosis in suspended, trypsinized cells. These results demonstrate that cell-cell contact may be fundamental control mechanism governing cell viability and that the junctional protein plakoglobin is a key regulator of this process. These findings could have significant implications for understanding cell adhesion, modeling disease progression, developing therapeutics and improving the viability of tissue engineering protocols. These results provide a solid foundation for future characterization and manipulation of viable cell sheets for cell sheet engineering purpose.

There is a need to characterize biomechanical cell-cell interactions, but due to a lack of suitable experimental methods, relevant *in vitro* experimental data are often masked by cell-substrate interactions. In project 2 we presented a novel method to generate partially-lifted substrate-free cell sheets which engage primarily in cell-cell interactions, yet are amenable to biological and chemical perturbations and, importantly, mechanical conditioning. Results demonstrate that the mechanical strength and cohesion of the substrate-free cell sheets strongly depend on integrity of the actomyosin cytoskeleton and the cell-cell junctional protein plakoglobin. Both actin and plakoglobin are significantly reinforced at junctions with mechanical

conditioning. These results represent a first systematic examination of mechanical conditioning and the cytoskeleton on cells with primarily intercellular interactions.

Cardiac cell sheet tissue engineering has recently emerged as a promising alternative therapeutic option for heart diseases. However, the cardiac sheets harvested via currently available techniques suffer several drawbacks such as fragility and shrinking. To address these drawbacks, in Project 3 we further refined the partial-lift technique. Results show that mechanical conditioning resulted in junctional reinforcement. Further results demonstrate that the mechanical strength and cohesion of the substrate-free cardiac sheets strongly depend on integrity of the actin cytoskeleton and the cell junctional protein plakoglobin. Moreover, we showed mechanical conditioning could enhance contraction, calcium signaling, alter viscoelastic property, and thus improve the functional cell-cell coupling in the cardiac sheets. Direct experimental investigations on cardiac cell sheets without interference of cell-substrate interactions will greatly enhance our understanding of cell-cell interactions and improve cardiac cell sheets mechanical properties. For tissue engineering purpose, our dispase-based partial-lift cell sheet harvesting method has the advantage of being biocompatible, easily applicable, rapidly collectable and stretchable, compared to currently available techniques. This simple yet powerful partial lift technique has enormous potential for fabricating clinically applicable cardiac tissues.

Benefiting from collaboration between molecular techniques and biomedical engineering methods, the study of cell junctions is moving at a rapid pace. Specifically for scaffold-less cardiac sheet engineering, future research is likely to focus on improving our ability to find the right (1) stem cell sources (such as induced pluripotent stem cells) and (2) biomimetic culture condition (such as specific physiological stimulation regimen and bioreactor design considerations). Though many challenges remain, this technology platform presents

exciting new opportunities for a wide variety of applications such as for studies in developmental pathways, disease modeling, drug discovery, predictive cardiotoxicity and ultimately cardiac regeneration.

References

1. Kobielak A, Fuchs E (2006) Links between alpha-catenin, NF-kappaB, and squamous cell carcinoma in skin. Proc Natl Acad Sci U S A 103: 2322-2327.

2. Maniotis AJ, Chen CS, Ingber DE (1997) Demonstration of mechanical connections between integrins, cytoskeletal filaments, and nucleoplasm that stabilize nuclear structure. Proc Natl Acad Sci U S A 94: 849-854.

3. Geiger B, Bershadsky A (2002) Exploring the neighborhood: adhesion-coupled cell mechanosensors. Cell 110: 139-142.

4. Matthews BD, Overby DR, Mannix R, Ingber DE (2006) Cellular adaptation to mechanical stress: role of integrins, Rho, cytoskeletal tension and mechanosensitive ion channels. J Cell Sci 119: 508-518.

5. Mannix RJ, Kumar S, Cassiola F, Montoya-Zavala M, Feinstein E, et al. (2008) Nanomagnetic actuation of receptor-mediated signal transduction. Nat Nanotechnol 3: 36-40.

6. Chen CS, Mrksich M, Huang S, Whitesides GM, Ingber DE (1997) Geometric control of cell life and death. Science 276: 1425-1428.

7. Cadigan KM, Peifer M (2009) Wnt signaling from development to disease: insights from model systems. Cold Spring Harb Perspect Biol 1: a002881.

8. Franke WW (2009) Discovering the molecular components of intercellular junctions--a historical view. Cold Spring Harb Perspect Biol 1: a003061.

9. Green KJ, Getsios S, Troyanovsky S, Godsel LM (2010) Intercellular junction assembly, dynamics, and homeostasis. Cold Spring Harb Perspect Biol 2: a000125.

10. Huang H, Cruz F, Bazzoni G (2006) Junctional adhesion molecule-A regulates cell migration and resistance to shear stress. J Cell Physiol 209: 122-130.

11. Wei Q, Hariharan V, Huang H (2011) Cell-cell contact preserves cell viability via plakoglobin. PLoS One 6: e27064.

12. Wei Q, Reidler D, Shen MY, Huang H (2013) Keratinocyte cytoskeletal roles in cell sheet engineering. BMC Biotechnol 13: 17.

13. Wei Q, Huang H (2013) Insights into the role of cell-cell junctions in physiology and disease. Int Rev Cell Mol Biol 306: 187-221.

14. Yoshioka J, Prince RN, Huang H, Perkins SB, Cruz FU, et al. (2005) Cardiomyocyte hypertrophy and degradation of connexin43 through spatially restricted autocrine/paracrine heparin-binding EGF. Proc Natl Acad Sci U S A 102: 10622-10627.

15. Abedin M, King N (2008) The premetazoan ancestry of cadherins. Science 319: 946-948.

16. Adams CL, Nelson WJ, Smith SJ (1996) Quantitative analysis of cadherin-catenin-actin reorganization during development of cell-cell adhesion. J Cell Biol 135: 1899-1911.

17. Bloor JW, Kiehart DP (2002) Drosophila RhoA regulates the cytoskeleton and cell-cell adhesion in the developing epidermis. Development 129: 3173-3183.

18. Cavey M, Rauzi M, Lenne PF, Lecuit T (2008) A two-tiered mechanism for stabilization and immobilization of E-cadherin. Nature 453: 751-756.

19. Knudsen KA, Wheelock MJ (1992) Plakoglobin, or an 83-kD homologue distinct from beta-catenin, interacts with E-cadherin and N-cadherin. J Cell Biol 118: 671-679.

20. Hoshino T, Sakisaka T, Baba T, Yamada T, Kimura T, et al. (2005) Regulation of E-cadherin endocytosis by nectin through afadin, Rap1, and p120ctn. J Biol Chem 280: 24095-24103.

21. Nose A, Nagafuchi A, Takeichi M (1988) Expressed recombinant cadherins mediate cell sorting in model systems. Cell 54: 993-1001.

22. Bierkamp C, McLaughlin KJ, Schwarz H, Huber O, Kemler R (1996) Embryonic heart and skin defects in mice lacking plakoglobin. Dev Biol 180: 780-785.

23. Chen X, Bonne S, Hatzfeld M, van Roy F, Green KJ (2002) Protein binding and functional characterization of plakophilin 2. Evidence for its diverse roles in desmosomes and beta -catenin signaling. J Biol Chem 277: 10512-10522.

24. Bagnat M, Cheung ID, Mostov KE, Stainier DY (2007) Genetic control of single lumen formation in the zebrafish gut. Nat Cell Biol 9: 954-960.

25. Carlton VE, Harris BZ, Puffenberger EG, Batta AK, Knisely AS, et al. (2003) Complex inheritance of familial hypercholanemia with associated mutations in TJP2 and BAAT. Nat Genet 34: 91-96.

26. Abrams CK, Freidin MM, Verselis VK, Bargiello TA, Kelsell DP, et al. (2006) Properties of human connexin 31, which is implicated in hereditary dermatological disease and deafness. Proc Natl Acad Sci U S A 103: 5213-5218.

27. Anselmi F, Hernandez VH, Crispino G, Seydel A, Ortolano S, et al. (2008) ATP release through connexin hemichannels and gap junction transfer of second messengers propagate Ca2+ signals across the inner ear. Proc Natl Acad Sci U S A 105: 18770-18775.

28. Bergoffen J, Scherer SS, Wang S, Scott MO, Bone LJ, et al. (1993) Connexin mutations in X-linked Charcot-Marie-Tooth disease. Science 262: 2039-2042.

29. Holen I, Whitworth J, Nutter F, Evans A, Brown HK, et al. (2012) Loss of plakoglobin promotes decreased cell-cell contact, increased invasion, and breast cancer cell dissemination in vivo. Breast Cancer Res 14: R86.

30. Green KJ, Getsios S, Troyanovsky S, Godsel LM (2010) Intercellular Junction Assembly, Dynamics, and Homeostasis. Cold Spring Harbor Perspectives in Biology 2: -.

31. Stepniak E, Radice GL, Vasioukhin V (2009) Adhesive and signaling functions of cadherins and catenins in vertebrate development. Cold Spring Harb Perspect Biol 1: a002949.

32. Cavey M, Lecuit T (2009) Molecular bases of cell-cell junctions stability and dynamics. Cold Spring Harb Perspect Biol 1: a002998.

33. McCrea PD, Gu D, Balda MS (2009) Junctional music that the nucleus hears: cell-cell contact signaling and the modulation of gene activity. Cold Spring Harb Perspect Biol 1: a002923.

34. Walters BD, Stegemann JP (2013) Strategies for directing the structure and function of three-dimensional collagen biomaterials across length scales. Acta Biomater.

35. de Peppo GM, Marcos-Campos I, Kahler DJ, Alsalman D, Shang L, et al. (2013) Engineering bone tissue substitutes from human induced pluripotent stem cells. Proc Natl Acad Sci U S A 110: 8680-8685.

36. Shimizu T, Yamato M, Kikuchi A, Okano T (2003) Cell sheet engineering for myocardial tissue reconstruction. Biomaterials 24: 2309-2316.

37. Yang J, Yamato M, Shimizu T, Sekine H, Ohashi K, et al. (2007) Reconstruction of functional tissues with cell sheet engineering. Biomaterials 28: 5033-5043.

38. Correia C, Bhumiratana S, Yan LP, Oliveira AL, Gimble JM, et al. (2012) Development of silk-based scaffolds for tissue engineering of bone from human adipose-derived stem cells. Acta Biomater 8: 2483-2492.

39. Godier-Furnemont AF, Martens TP, Koeckert MS, Wan L, Parks J, et al. (2011) Composite scaffold provides a cell delivery platform for cardiovascular repair. Proc Natl Acad Sci U S A 108: 7974-7979.

40. Hersch N, Wolters B, Dreissen G, Springer R, Kirchgessner N, et al. (2013) The constant beat: cardiomyocytes adapt their forces by equal contraction upon environmental stiffening. Biol Open 2: 351-361.

41. Majkut SF, Discher DE (2012) Cardiomyocytes from late embryos and neonates do optimal work and striate best on substrates with tissue-level elasticity: metrics and mathematics. Biomech Model Mechanobiol 11: 1219-1225.

42. Jacot JG, McCulloch AD, Omens JH (2008) Substrate stiffness affects the functional maturation of neonatal rat ventricular myocytes. Biophys J 95: 3479-3487.

43. Harris AR, Peter L, Bellis J, Baum B, Kabla AJ, et al. (2012) Characterizing the mechanics of cultured cell monolayers. Proc Natl Acad Sci U S A 109: 16449-16454.

44. Jamora C, Fuchs E (2002) Intercellular adhesion, signalling and the cytoskeleton. Nat Cell Biol 4: E101-108.

45. El-Amraoui A, Petit C (2013) Cadherin defects in inherited human diseases. Prog Mol Biol Transl Sci 116: 361-384.

46. Lai-Cheong JE, Arita K, McGrath JA (2007) Genetic diseases of junctions. J Invest Dermatol 127: 2713-2725.

47. Kottke MD, Delva E, Kowalczyk AP (2006) The desmosome: cell science lessons from human diseases. J Cell Sci 119: 797-806.

48. Brooke MA, Nitoiu D, Kelsell DP (2012) Cell-cell connectivity: desmosomes and disease. J Pathol 226: 158-171.

49. Hesketh GG, Van Eyk JE, Tomaselli GF (2009) Mechanisms of gap junction traffic in health and disease. J Cardiovasc Pharmacol 54: 263-272.

50. Hamosh A, Scott AF, Amberger JS, Bocchini CA, McKusick VA (2005) Online Mendelian Inheritance in Man (OMIM), a knowledgebase of human genes and genetic disorders. Nucleic Acids Res 33: D514-517.

51. McKusick VA (2007) Mendelian Inheritance in Man and its online version, OMIM. Am J Hum Genet 80: 588-604.

52. Green KJ, Gaudry CA (2000) Are desmosomes more than tethers for intermediate filaments? Nat Rev Mol Cell Biol 1: 208-216.

53. McGrath JA, McMillan JR, Shemanko CS, Runswick SK, Leigh IM, et al. (1997) Mutations in the plakophilin 1 gene result in ectodermal dysplasia/skin fragility syndrome. Nat Genet 17: 240-244.

54. Amagai M, Klaus-Kovtun V, Stanley JR (1991) Autoantibodies against a novel epithelial cadherin in pemphigus vulgaris, a disease of cell adhesion. Cell 67: 869-877.

55. Ishii K, Amagai M, Hall RP, Hashimoto T, Takayanagi A, et al. (1997) Characterization of autoantibodies in pemphigus using antigen-specific enzyme-linked immunosorbent assays with baculovirus-expressed recombinant desmogleins. J Immunol 159: 2010-2017.

56. Endo H, Rees TD, Hallmon WW, Kuyama K, Nakadai M, et al. (2008) Disease progression from mucosal to mucocutaneous involvement in a patient with desquamative gingivitis associated with pemphigus vulgaris. J Periodontol 79: 369-375.

57. Ding X, Aoki V, Mascaro JM, Jr., Lopez-Swiderski A, Diaz LA, et al. (1997) Mucosal and mucocutaneous (generalized) pemphigus vulgaris show distinct autoantibody profiles. J Invest Dermatol 109: 592-596.

58. Kalantari-Dehaghi M, Anhalt GJ, Camilleri MJ, Chernyavsky AI, Chun S, et al. (2013) Pemphigus vulgaris autoantibody profiling by proteomic technique. PLoS One 8: e57587.

59. Bierkamp C, McLaughlin KJ, Schwarz H, Huber O, Kemler R (1996) Embryonic heart and skin defects in mice lacking plakoglobin. Developmental Biology 180: 780-785.

60. McKoy G, Protonotarios N, Crosby A, Tsatsopoulou A, Anastasakis A, et al. (2000) Identification of a deletion in plakoglobin in arrhythmogenic right ventricular

cardiomyopathy with palmoplantar keratoderma and woolly hair (Naxos disease). Lancet 355: 2119-2124.

61. Asimaki A, Syrris P, Wichter T, Matthias P, Saffitz JE, et al. (2007) A novel dominant mutation in plakoglobin causes arrhythmogenic right ventricular cardiomyopathy. Am J Hum Genet 81: 964-973.

62. Corrado D, Basso C, Thiene G, McKenna WJ, Davies MJ, et al. (1997) Spectrum of clinicopathologic manifestations of arrhythmogenic right ventricular cardiomyopathy/dysplasia: a multicenter study. J Am Coll Cardiol 30: 1512-1520.

63. Garcia-Gras E, Lombardi R, Giocondo MJ, Willerson JT, Schneider MD, et al. (2006) Suppression of canonical Wnt/beta-catenin signaling by nuclear plakoglobin recapitulates phenotype of arrhythmogenic right ventricular cardiomyopathy. J Clin Invest 116: 2012-2021.

64. Miravet S, Piedra J, Miro F, Itarte E, Garcia de Herreros A, et al. (2002) The transcriptional factor Tcf-4 contains different binding sites for beta-catenin and plakoglobin. J Biol Chem 277: 1884-1891.

65. Williams BO, Barish GD, Klymkowsky MW, Varmus HE (2000) A comparative evaluation of beta-catenin and plakoglobin signaling activity. Oncogene 19: 5720-5728.

66. Zhurinsky J, Shtutman M, Ben-Ze'ev A (2000) Differential mechanisms of LEF/TCF family-dependent transcriptional activation by beta-catenin and plakoglobin. Mol Cell Biol 20: 4238-4252.

67. Sobolik-Delmaire T, Reddy R, Pashaj A, Roberts BJ, Wahl JK, 3rd (2010) Plakophilin-1 localizes to the nucleus and interacts with single-stranded DNA. J Invest Dermatol 130: 2638-2646.

68. Bonne S, van Hengel J, Nollet F, Kools P, van Roy F (1999) Plakophilin-3, a novel armadillo-like protein present in nuclei and desmosomes of epithelial cells. J Cell Sci 112 (Pt 14): 2265-2276.

69. Stehbens SJ, Paterson AD, Crampton MS, Shewan AM, Ferguson C, et al. (2006) Dynamic microtubules regulate the local concentration of E-cadherin at cell-cell contacts. J Cell Sci 119: 1801-1811.

70. Grindstaff KK, Bacallao RL, Nelson WJ (1998) Apiconuclear organization of microtubules does not specify protein delivery from the trans-Golgi network to different membrane domains in polarized epithelial cells. Mol Biol Cell 9: 685-699.

71. Michaelson JE, Huang H (2012) Cell-cell junctional proteins in cardiovascular mechanotransduction. Ann Biomed Eng 40: 568-577.

72. McCain ML, Parker KK (2011) Mechanotransduction: the role of mechanical stress, myocyte shape, and cytoskeletal architecture on cardiac function. Pflugers Arch 462: 89-104.

73. le Duc Q, Shi Q, Blonk I, Sonnenberg A, Wang N, et al. (2010) Vinculin potentiates E-cadherin mechanosensing and is recruited to actin-anchored sites within adherens junctions in a myosin II-dependent manner. J Cell Biol 189: 1107-1115.

74. Liu Z, Tan JL, Cohen DM, Yang MT, Sniadecki NJ, et al. (2010) Mechanical tugging force regulates the size of cell-cell junctions. Proc Natl Acad Sci U S A 107: 9944-9949.

75. Yamada K, Green KG, Samarel AM, Saffitz JE (2005) Distinct pathways regulate expression of cardiac electrical and mechanical junction proteins in response to stretch. Circ Res 97: 346-353.

76. Huang H, Asimaki A, Lo D, McKenna W, Saffitz J (2008) Disparate effects of different mutations in plakoglobin on cell mechanical behavior. Cell Motil Cytoskeleton 65: 964-978.

77. Trepat X, Wasserman MR, Angelini TE, Millet E, Weitz DA, et al. (2009) Physical forces during collective cell migration. Nat Phys 5: 426-430.

78. Tseng Q, Duchemin-Pelletier E, Deshiere A, Balland M, Guillou H, et al. (2012) Spatial organization of the extracellular matrix regulates cell-cell junction positioning. Proc Natl Acad Sci U S A 109: 1506-1511.

79. Ting LH, Jahn JR, Jung JI, Shuman BR, Feghhi S, et al. (2012) Flow mechanotransduction regulates traction forces, intercellular forces, and adherens junctions. Am J Physiol Heart Circ Physiol 302: H2220-2229.

80. Shao JY, Xu G, Guo P (2004) Quantifying cell-adhesion strength with micropipette manipulation: principle and application. Front Biosci 9: 2183-2191.

81. Benjamin JM, Kwiatkowski AV, Yang C, Korobova F, Pokutta S, et al. (2010) AlphaE-catenin regulates actin dynamics independently of cadherin-mediated cell-cell adhesion. J Cell Biol 189: 339-352.

82. Franzen CA, Todorovic V, Desai BV, Mirzoeva S, Yang XJ, et al. (2012) The desmosomal armadillo protein plakoglobin regulates prostate cancer cell adhesion and motility through vitronectin-dependent Src signaling. PLoS One 7: e42132.

83. Akiyama Y, Kikuchi A, Yamato M, Okano T (2004) Ultrathin poly(N-isopropylacrylamide) grafted layer on polystyrene surfaces for cell adhesion/detachment control. Langmuir 20: 5506-5511.

84. Tsuda Y, Kikuchi A, Yamato M, Sakurai Y, Umezu M, et al. (2004) Control of cell adhesion and detachment using temperature and thermoresponsive copolymer grafted culture surfaces. J Biomed Mater Res A 69: 70-78.

85. Hui EE, Bhatia SN (2007) Micromechanical control of cell-cell interactions. Proc Natl Acad Sci U S A 104: 5722-5726.

86. Califano J, Reinhart-King C (2008) A Balance of Substrate Mechanics and Matrix Chemistry Regulates Endothelial Cell Network Assembly. Cellular and Molecular Bioengineering 1: 122-132.

87. Maruthamuthu V, Sabass B, Schwarz US, Gardel ML (2011) Cell-ECM traction force modulates endogenous tension at cell-cell contacts. Proc Natl Acad Sci U S A 108: 4708-4713.

88. Rakshit S, Zhang Y, Manibog K, Shafraz O, Sivasankar S (2012) Ideal, catch, and slip bonds in cadherin adhesion. Proc Natl Acad Sci U S A 109: 18815-18820.

89. Ganz A, Lambert M, Saez A, Silberzan P, Buguin A, et al. (2006) Traction forces exerted through N-cadherin contacts. Biol Cell 98: 721-730.

90. Roger VL, Go AS, Lloyd-Jones DM, Adams RJ, Berry JD, et al. (2011) Heart disease and stroke statistics--2011 update: a report from the American Heart Association. Circulation 123: e18-e209.

91. Cowie MR, Mosterd A, Wood DA, Deckers JW, Poole-Wilson PA, et al. (1997) The epidemiology of heart failure. Eur Heart J 18: 208-225.

92. Laflamme MA, Murry CE (2005) Regenerating the heart. Nat Biotechnol 23: 845-856.

93. Beltrami AP, Urbanek K, Kajstura J, Yan SM, Finato N, et al. (2001) Evidence that human cardiac myocytes divide after myocardial infarction. N Engl J Med 344: 1750-1757.

94. Segers VF, Lee RT (2010) Protein therapeutics for cardiac regeneration after myocardial infarction. J Cardiovasc Transl Res 3: 469-477.

95. Lloyd-Jones DM (2001) The risk of congestive heart failure: sobering lessons from the Framingham Heart Study. Curr Cardiol Rep 3: 184-190.

96. Boyle A (2009) Current status of cardiac transplantation and mechanical circulatory support. Curr Heart Fail Rep 6: 28-33.

97. Jeevanandam V, Furukawa S, Prendergast TW, Todd BA, Eisen HJ, et al. (1996) Standard criteria for an acceptable donor heart are restricting heart transplantation. Ann Thorac Surg 62: 1268-1275.

98. Lindenfeld J, Miller GG, Shakar SF, Zolty R, Lowes BD, et al. (2004) Drug therapy in the heart transplant recipient: part I: cardiac rejection and immunosuppressive drugs. Circulation 110: 3734-3740.

99. Ye KY, Black LD, 3rd (2011) Strategies for tissue engineering cardiac constructs to affect functional repair following myocardial infarction. J Cardiovasc Transl Res 4: 575-591.

100. Laflamme MA, Zbinden S, Epstein SE, Murry CE (2007) Cell-based therapy for myocardial ischemia and infarction: pathophysiological mechanisms. Annu Rev Pathol 2: 307-339.

101. Beitnes JO, Hopp E, Lunde K, Solheim S, Arnesen H, et al. (2009) Long-term results after intracoronary injection of autologous mononuclear bone marrow cells in acute myocardial infarction: the ASTAMI randomised, controlled study. Heart 95: 1983-1989.

102. Leor J, Gerecht S, Cohen S, Miller L, Holbova R, et al. (2007) Human embryonic stem cell transplantation to repair the infarcted myocardium. Heart 93: 1278-1284.

103. Meyer GP, Wollert KC, Lotz J, Steffens J, Lippolt P, et al. (2006) Intracoronary bone marrow cell transfer after myocardial infarction: eighteen months' follow-up data from the randomized, controlled BOOST (BOne marrOw transfer to enhance ST-elevation infarct regeneration) trial. Circulation 113: 1287-1294.

104. Fujita H, Shimizu K, Nagamori E (2009) Application of a cell sheet-polymer film complex with temperature sensitivity for increased mechanical strength and cell alignment capability. Biotechnol Bioeng 103: 370-377.

105. Ito A, Ino K, Hayashida M, Kobayashi T, Matsunuma H, et al. (2005) Novel methodology for fabrication of tissue-engineered tubular constructs using magnetite nanoparticles and magnetic force. Tissue Eng 11: 1553-1561.

106. Shimizu T, Yamato M, Isoi Y, Akutsu T, Setomaru T, et al. (2002) Fabrication of pulsatile cardiac tissue grafts using a novel 3-dimensional cell sheet manipulation technique and temperature-responsive cell culture surfaces. Circulation Research 90: E40-E48.

107. Vunjak-Novakovic G, Tandon N, Godier A, Maidhof R, Marsano A, et al. (2010) Challenges in cardiac tissue engineering. Tissue Eng Part B Rev 16: 169-187.

108. Wang F, Guan J (2010) Cellular cardiomyoplasty and cardiac tissue engineering for myocardial therapy. Adv Drug Deliv Rev 62: 784-797.

109. Shimizu T, Yamato M, Isoi Y, Akutsu T, Setomaru T, et al. (2002) Fabrication of pulsatile cardiac tissue grafts using a novel 3-dimensional cell sheet manipulation technique and temperature-responsive cell culture surfaces. Circ Res 90: e40.

110. Masuda S, Shimizu T, Yamato M, Okano T (2008) Cell sheet engineering for heart tissue repair. Adv Drug Deliv Rev 60: 277-285.

111. Zhuang J, Yamada KA, Saffitz JE, Kleber AG (2000) Pulsatile stretch remodels cell-to-cell communication in cultured myocytes. Circ Res 87: 316-322.

112. Zhang Y, Kanter EM, Yamada KA (2010) Remodeling of cardiac fibroblasts following myocardial infarction results in increased gap junction intercellular communication. Cardiovasc Pathol 19: e233-240.

113. Hussain W, Patel PM, Chowdhury RA, Cabo C, Ciaccio EJ, et al. (2010) The Renin-Angiotensin system mediates the effects of stretch on conduction velocity, connexin43 expression, and redistribution in intact ventricle. J Cardiovasc Electrophysiol 21: 1276-1283.

114. Kohl P, Hunter P, Noble D (1999) Stretch-induced changes in heart rate and rhythm: clinical observations, experiments and mathematical models. Prog Biophys Mol Biol 71: 91-138.

115. Zhang Y, Sekar RB, McCulloch AD, Tung L (2008) Cell cultures as models of cardiac mechanoelectric feedback. Prog Biophys Mol Biol 97: 367-382.

116. Rauzi M, Verant P, Lecuit T, Lenne PF (2008) Nature and anisotropy of cortical forces orienting Drosophila tissue morphogenesis. Nat Cell Biol 10: 1401-1410.

117. Levine E, Lee CH, Kintner C, Gumbiner BM (1994) Selective disruption of E-cadherin function in early Xenopus embryos by a dominant negative mutant. Development 120: 901-909.

118. Davidson LA, Keller R, DeSimone DW (2004) Assembly and remodeling of the fibrillar fibronectin extracellular matrix during gastrulation and neurulation in Xenopus laevis. Dev Dyn 231: 888-895.

119. Davidson LA, Marsden M, Keller R, Desimone DW (2006) Integrin alpha5beta1 and fibronectin regulate polarized cell protrusions required for Xenopus convergence and extension. Curr Biol 16: 833-844.

120. Krishnan R, Klumpers DD, Park CY, Rajendran K, Trepat X, et al. (2011) Substrate stiffening promotes endothelial monolayer disruption through enhanced physical forces. Am J Physiol Cell Physiol 300: C146-154.

121. Rorth P (2009) Collective cell migration. Annu Rev Cell Dev Biol 25: 407-429.

122. Huttenlocher A, Lakonishok M, Kinder M, Wu S, Truong T, et al. (1998) Integrin and cadherin synergy regulates contact inhibition of migration and motile activity. J Cell Biol 141: 515-526.

123. Eschenhagen T, Fink C, Remmers U, Scholz H, Wattchow J, et al. (1997) Three-dimensional reconstitution of embryonic cardiomyocytes in a collagen matrix: a new heart muscle model system. FASEB J 11: 683-694.

124. Zimmermann WH, Melnychenko I, Wasmeier G, Didie M, Naito H, et al. (2006) Engineered heart tissue grafts improve systolic and diastolic function in infarcted rat hearts. Nat Med 12: 452-458.

125. Li D, Zhou J, Wang L, Shin ME, Su P, et al. (2010) Integrated biochemical and mechanical signals regulate multifaceted human embryonic stem cell functions. J Cell Biol 191: 631-644.

126. Rheinwald JG, Hahn WC, Ramsey MR, Wu JY, Guo Z, et al. (2002) A two-stage, p16(INK4A)- and p53-dependent keratinocyte senescence mechanism that limits replicative potential independent of telomere status. Mol Cell Biol 22: 5157-5172.

127. Takeuchi A, Fukazawa S, Chida K, Taguchi M, Shirataka M, et al. (2012) Semi-automatic counting of connexin 32s immunolocalized in cultured fetal rat hepatocytes using image processing. Acta Histochem 114: 318-326.

128. Hartig SM (2013) Basic image analysis and manipulation in ImageJ. Curr Protoc Mol Biol Chapter 14: Unit14 15.

129. Jensen EC (2013) Quantitative analysis of histological staining and fluorescence using ImageJ. Anat Rec (Hoboken) 296: 378-381.

130. Calautti E, Cabodi S, Stein PL, Hatzfeld M, Kedersha N, et al. (1998) Tyrosine phosphorylation and src family kinases control keratinocyte cell-cell adhesion. J Cell Biol 141: 1449-1465.

131. Yin T, Getsios S, Caldelari R, Kowalczyk AP, Muller EJ, et al. (2005) Plakoglobin suppresses keratinocyte motility through both cell-cell adhesion-dependent and -independent mechanisms. Proc Natl Acad Sci U S A 102: 5420-5425.

132. Huen AC, Park JK, Godsel LM, Chen X, Bannon LJ, et al. (2002) Intermediate filament-membrane attachments function synergistically with actin-dependent contacts to regulate intercellular adhesive strength. J Cell Biol 159: 1005-1017.

133. Ingber DE, Folkman J (1989) Mechanochemical switching between growth and differentiation during fibroblast growth factor-stimulated angiogenesis in vitro: role of extracellular matrix. J Cell Biol 109: 317-330.

134. Gallant ND, Michael KE, Garcia AJ (2005) Cell adhesion strengthening: contributions of adhesive area, integrin binding, and focal adhesion assembly. Mol Biol Cell 16: 4329-4340.

135. Ingber DE (2008) Tensegrity-based mechanosensing from macro to micro. Prog Biophys Mol Biol 97: 163-179.

136. Caca K, Kolligs FT, Ji X, Hayes M, Qian J, et al. (1999) Beta- and gamma-catenin mutations, but not E-cadherin inactivation, underlie T-cell factor/lymphoid enhancer factor transcriptional deregulation in gastric and pancreatic cancer. Cell Growth Differ 10: 369-376.

137. Kolligs FT, Kolligs B, Hajra KM, Hu G, Tani M, et al. (2000) gamma-catenin is regulated by the APC tumor suppressor and its oncogenic activity is distinct from that of beta-catenin. Genes Dev 14: 1319-1331.

138. Maeda O, Usami N, Kondo M, Takahashi M, Goto H, et al. (2004) Plakoglobin (gamma-catenin) has TCF/LEF family-dependent transcriptional activity in beta-catenin-deficient cell line. Oncogene 23: 964-972.

139. Condeelis J, Segall JE (2003) Intravital imaging of cell movement in tumours. Nat Rev Cancer 3: 921-930.

140. Sommers CL, Gelmann EP, Kemler R, Cowin P, Byers SW (1994) Alterations in beta-catenin phosphorylation and plakoglobin expression in human breast cancer cells. Cancer Res 54: 3544-3552.

141. Aberle H, Bierkamp C, Torchard D, Serova O, Wagner T, et al. (1995) The human plakoglobin gene localizes on chromosome 17q21 and is subjected to loss of heterozygosity in breast and ovarian cancers. Proc Natl Acad Sci U S A 92: 6384-6388.

142. Simcha I, Geiger B, Yehuda-Levenberg S, Salomon D, Ben-Ze'ev A (1996) Suppression of tumorigenicity by plakoglobin: an augmenting effect of N-cadherin. J Cell Biol 133: 199-209.

143. Denk C, Hulsken J, Schwarz E (1997) Reduced gene expression of E-cadherin and associated catenins in human cervical carcinoma cell lines. Cancer Lett 120: 185-193.

144. Giroldi LA, Bringuier PP, Shimazui T, Jansen K, Schalken JA (1999) Changes in cadherin-catenin complexes in the progression of human bladder carcinoma. Int J Cancer 82: 70-76.

145. Winn RA, Bremnes RM, Bemis L, Franklin WA, Miller YE, et al. (2002) gamma-Catenin expression is reduced or absent in a subset of human lung cancers and re-expression inhibits transformed cell growth. Oncogene 21: 7497-7506.

146. Pantel K, Passlick B, Vogt J, Stosiek P, Angstwurm M, et al. (1998) Reduced expression of plakoglobin indicates an unfavorable prognosis in subsets of patients with non-small-cell lung cancer. J Clin Oncol 16: 1407-1413.

147. Kanazawa Y, Ueda Y, Shimasaki M, Katsuda S, Yamamoto N, et al. (2008) Down-regulation of plakoglobin in soft tissue sarcoma is associated with a higher risk of pulmonary metastasis. Anticancer Res 28: 655-664.

148. Narkio-Makela M, Pukkila M, Lagerstedt E, Virtaniemi J, Pirinen R, et al. (2009) Reduced gamma-catenin expression and poor survival in oral squamous cell carcinoma. Arch Otolaryngol Head Neck Surg 135: 1035-1040.

149. Aktary Z, Chapman K, Lam L, Lo A, Ji C, et al. (2010) Plakoglobin interacts with and increases the protein levels of metastasis suppressor Nm23-H2 and regulates the expression of Nm23-H1. Oncogene 29: 2118-2129.

150. Kurosawa H (2007) Methods for inducing embryoid body formation: in vitro differentiation system of embryonic stem cells. J Biosci Bioeng 103: 389-398.

151. Shimizu T, Yamato M, Kikuchi A, Okano T (2001) Two-dimensional manipulation of cardiac myocyte sheets utilizing temperature-responsive culture dishes augments the pulsatile amplitude. Tissue Eng 7: 141-151.

152. Georges-Labouesse EN, George EL, Rayburn H, Hynes RO (1996) Mesodermal development in mouse embryos mutant for fibronectin. Dev Dyn 207: 145-156.

153. Numaguchi K, Eguchi S, Yamakawa T, Motley ED, Inagami T (1999) Mechanotransduction of rat aortic vascular smooth muscle cells requires RhoA and intact actin filaments. Circ Res 85: 5-11.

154. Ehrlicher AJ, Nakamura F, Hartwig JH, Weitz DA, Stossel TP (2011) Mechanical strain in actin networks regulates FilGAP and integrin binding to filamin A. Nature 478: 260-263.

155. Mathieu PS, Loboa EG (2012) Cytoskeletal and focal adhesion influences on mesenchymal stem cell shape, mechanical properties, and differentiation down osteogenic, adipogenic, and chondrogenic pathways. Tissue Eng Part B Rev 18: 436-444.

156. Trepat X, Deng L, An SS, Navajas D, Tschumperlin DJ, et al. (2007) Universal physical responses to stretch in the living cell. Nature 447: 592-595.

157. Vogel V, Sheetz M (2006) Local force and geometry sensing regulate cell functions. Nat Rev Mol Cell Biol 7: 265-275.

158. Koetsier JL, Amargo EV, Todorovic V, Green KJ, Godsel LM (2013) Plakophilin 2 Affects Cell Migration by Modulating Focal Adhesion Dynamics and Integrin Protein Expression. J Invest Dermatol.

159. Kushida A, Yamato M, Isoi Y, Kikuchi A, Okano T (2005) A noninvasive transfer system for polarized renal tubule epithelial cell sheets using temperature-responsive culture dishes. Eur Cell Mater 10: 23-30; discussion 23-30.

160. Nishida K, Yamato M, Hayashida Y, Watanabe K, Yamamoto K, et al. (2004) Corneal reconstruction with tissue-engineered cell sheets composed of autologous oral mucosal epithelium. N Engl J Med 351: 1187-1196.

161. Shimizu T, Yamato M, Akutsu T, Shibata T, Isoi Y, et al. (2002) Electrically communicating three-dimensional cardiac tissue mimic fabricated by layered cultured cardiomyocyte sheets. J Biomed Mater Res 60: 110-117.

162. Moore A, Donahue CJ, Bauer KD, Mather JP (1998) Simultaneous measurement of cell cycle and apoptotic cell death. Methods Cell Biol 57: 265-278.

163. Yoshioka J, Schulze PC, Cupesi M, Sylvan JD, MacGillivray C, et al. (2004) Thioredoxin-interacting protein controls cardiac hypertrophy through regulation of thioredoxin activity. Circulation 109: 2581-2586.

164. Yin T, Getsios S, Caldelari R, Godsel LM, Kowalczyk AP, et al. (2005) Mechanisms of plakoglobin-dependent adhesion: desmosome-specific functions in assembly and regulation by epidermal growth factor receptor. J Biol Chem 280: 40355-40363.

165. Shen MY, Michaelson J, Huang H (2013) Rheological responses of cardiac fibroblasts to mechanical stretch. Biochem Biophys Res Commun 430: 1028-1033.

166. Michaelson J, Choi H, So P, Huang H (2012) Depth-resolved cellular microrheology using HiLo microscopy. Biomed Opt Express 3: 1241-1255.

167. Ingber DE (2003) Tensegrity II. How structural networks influence cellular information processing networks. J Cell Sci 116: 1397-1408.

168. Bershadsky AD, Balaban NQ, Geiger B (2003) Adhesion-dependent cell mechanosensitivity. Annu Rev Cell Dev Biol 19: 677-695.

169. Gardel ML, Shin JH, MacKintosh FC, Mahadevan L, Matsudaira P, et al. (2004) Elastic behavior of cross-linked and bundled actin networks. Science 304: 1301-1305.

170. Storm C, Pastore JJ, MacKintosh FC, Lubensky TC, Janmey PA (2005) Nonlinear elasticity in biological gels. Nature 435: 191-194.

171. Ladoux B, Anon E, Lambert M, Rabodzey A, Hersen P, et al. (2010) Strength dependence of cadherin-mediated adhesions. Biophys J 98: 534-542.

172. Papusheva E, Heisenberg CP (2010) Spatial organization of adhesion: force-dependent regulation and function in tissue morphogenesis. EMBO J 29: 2753-2768.

173. Kondoh H, Sawa Y, Miyagawa S, Sakakida-Kitagawa S, Memon IA, et al. (2006) Longer preservation of cardiac performance by sheet-shaped myoblast implantation in dilated cardiomyopathic hamsters. Cardiovasc Res 69: 466-475.

174. Ito A, Ino K, Kobayashi T, Honda H (2005) The effect of RGD peptide-conjugated magnetite cationic liposomes on cell growth and cell sheet harvesting. Biomaterials 26: 6185-6193.

175. Tiwari A, Punshon G, Kidane A, Hamilton G, Seifalian AM (2003) Magnetic beads (Dynabead) toxicity to endothelial cells at high bead concentration: implication for tissue engineering of vascular prosthesis. Cell Biol Toxicol 19: 265-272.

176. Inaba R, Khademhosseini A, Suzuki H, Fukuda J (2009) Electrochemical desorption of self-assembled monolayers for engineering cellular tissues. Biomaterials 30: 3573-3579.

177. Stenn KS, Link R, Moellmann G, Madri J, Kuklinska E (1989) Dispase, a neutral protease from Bacillus polymyxa, is a powerful fibronectinase and type IV collagenase. J Invest Dermatol 93: 287-290.

178. Solomon DE (2002) An in vitro examination of an extracellular matrix scaffold for use in wound healing. Int J Exp Pathol 83: 209-216.

179. Nagai N, Yunoki S, Satoh Y, Tajima K, Munekata M (2004) A method of cell-sheet preparation using collagenase digestion of salmon atelocollagen fibrillar gel. J Biosci Bioeng 98: 493-496.

180. Lim LS, Riau A, Poh R, Tan DT, Beuerman RW, et al. (2009) Effect of dispase denudation on amniotic membrane. Mol Vis 15: 1962-1970.

181. Bursac N, Loo Y, Leong K, Tung L (2007) Novel anisotropic engineered cardiac tissues: studies of electrical propagation. Biochem Biophys Res Commun 361: 847-853.

182. Kresh JY, Chopra A (2011) Intercellular and extracellular mechanotransduction in cardiac myocytes. Pflugers Arch 462: 75-87.

183. Hammerling B, Grund C, Boda-Heggemann J, Moll R, Franke WW (2006) The complexus adhaerens of mammalian lymphatic endothelia revisited: a junction even more complex than hitherto thought. Cell Tissue Res 324: 55-67.

184. Goossens S, Janssens B, Bonne S, De Rycke R, Braet F, et al. (2007) A unique and specific interaction between alphaT-catenin and plakophilin-2 in the area composita, the mixed-type junctional structure of cardiac intercalated discs. J Cell Sci 120: 2126-2136.

185. Mahoney MG, Muller EJ, Koch PJ (2010) Desmosomes and desmosomal cadherin function in skin and heart diseases-advancements in basic and clinical research. Dermatol Res Pract 2010.

186. Volk T, Fessler LI, Fessler JH (1990) A role for integrin in the formation of sarcomeric cytoarchitecture. Cell 63: 525-536.

187. Pollard TD, Cooper JA (2009) Actin, a central player in cell shape and movement. Science 326: 1208-1212.

188. Blaauw E, van Nieuwenhoven FA, Willemsen P, Delhaas T, Prinzen FW, et al. (2010) Stretch-induced hypertrophy of isolated adult rabbit cardiomyocytes. Am J Physiol Heart Circ Physiol 299: H780-787.

189. Cadre BM, Qi M, Eble DM, Shannon TR, Bers DM, et al. (1998) Cyclic stretch down-regulates calcium transporter gene expression in neonatal rat ventricular myocytes. J Mol Cell Cardiol 30: 2247-2259.

190. de Jonge HW, Dekkers DH, Houtsmuller AB, Sharma HS, Lamers JM (2007) Differential Signaling and Hypertrophic Responses in Cyclically Stretched vs Endothelin-1 Stimulated Neonatal Rat Cardiomyocytes. Cell Biochem Biophys 47: 21-32.

191. Simpson DG, Majeski M, Borg TK, Terracio L (1999) Regulation of cardiac myocyte protein turnover and myofibrillar structure in vitro by specific directions of stretch. Circ Res 85: e59-69.

192. Lokuta A, Kirby MS, Gaa ST, Lederer WJ, Rogers TB (1994) On establishing primary cultures of neonatal rat ventricular myocytes for analysis over long periods. J Cardiovasc Electrophysiol 5: 50-62.

193. Miragoli M, Gaudesius G, Rohr S (2006) Electrotonic modulation of cardiac impulse conduction by myofibroblasts. Circ Res 98: 801-810.

194. Straight AF, Cheung A, Limouze J, Chen I, Westwood NJ, et al. (2003) Dissecting temporal and spatial control of cytokinesis with a myosin II Inhibitor. Science 299: 1743-1747.

195. Kwan HY, Huang Y, Yao X (2000) Store-operated calcium entry in vascular endothelial cells is inhibited by cGMP via a protein kinase G-dependent mechanism. J Biol Chem 275: 6758-6763.

196. Klauke N, Smith G, Cooper JM (2010) Regional electroporation of single cardiac myocytes in a focused electric field. Anal Chem 82: 585-592.

197. Selvaggi L, Salemme M, Vaccaro C, Pesce G, Rusciano G, et al. (2010) Multiple-Particle-Tracking to investigate viscoelastic properties in living cells. Methods 51: 20-26.

198. Wirtz D (2009) Particle-tracking microrheology of living cells: principles and applications. Annu Rev Biophys 38: 301-326.

199. Tseng Y, Kole TP, Wirtz D (2002) Micromechanical mapping of live cells by multiple-particle-tracking microrheology. Biophys J 83: 3162-3176.

200. Garcia-Gras E, Lombardi R, Giocondo MJ, Willerson JT, Schneider MD, et al. (2006) Suppression of canonical Wnt/beta-catenin signaling by nuclear plakoglobin recapitulates phenotype of arrhythmogenic right ventricular cardiomyopathy. Journal of Clinical Investigation 116: 2012-2021.

201. Iribe G, Kohl P (2008) Axial stretch enhances sarcoplasmic reticulum Ca2+ leak and cellular Ca2+ reuptake in guinea pig ventricular myocytes: experiments and models. Prog Biophys Mol Biol 97: 298-311.

202. Bers DM (2000) Calcium fluxes involved in control of cardiac myocyte contraction. Circ Res 87: 275-281.

203. O'Rourke B, Kass DA, Tomaselli GF, Kaab S, Tunin R, et al. (1999) Mechanisms of altered excitation-contraction coupling in canine tachycardia-induced heart failure, I: experimental studies. Circ Res 84: 562-570.

204. Pogwizd SM, Qi M, Yuan W, Samarel AM, Bers DM (1999) Upregulation of Na(+)/Ca(2+) exchanger expression and function in an arrhythmogenic rabbit model of heart failure. Circ Res 85: 1009-1019.

205. Ito S, Kume H, Naruse K, Kondo M, Takeda N, et al. (2008) A novel Ca2+ influx pathway activated by mechanical stretch in human airway smooth muscle cells. Am J Respir Cell Mol Biol 38: 407-413.

206. Minin AA, Kulik AV, Gyoeva FK, Li Y, Goshima G, et al. (2006) Regulation of mitochondria distribution by RhoA and formins. J Cell Sci 119: 659-670.

207. Lee JS, Chang MI, Tseng Y, Wirtz D (2005) Cdc42 mediates nucleus movement and MTOC polarization in Swiss 3T3 fibroblasts under mechanical shear stress. Mol Biol Cell 16: 871-880.

208. Lee JS, Panorchan P, Hale CM, Khatau SB, Kole TP, et al. (2006) Ballistic intracellular nanorheology reveals ROCK-hard cytoplasmic stiffening response to fluid flow. J Cell Sci 119: 1760-1768.

209. Walcott S, Sun SX (2010) A mechanical model of actin stress fiber formation and substrate elasticity sensing in adherent cells. Proc Natl Acad Sci U S A 107: 7757-7762.

210. Sigurdson W, Ruknudin A, Sachs F (1992) Calcium imaging of mechanically induced fluxes in tissue-cultured chick heart: role of stretch-activated ion channels. Am J Physiol 262: H1110-1115.

211. Yamazaki T, Komuro I, Kudoh S, Zou Y, Nagai R, et al. (1998) Role of ion channels and exchangers in mechanical stretch-induced cardiomyocyte hypertrophy. Circ Res 82: 430-437.

212. Jugdutt BI (2003) Ventricular remodeling after infarction and the extracellular collagen matrix: when is enough enough? Circulation 108: 1395-1403.